

EPIGENETIC MECHANISMS GOVERNING BEHAVIORAL REPROGRAMMING IN THE  
*ANT CAMPONOTUS FLORIDANUS*

Riley John Graham

A DISSERTATION

in

Biology

Presented to the Faculties of the University of Pennsylvania

in

Partial Fulfillment of the Requirements for the

Degree of Doctor of Philosophy

2018

Supervisor of Dissertation

---

Shelley L. Berger

Daniel S. Och University Professor, Professor of Cell and Developmental Biology and Professor of Biology

Graduate Group Chairperson

---

Michael Lampson

Associate Professor of Biology and Graduate Chair in Biology

Dissertation Committee

Nancy Bonini, Florence R.C. Murray Professor of Biology

Roberto Bonasio, Assistant Professor of Cell and Developmental Biology

Mia Levine, Assistant Professor of Biology

Timothy Linksvayer, Associate Professor of Biology

## DEDICATION

I dedicate this work to Elizabeth, for passing her love for science and nature on to her sons.  
And to Olivia, for breathing new life into us all. May this thesis help you along your own journey.  
And to Colleen, who treated the students in her care to unwavering kindness and support.

## ACKNOWLEDGMENT

I am indebted to my advisor, Shelley L. Berger, who has been a courageous advocate for her students, our ant models, and the epigenetics community. I am entirely grateful for her support.

I would like to thank Nancy Bonini, Roberto Bonasio, Mia Levina, and Tim Linksvayer for their insightful comments and suggestions that helped mold this work into its best form.

Dr. Linksvayer welcomed me into the Penn community, and invited me out to find ants in Fairmount Park. I'm proud to have spent time with him in the field, in classrooms, and in his lab.

I would like to thank Doris Wagner and Michael Lampson, who have been exceptionally supportive and accessible graduate chairs, and always encouraged me to keep pushing ahead.

Karl Glastad for assuming the role of energy in its purest form and sharing it around, etc.

Cristina Brady for sustaining the colony (I don't mean ants), and being a true friend.

Dan Simola for his guru-level mentoring, and brilliant character. Free will is alive and well.

## ABSTRACT

### EPIGENETIC MECHANISMS GOVERNING BEHAVIORAL REPROGRAMMING IN THE ANT *CAMPONOTUS FLORIDANUS*

Riley J. Graham

Shelley L. Berger

Eusocial insect colonies divide behaviors among specialist groups called castes. In some species, caste identity is determined by the interaction of endogenous (e.g. genomic) and exogenous (e.g. juvenile hormone from nurses) signals during larval development, suggesting epigenetic mechanisms underlie plastic traits tied to caste identity. Previous work demonstrated a link between patterns of histone H3 lysine 27 acetylation (H3K27ac) and caste-specific gene expression in Major and Minor workers of the ant *Camponotus floridanus*, and we hypothesized caste-specific behaviors such as foraging may be similarly regulated by histone acetylation. To test this hypothesis, we fed mature (~30d old) Majors and Minors with histone deacetylase inhibitors (HDACi), and CBP-dependent histone acetyl transferase inhibitors (HATi). We observed foraging enhancement after HDACi, and foraging suppression after HATi in Minors. Curiously, we did not observe increased foraging in HDACi treated mature (~30d) Majors. However, HDACi injections in callow (0-1d old) Majors succeeded in causing stable reprogramming of foraging behavior, indicating a critical period, or 'window' of epigenetic sensitivity to HDACi exists in young majors. To address this possibility, we injected Majors with HDACi in a time course and observed juvenile (d0-d5) Majors are susceptible to reprogramming, whereas mature (d10) Majors are not. To assess innate differences in the brain between castes, we conducted an RNA-seq study in untreated Major and Minor workers 0, 5, and 10 days old, and detected caste-specific patterns of juvenile hormone and ecdysone signaling. Finally, to characterize the transcriptional and epigenetic effects of reprogramming, we conducted RNA-seq in HDACi treated Major brains, and detected consistent upregulation of members of the neuron restrictive silencing factor (NRSF/REST) repressive complex (e.g. CoREST, RPD3, ttk). Notably, the top downregulated gene after HDACi is juvenile hormone esterase (JHe), which antagonizes JH signaling and inhibits foraging behavior in many eusocial insects. Thus, our results suggest REST/CoREST-mediated repression of JHe may be a significant source of stable changes to foraging in behaviorally reprogrammed Majors.

## TABLE OF CONTENTS

<b>DEDICATION .....</b>	<b>II</b>
<b>ACKNOWLEDGMENT.....</b>	<b>III</b>
<b>ABSTRACT .....</b>	<b>IV</b>
<b>CHAPTER 1: INTRODUCTION .....</b>	<b>1</b>
From Waddington to behavioral epigenetics .....	1
Epigenetic processes link gene expression and chromatin structure .....	2
The histone language and behavior.....	3
Eusocial insects are new model organisms for behavioral epigenetics .....	4
Caste identity involves changes in gene expression and hPTMs.....	5
Chapter 1 Bibliography.....	7
<b>CHAPTER 2: EPIGENETIC (RE)PROGRAMMING OF CASTE-SPECIFIC BEHAVIOR IN THE ANT CAMPONOTUS FLORIDANUS .....</b>	<b>11</b>
Background .....	11
C. floridanus workers exhibit caste-specific behaviors.....	12
Histone deacetylases inhibit foraging and scouting behaviors.....	15
CBP-dependent histone acetylation regulates foraging and scouting behaviors .....	18
HDAC inhibition induces and sustains Minor-like foraging behavior in Majors .....	23
Ant colonies and husbandry .....	28
Caste and age identification.....	28
Foraging assays and analyses .....	29
Reverse transcription quantitative polymerase chain reaction (RT-qPCR) sample preparation and analyses.....	30
Chromatin immunoprecipitation .....	30

Foraging assays for pharmacologically treated ants.....	31
Preparation of RNA-seq libraries .....	32
Preparation of ChIP-seq libraries.....	33
Analysis of RNA-seq and ChIP-seq data.....	33
Brain injection procedure.....	34
RNAi-mediated mRNA knockdown and analysis.....	34
Chapter 2 Bibliography.....	36
<b>CHAPTER 3: BEHAVIORAL REPROGRAMMING BY HDACI CAUSES A TARGETED TRANSCRIPTIONAL RESPONSE DURING A CRITICAL PERIOD OF EPIGENETIC SENSITIVITY. ....</b>	<b>40</b>
Background .....	40
Caste identity and early maturation stimulate transcriptional change in worker brains .....	42
Ecdysteroid factors are differentially expressed in <i>Cflo</i> worker brains by caste .....	44
GABA signaling factors related to <i>Dmel</i> feeding behavior are upregulated in Minors.....	46
Mediators of heterochromatin and euchromatin indicate a period of epigenetic plasticity during maturation .....	48
A time course of pharmacologic treatments in Majors indicates a critical period for behavioral reprogramming in early development.....	50
HDACi treatments induce rapid transcriptional change in d5 Major brains .....	51
E3 ubiquitin ligases with RING-domain cofactors are induced by HDACi.....	54
Chromatin modifiers are induced by HDACi.....	55
HDACi induced Rho GTPases indicate non-canonical Shh/Smoothed activation.....	57
The insect CoREST repressive complex is activated by HDACi in d5 Majors.....	57
Two antagonists of JH function, JHe and JHEH, are silenced by HDACi.....	59
Induction of the CoREST complex is not observed in mature (d10) Majors.....	60
Global and targeted changes in H3K27ac, but not H3K27me3, due to HDACi .....	61
HDACi response genes gain H3K27ac peaks upstream of TSS after treatment.....	62
Discussion .....	65

Materials and Methods.....	67
Ant collection and husbandry.....	67
Caste and age determination .....	67
Untreated Cflo collection and dissection .....	67
mRNA-seq sample preparation .....	68
RNA-seq analysis pipeline .....	68
Injections .....	69
Foraging behavior analysis.....	69
Preparation of ChIP-seq samples.....	70
Native ChIP-seq sample preparation .....	70
ChIP-seq analysis pipeline.....	71
Chapter 3 Bibliography .....	71
<b>CHAPTER 4: DISCUSSION .....</b>	<b>77</b>
Histone acetylation dynamics influence caste identity and behavior .....	77
Ecdysteroid and JH signaling is linked to HDAC function.....	78
Minor GABA and Grd expansion supports GABA role in DoL .....	79
Caste DEGs have established function in circadian clock regulation.....	79
Neuropeptides corazonin and neuroparsin antagonize vitellogenin in non-reproductive workers.....	80
Elevated heat shock protein in Majors signals a role in caste longevity .....	81
DEGs in untreated samples indicate targeted transcriptional differences in behaviorally relevant pathways between castes.....	82
One Really Interesting New Gene to rule them all.....	82
Manipulation of HDAC function reprograms behavior and transcription .....	84
Current model for stable reprogramming of foraging behavior by HDACi .....	85
Future directions .....	87
Chapter 4 Bibliography .....	89

## CHAPTER 1: Introduction

### From Waddington to behavioral epigenetics

The term 'epigenetics' was introduced to describe the interaction of genes and their products in the 1940s by Conrad Waddington, who realized systems of gene regulation are needed for the ordered process of embryological development<sup>1,2</sup>. Today, epigenetics broadly describes molecular mechanisms of the genome that orchestrate dynamic temporal and spatial patterns of gene expression<sup>1</sup>. Epigenetic processes are essential for the elaboration of phenotypically distinct cell types from a single genome, and are thus key factors regulating development in multicellular life<sup>3</sup>. Epigenetic mechanisms are a platform for stable molecular memory, in that these processes can alter cellular traits based on previously experienced stimuli, and propagate those traits through subsequent cell divisions<sup>2</sup>. Additionally, errors in epigenetic function are a central focus of clinical research for many developmental disorders<sup>4</sup>, neurological diseases<sup>5</sup>, and cancer states<sup>6</sup>, demonstrating the exceptional phenotypic plasticity orchestrated by epigenetic mechanisms during development and adulthood.

In the last two decades, epigenetic features of the genome, including DNA-methylation<sup>7, 8</sup>,<sup>9</sup> histone modifications<sup>10,11,12</sup>, and long non-coding RNAs<sup>13</sup> have arisen as components of behavior. After the Kandel lab's transformative work describing molecular players in synaptic plasticity in the sea slug *Aplysia*<sup>14</sup>, one of the focal genes, CREB binding protein (CBP) and its paralog p300 were shown to be histone modifying enzymes. Wood et. al. showed the histone modifying acetyltransferase (HAT) domain of CREB binding protein (CBP) is required during the formation of memories<sup>15</sup>. Strikingly, memory and synaptic plasticity are enhanced in the presence of histone deacetylase inhibitors (HDACi), which block the removal of histone acetylation. These findings support the idea that histone modifications (hPTMs) are key epigenetic factors contributing to behavior, and indeed, hPTMs have been shown to influence neurotransmitter secretion<sup>16</sup>, axon and dendritic growth<sup>17</sup>, neuronal cell identity<sup>18</sup>, and other behaviorally relevant processes. Hence, the emerging fields of behavioral epigenetics and neuroepigenetics are rapidly

growing as new pathways linking molecular and behavioral memory to epigenetic mechanisms are identified. Importantly, dynamic histone modification appears to be a crucial substrate for cellular and behavioral memory.

### **Epigenetic processes link gene expression and chromatin structure**

Histone proteins and their enzymatic partners structurally organize DNA into transcriptionally active and inactive states<sup>19</sup>. The core histone molecule is a protein octamer comprised of two H2A/H2B histone protein dimers in complex with a histone H3/H4 tetramer. Negative charge sites on the DNA backbone form 142 hydrogen bonds with positively charged sites on histone proteins, causing 147 base pair segments of DNA to coil around a single histone octamer to form a nucleosome<sup>20</sup>. Nucleosomes are the fundamental unit of chromatin, and the dynamic organization of nucleosomes within the genome modulates access to transcription factor (TF) binding sites, enhancers, transcription start sites (TSSs) and other DNA regulatory elements<sup>21</sup>. Through these mechanisms, chromatin organization influences gene expression during development, disease, and behavior.

Histone post-translational modifications (hPTMs) are covalent chemical tags that alter the binding forces between DNA and histone proteins and can recruit cofactors<sup>22,23</sup>. hPTMs are added to the unstructured tails and globular domains of histone proteins by 'writers'. Writers can be transcriptionally activating or silencing depending on the downstream effect of their target modification. The HAT domain of CBP, for example, acetylates lysine 27 on histone H3 (H3K27ac) and causes an activating effect. In contrast, the histone methyltransferase (HMT) EZH2 tri-methylates the same target lysine on H3 (H3K27me3), and causes a silencing effect<sup>24</sup>. 'Eraser' enzymes remove histone modifications and are also either silencing (e.g. via removal of H3K27ac) or activating (e.g. via removal of H3K27me3). Thus, the activities of writer and eraser enzymes encode context-specific patterns of hPTMs that alter downstream gene expression<sup>25</sup>.

A variety of hPTMs decorate eukaryotic chromatin to form a 'histone language', which is dynamically edited by writers and erasers, and interpreted by factors known as 'readers'<sup>22</sup>.

Readers recognize and bind specific hPTMs and can directly alter gene expression or recruit regulatory cofactors. Thus, due to their direct (e.g. structural) and indirect (e.g. cofactor mediated) effects on chromatin and DNA accessibility, hPTMs and their enzymatic partners are important components of epigenetic gene regulation. hPTMs are dynamically regulated during development and at adulthood, and can be altered in response to sensory stimuli <sup>26</sup>. Therefore, the language of histone modifications is of interest in recent efforts to understand how epigenetic processes function in behavior <sup>27</sup>. Indeed, histone modifiers are among the most well-characterized epigenetic components of learning and memory, highlighting their role in behavior.

### **The histone language and behavior**

Animal behaviors arise from the interaction of endogenous (e.g. genomic) and exogenous (e.g. sensory) cues, and adaptive behaviors require neuronal tissues to respond to sensory stimuli by altering the timing and location of gene expression. Decades of research into the molecular basis of memory indicate epigenetic mechanisms, and histone modifications in particular, regulate changes in gene expression during memory formation <sup>28, 29, 30</sup>. One of the most established links between hPTMs and behavior is the role of CBP in learning and memory.

During memory formation, CBP acetylates H3K27 sites upstream of immediate early genes in neurons <sup>31</sup>, leading to a regulatory cascade of protein synthesis required for memory stabilization (i.e. consolidation) <sup>32</sup>. Inhibition of CBP's HAT domain leads to memory defects, as does inhibition of CBP's KIX domain, which is the binding surface that specifically recognizes CBP's DNA-binding cofactor, CREB <sup>33</sup>. Binding of CBP to CREB and catalytic acetylation of H3K27 (H3K27ac) sites by CBP's HAT domain are thus required in memory, and hence H3K27ac is an attractive target for studies of epigenetic regulation in memory and behavior.

Changes in neural cell identity during development and adulthood also strongly influence behavior, and hPTMs are important regulators of cellular differentiation pathways in the brain <sup>34</sup>. During development, neural stem cells (NSCs) follow well-characterized differentiation programs to become one of many possible neural cell subtypes. As a consequence, hPTM enrichment and

transcription are correlated within these subtypes, suggesting differentiation is, in part, orchestrated by histone modifying enzymes. RE-1 silencing transcription factor (REST) and its corepressor CoREST recruit histone modifying enzymes RPD3/HDAC1, LSD1, and other cofactors during neurogenesis and differentiation<sup>35,36</sup>. Interestingly, invertebrates lack REST, and the DNA-binding cofactor for CoREST in insects, tramtrack (ttk), has a conserved role in recruiting CoREST and its epigenetic cofactors to regulate expression in insects<sup>37</sup>. Together, these findings highlight the central role of histone modifying complexes in the stable changes to neuronal structure and function that underlie behavioral variation.

We have established the use of eusocial insect models to address emergent questions in behavioral epigenetics, due to their extraordinary system of caste identity, which programs differences between individual colony members in morphology and behavior during development and at adulthood through epigenetic mechanisms<sup>38</sup>.

### **Eusocial insects are new model organisms for behavioral epigenetics**

Eusocial insect species (e.g. ants, bees, wasps, and termites) express specialized morphological and behavioral groups of individuals, called castes<sup>39</sup>. These castes facilitate division of labor (DoL) strategies, which distribute tasks to morphological and behavioral specialists<sup>40</sup>. A classic example in eusocial insects is the separation of reproductive and non-reproductive tasks between royal (e.g. queen) and non-royal (e.g. worker) female castes. Strongly caste-biased behaviors, such as foraging, indicate neurologic differences may 'program' different responses to sensory stimuli between castes. Programmed responses indicate underlying differences in gene function in nervous tissues, which are likely controlled by epigenetic regulators. Thus, the sophisticated organization of behaviors within eusocial insect colonies is a powerful system for the study of behavioral epigenetics and neuroepigenetics<sup>41</sup>.

Whereas some eusocial species demonstrate reproductive plasticity and low phenotypic distinction between castes<sup>42,43</sup>, our study model, the ant *Camponotus floridanus* (*Cflo*), exhibits rigid separation of reproductive tasks between morphologically distinct queen and female worker

castes<sup>44</sup>. *Camponotus* colonies are founded by a single diploid queen (e.g. haplometrosis), who mates with a single haploid male<sup>45</sup>. All diploid workers inherit the haploid male's single chromosome, and one of two potential maternal chromosomes, causing high genetic relatedness ( $r = \sim .75$ ) among siblings. Nonetheless, *Cflo* colonies express morphologically and behaviorally distinct worker castes, called Majors and Minors. Rather than acting through genetic determinants of phenotypic variation (i.e. alleles), ant embryos are thought to be 'multipotent', and caste identity is assigned during larval development in response to exogenous cues<sup>46</sup>. Thus, the exceptional phenotypic variation arising from genetically similar, yet multipotent, embryos argues that epigenetic factors underlie morphological and behavioral caste identity.

Ant models exhibit exceptional traits for the study of behavioral epigenetics, including sophisticated social behaviors, a full complement of epigenetic mechanisms found in eukaryotes, and tractability for CRISPR, RNAi, and other molecular tools<sup>41,42,43</sup>. Our research group, along with our collaborators, has pioneered the use of eusocial insects in the study of epigenetic processes and have developed methods for RNAi<sup>42</sup>, (also, Chapter 2) and CRISPR targeted mutagenesis<sup>43</sup>. Further, we have prepared next generation sequencing (NGS) libraries from a variety of ant tissues (e.g. RNA-seq, ChIP-seq)<sup>42,44</sup> (also, Chapter 2 & Chapter 3) demonstrating these ant species are amenable to contemporary molecular tools. Through our efforts to advance eusocial insects as model systems, we have observed an important role for hPTMs in organizing transcriptional differences between castes.

### **Caste identity involves changes in gene expression and hPTMs**

Significant support for the advancement of *Cflo* as a model species was gained through our publication of a genome assembly for it, along with another ant species<sup>47</sup>. Early efforts to detect transcriptional differences between castes found distinct mRNA profiles between head+thorax tissue samples in Major and Minor workers. This stimulated a screen of hPTMs in Major and Minor castes, which detected a link between caste identity and patterns of H3K27ac enrichment in *Cflo*. This study characterized caste-specific regions of H3K27ac enrichment that

correlate with caste-specific transcription<sup>44</sup>. Interestingly, in head+thorax samples, Minor-specific hPTM patterns correlate with neuronal gene expression, and Major-specific hPTMs correlate with genes related to muscle function and growth. Together, these results indicate alternative transcription programs between Major and Minor tissues are caused by differences in hPTM enrichment. In addition to striking morphological differences between *Cflo* worker castes, we observed a significant difference in foraging behavior between adult *Cflo* worker castes, and sought to understand how regulation of the epigenome in worker brains might contribute to behavioral differences between castes.

Based on our observations of caste-specific H3K27ac, transcription, and foraging behavior, we hypothesized HAT and HDAC enzymes encode specific patterns of histone acetylation in the brain of each caste, leading to epigenetic control of DoL. To address this question, we pursued experimental approaches targeting HATs and HDACs, and found HDACi treatments increased foraging activity. We developed microinjection methods, and found HDACi resulted in reprogramming of foraging behavior in newly eclosed Majors. We screened for caste-biased genes and detected differential expression of steroid hormones (e.g prothoracicotropic hormone, Ariadne-1; see Ch. 3) known to regulate development and foraging in insects. We then treated Major workers with HDACi in a time course during early maturation (d0-d10), and detected a 'window' of sensitivity to reprogramming in Majors. Finally, we characterized transcriptional and chromatin changes resulting from HDACi injections, and detected a reproducible response implicating the REST/tramtrack co-repressor complex in behavioral reprogramming.

## Chapter 1 Bibliography

1. Jablonka E, Lamb MJ. The changing concept of epigenetics. *Annals of the New York Academy of Sciences*. 2002 Dec 1;981(1):82-96.
2. Bonasio R, Tu S, Reinberg D. Molecular Signals of Epigenetic States. *Science (New York, NY)*. 2010;330(6004):612-616. doi:10.1126/science.1191078.
3. Boland MJ, Nazor KL, Loring JF. Epigenetic regulation of pluripotency and differentiation. *Circulation research*. 2014;115(2):311-324. doi:10.1161/CIRCRESAHA.115.301517.
4. Kubota T. Epigenetics in congenital diseases and pervasive developmental disorders. *Environmental Health and Preventive Medicine*. 2008;13(1):3-7. doi:10.1007/s12199-007-0008-7.
5. Landgrave-Gómez J, Mercado-Gómez O, Guevara-Guzmán R. Epigenetic mechanisms in neurological and neurodegenerative diseases. *Frontiers in Cellular Neuroscience*. 2015;9:58. doi:10.3389/fncel.2015.00058.
6. Dawson, Mark A., and Tony Kouzarides. "Cancer epigenetics: from mechanism to therapy." *Cell* 150.1 (2012): 12-27.
7. Saunderson, Emily A., et al. "Stress-induced gene expression and behavior are controlled by DNA methylation and methyl donor availability in the dentate gyrus." *Proceedings of the National Academy of Sciences* 113.17 (2016): 4830-4835.
8. Szyf, Moshe. "DNA methylation, behavior and early life adversity." *Journal of Genetics and Genomics* 40.7 (2013): 331-338.
9. Roth TL. Epigenetic mechanisms in the development of behavior: advances, challenges, and future promises of a new field. *Development and psychopathology*. 2013;25(4 0 2):1279-1291. doi:10.1017/S0954579413000618.
10. Sun H, Kennedy PJ, Nestler EJ. Epigenetics of the Depressed Brain: Role of Histone Acetylation and Methylation. *Neuropsychopharmacology*. 2013;38(1):124-137. doi:10.1038/npp.2012.73.
11. Dias, Brian G., et al. "Epigenetic mechanisms underlying learning and the inheritance of learned behaviors." *Trends in neurosciences* 38.2 (2015): 96-107.
12. K. E. Hawkins, J. D. Sweatt, Chapter 23 - Epigenetics of Memory Processes, Handbook of Epigenetics (2nd Edition), Academic Press, 2017, Pages 347-358, ISBN 9780128053881, <https://doi.org/10.1016/B978-0-12-805388-1.00023-7>.
13. Spadaro PA, Flavell CR, Widagdo J, et al. Long noncoding RNA-directed epigenetic regulation of gene expression is associated with anxiety-like behavior in mice. *Biological psychiatry*. 2015;78(12):848-859. doi:10.1016/j.biopsych.2015.02.004.
14. Hawkins, Robert D., Eric R. Kandel, and Craig H. Bailey. "Molecular mechanisms of memory storage in Aplysia." *The Biological Bulletin* 210.3 (2006): 174-191.

15. Wood MA, Attner MA, Oliveira AMM, Brindle PK, Abel T. A transcription factor-binding domain of the coactivator CBP is essential for long-term memory and the expression of specific target genes. *Learning & Memory*. 2006;13(5):609-617. doi:10.1101/lm.213906.
16. Banerjee K, Akiba Y, Baker H, Cave JW. Epigenetic control of neurotransmitter expression in olfactory bulb interneurons. *International journal of developmental neuroscience: the official journal of the International Society for Developmental Neuroscience*. 2013;31(6):415-423. doi:10.1016/j.ijdevneu.2012.11.009.
17. Trakhtenberg EF, Goldberg JL. Epigenetic regulation of axon and dendrite growth. *Frontiers in Molecular Neuroscience*. 2012;5:24. doi:10.3389/fnmol.2012.00024.
18. Yao, Bing, and Peng Jin. "Unlocking epigenetic codes in neurogenesis." *Genes & development* 28.12 (2014): 1253-1271.
19. Tchakovnikarova, Iva A., and Robert E. Kingston. "Beyond the Histone Code: A Physical Map of Chromatin States." *Molecular cell* 69.1 (2018): 5-7.
20. Cutter A, Hayes JJ. A Brief Review of Nucleosome Structure. *FEBS letters*. 2015;589(20 0 0):2914-2922. doi:10.1016/j.febslet.2015.05.016.
21. Radman-Livaja M, Rando OJ. Nucleosome positioning: how is it established, and why does it matter? *Developmental biology*. 2010;339(2):258-266. doi:10.1016/j.ydbio.2009.06.012.
22. Berger, Shelley L. "Histone modifications in transcriptional regulation." *Current opinion in genetics & development* 12.2 (2002): 142-148.
23. Tessarz, Peter, and Tony Kouzarides. "Histone core modifications regulating nucleosome structure and dynamics." *Nature reviews Molecular cell biology* 15.11 (2014): 703.
24. Cao, Ru, et al. "Role of histone H3 lysine 27 methylation in Polycomb-group silencing." *Science* 298.5595 (2002): 1039-1043.
25. Goldberg, Aaron D., C. David Allis, and Emily Bernstein. "Epigenetics: a landscape takes shape." *Cell* 128.4 (2007): 635-638.
26. Riccio, Antonella. "Dynamic epigenetic regulation in neurons: enzymes, stimuli and signaling pathways." *Nature neuroscience* 13.11 (2010): 1330.
27. Gräff, Johannes, and Isabelle M. Mansuy. "Epigenetic codes in cognition and behaviour." *Behavioural brain research* 192.1 (2008): 70-87.
28. Levenson, Jonathan M., and J. David Sweatt. "Epigenetic mechanisms in memory formation." *Nature Reviews Neuroscience* 6.2 (2005): 108.
29. Martin, Kelsey C., and Yi E. Sun. "To learn better, keep the HAT on." *Neuron* 42.6 (2004): 879-881.

30. Alarcón, Juan M., et al. "Chromatin acetylation, memory, and LTP are impaired in CBP+/- mice: a model for the cognitive deficit in Rubinstein-Taybi syndrome and its amelioration." *Neuron* 42.6 (2004): 947-959.
31. Bahrami, Shahram, and Finn Drabløs. "Gene regulation in the immediate-early response process." *Advances in biological regulation* 62 (2016): 37-49.
32. Korzus, Edward, Michael G. Rosenfeld, and Mark Mayford. "CBP histone acetyltransferase activity is a critical component of memory consolidation." *Neuron* 42.6 (2004): 961-972.
33. Wood, Marcelo A., et al. "A transcription factor-binding domain of the coactivator CBP is essential for long-term memory and the expression of specific target genes." *Learning & Memory* 13.5 (2006): 609-617.
34. Hsieh, Jenny, et al. "Histone deacetylase inhibition-mediated neuronal differentiation of multipotent adult neural progenitor cells." *Proceedings of the National Academy of Sciences of the United States of America* 101.47 (2004): 16659-16664.
35. Ballas, Nurit, and Gail Mandel. "The many faces of REST oversee epigenetic programming of neuronal genes." *Current opinion in neurobiology* 15.5 (2005): 500-506.
36. Abrajano, Joseph J., et al. "REST and CoREST modulate neuronal subtype specification, maturation and maintenance." *PloS one* 4.12 (2009): e7936.
37. Dallman, Julia E., et al. "A conserved role but different partners for the transcriptional corepressor CoREST in fly and mammalian nervous system formation." *Journal of Neuroscience* 24.32 (2004): 7186-7193.
38. Bonasio, Roberto. "The role of chromatin and epigenetics in the polyphenisms of ant castes." *Briefings in functional genomics* 13.3 (2014): 235-245.
39. Hölldobler, Bert, and Edward O. Wilson. *The ants*. Harvard University Press, 1990.
40. Robinson, Gene E. "Regulation of division of labor in insect societies." *Annual review of entomology* 37.1 (1992): 637-665.
41. Yan, Hua, et al. "Eusocial insects as emerging models for behavioural epigenetics." *Nature Reviews Genetics* 15.10 (2014): 677.
42. Gospocic, Janko, et al. "The neuropeptide corazonin controls social behavior and caste identity in ants." *Cell* 170.4 (2017): 748-759.
43. Yan, Hua, et al. "An engineered orco mutation produces aberrant social behavior and defective neural development in ants." *Cell* 170.4 (2017): 736-747.
44. Simola, Daniel F., et al. "A chromatin link to caste identity in the carpenter ant *Camponotus floridanus*." *Genome Research* (2012): gr-148361.
45. Mersch, Danielle P., Christine La Mendola, and Laurent Keller. "Camponotus fellah queens are singly mated." *Insectes Sociaux* 64.2 (2017): 269-276.

46. Rajakumar, Rajendhran, et al. "Ancestral developmental potential facilitates parallel evolution in ants." *Science* 335.6064 (2012): 79-82.
47. Bonasio, Roberto, et al. "Genomic comparison of the ants *Camponotus floridanus* and *Harpegnathos saltator*." *science* 329.5995 (2010): 1068-1071.

## **CHAPTER 2: Epigenetic (re)programming of caste-specific behavior in the ant *Camponotus floridanus***

*From Simola, Daniel F., et al. "Epigenetic (re) programming of caste-specific behavior in the ant Camponotus floridanus." Science 351.6268 (2016): aac6633. Reprinted with permission from AAAS.*

*Figures 1 – 5 were conducted by Riley Graham, Daniel Simola, and Cristina Brady.*

*Figures 6 – 8 were conducted by Daniel Simola with input from Riley Graham.*

*Figures 9 – 10 were conducted by Riley Graham with input from Daniel Simola and Cristina Brady.*

### **Background**

Eusocial insects organize themselves into behavioral castes whose regulation has been proposed to involve epigenetic processes, including histone modification. In the carpenter ant *Camponotus floridanus*, morphologically distinct worker castes called Minors and Majors exhibit pronounced differences in foraging and scouting behaviors. We found that these behaviors are regulated by histone acetylation likely catalyzed by the conserved acetyltransferase CBP. Transcriptome and chromatin analysis in brains of scouting Minors fed pharmacological inhibitors of CBP and histone deacetylases (HDACs) revealed hundreds of genes linked to hyperacetylated regions targeted by CBP. Majors rarely forage, but injection of a HDAC inhibitor or small interfering RNAs against the HDAC *Rpd3* into young Major brains induced and sustained foraging in a CBP-dependent manner. Our results suggest that behavioral plasticity in animals may be regulated in an epigenetic manner via histone modification.

Colonies of eusocial insects organize themselves into castes comprising individuals that exhibit specific behaviors over extended periods of time. This colony division of labor (DoL) is a key adaptation responsible for the ecological and evolutionary success of eusocial insects<sup>1-4</sup>. Different eusocial species have evolved unique strategies for regulating the expression of behavioral castes on the basis of age, morphology, and social context. The most fundamental examples of DoL involve the differentiation of individuals into sterile (worker) and reproductive (queen) castes. In addition, workers often express a variety of specialized behaviors depending

on age (e.g., the honey bee *Apis mellifera*<sup>2</sup>), body size (e.g., the fire ant *Solenopsis invicta*<sup>5</sup>), or both (e.g., formicid ants<sup>1-4,6</sup>).

The principles underlying the social control of behavior and the corresponding molecular mechanisms that regulate individual behavioral plasticity have been studied primarily in solitary species, such as the fly *Drosophila*<sup>7</sup>. Recently, obligately social insects, including the eusocial honey bee *A. mellifera* and carpenter ant *Camponotus floridanus*, have emerged as models of more complex behavior<sup>8-10</sup>. Findings in these species suggest that epigenetic processes, including DNA methylation<sup>11-15</sup>, and histone posttranslational modifications (hPTMs)<sup>16</sup>, may play key roles in regulating caste-based behavioral plasticity.

### **C. floridanus workers exhibit caste-specific behaviors**

To investigate the role of hPTMs in regulating ant behavioral castes, we studied *C. floridanus*<sup>12</sup>, which expresses two distinct female worker caste morphologies, called Minors and Majors (Fig 1A, right). These morphs are distinguished by head width and length of scape (basal antennal segment; a proxy for body size) and are produced in a 2:1 ratio of Minors to Majors in mature colonies. Although genetic factors may contribute to the quantitative variation in worker morphology the production of Minor and Major castes per se is likely not caused by allelic variation. Rather, workers are genetically related supersisters ( $r = 0.75$ ) resulting from a single diploid mother mating with a single haploid father<sup>17</sup>. Further, treatment of undifferentiated larvae with the DNA methylation inhibitor 5-aza-2'-deoxycytidine (5-aza-dC) increases head width and scape length in the resulting adults<sup>15</sup>.

A survey of hPTMs in *C. floridanus* indicated that several hPTMs, especially the acetylation of Lys<sup>27</sup> on histone H3 (H3K27ac), have distinct genome-wide patterns in the bodies and brains of Minors and Majors<sup>16</sup>. These differences can be attributed to differential localization of the conserved acetyltransferase and transcriptional coactivator CBP [cyclic adenosine monophosphate response element-binding protein (CREB) binding protein] in each caste, and they correspond to differences in gene expression<sup>16</sup>. In addition, a functional histone deacetylase

inhibitor (HDACi), the fatty acid 10-HDA, is a key component of royal jelly, an environmental regulator of queen production in honey bees<sup>18</sup>. Taken together, these findings suggest that hPTMs influence the generation of distinct castes in eusocial insects and that histone acetylation might regulate caste-based behavioral plasticity.

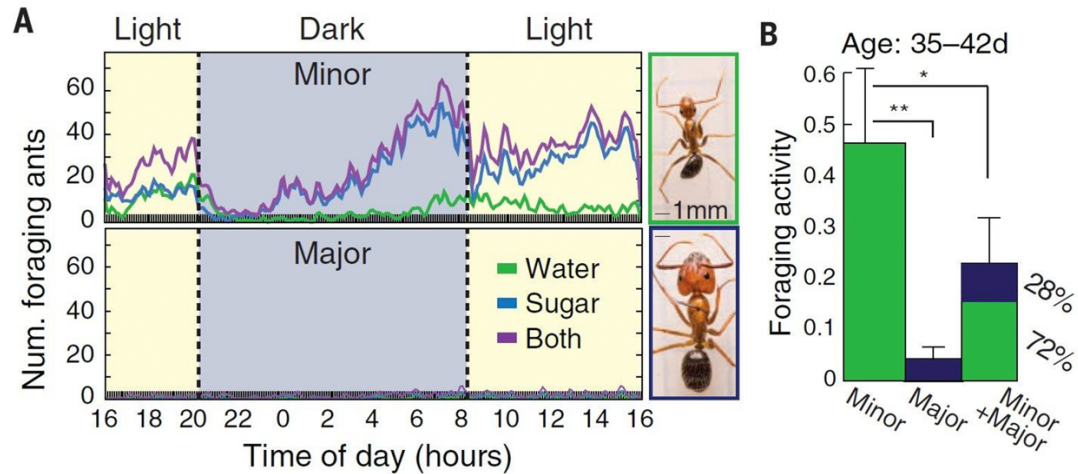


**Figure 1: Foraging is a strong caste-biased behavior in Minors**

(A) Circadian foraging activity for Minor (top) and Major (bottom) workers in a single monogamous colony. Photographs show representative Minor and Major workers (fig. S1, A and B). (B) Average foraging activity (defined in fig. S2A)  $\pm$  SE for 35- to 42-day-old Minors and Majors isolated and sugar-starved for 24 hours; rightmost column shows foraging activity for mixed cohorts of 10 Majors and 10 Minors of the same age.

To examine caste-based behavioral plasticity in *C. floridanus*, we fitted the nest of a 7-year-old queen-right (i.e., containing a queen) colony with a foraging arena and counted the number and caste of each ant that foraged out to feed on water or 20% sugar water over 24-hour periods (see Materials and Methods)<sup>19</sup>. Minors performed the vast majority of foraging, with a distinct circadian pattern and preference for sugar water (Fig. 1A). To control for effects of social interactions, we isolated 1-day-old ants and monitored their foraging behavior either in isolation for 10 days or when mixed with older, mature workers for 4 months. In both cases, Minors were the predominant foragers. To determine whether caste-based foraging may be a generic feature of *Camponotus* ants, we also assayed the sympatric species *C. tortuganus*. In both species,

Minors foraged but Majors did not, indicating that Minor and Major *Camponotus* workers display natural differences in foraging behavior<sup>20-22</sup>.

Age correlates with behavioral plasticity in eusocial insects, including other *Camponotus* species<sup>22</sup>. We therefore marked 1-day-old callows on a weekly basis in several queen-right colonies. We analyzed equal-sized cohorts of workers with identical colony background, caste morphology, and age ( $\pm 48$  hours) in an assay where either Minors or Majors were isolated from their natal nest and were water-starved (i.e., by withholding sugar) for 24 hours before foraging. Under these stringent conditions, Minors showed significantly greater foraging activity than age-matched Majors, although Majors did forage at a low rate (Fig. 1B). Moreover, mixed cohorts of age-matched Minors and Majors displayed lower foraging activity than Minors alone, yet only 28% of foraging was attributed to Majors (Fig. 1B).

Additionally, we analyzed foraging behavior as a function of starvation time, because Majors are physically larger and may have twice the food storage capacity of Minors. Majors required more than 9 days of starvation to match the foraging activity of Minors starved for only 24 hours (Mann-Whitney U test,  $P < 0.01$ ). Thus, Minors appear to be the predominant foragers

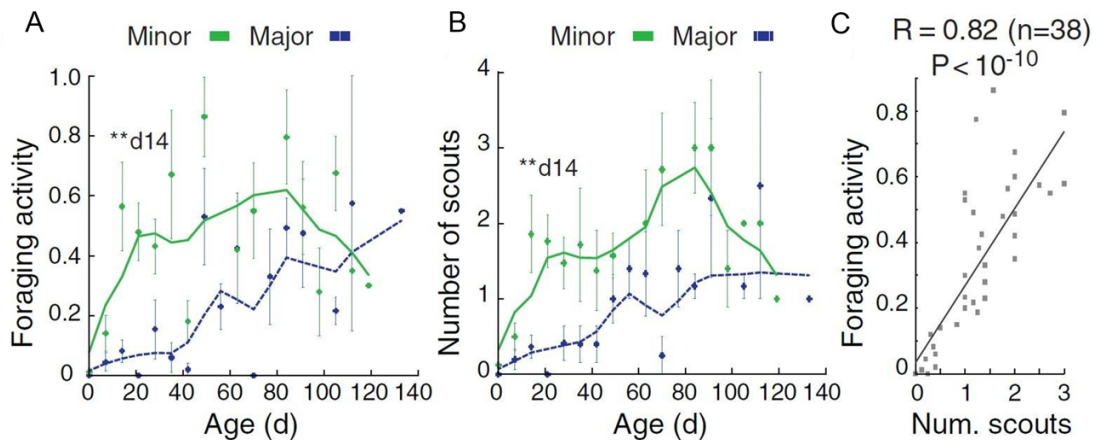


**Fig. 2: Foraging is influenced by caste identity and aging**

Foraging activity (A) and number of scouts (B) for Minors and Majors isolated and sugar-starved for 24 hours, as a function of adult age. Error bars denote SE over at least five independent replicates from six colonies. The earliest age of significant caste-differential behavior (day 14) is noted. Asterisks in (B) to (D) denote significance by Mann-Whitney U test: \* $P < 0.05$ , \*\* $P < 0.01$ . (E) Number of scouts versus foraging activity for data in (C) and (D). Pearson correlation coefficient is shown.

in queen-right colonies (Fig. 1A) as well as in young and mature (Fig. 1B) worker cohorts.

We also examined how caste and age affect the lead foragers, called scouts, which have been reported to constitute a distinct behavioral caste in a few eusocial species<sup>1, 20, 21, 23</sup> (see below). Scouts are the first ants to leave a nest, discover a food source, and return to the nest with this food, before recruiting additional ants to forage. Analysis of the number of scouts and foraging activity over 4 months revealed both caste- and age-based differences (Fig. 2, A and B). Minors exhibited significantly more foraging and scouting activity than did Majors by 14 days of age (Fig. 2, A and B). Also, the foraging speed of 60-day-old scouts was greater than that of 7-day-old scouts by as much as a factor of 6. We exclusively assayed ants that were naïve to a foraging arena, so these effects are not due to learning. Finally, the number of scouts in a cohort correlated strongly with the cohort's foraging activity (Fig. 2C); this finding suggests that scouts, which are predominantly Minors, determine a cohort's overall foraging activity<sup>24</sup>.

These results indicate that foraging and scouting behaviors in *C. floridanus* depend on caste morphology, age, and social context, consistent with observations in other ant species<sup>1-3, 20-23</sup>. They also support the view that eusocial species that express polymorphic worker castes have the potential for greater colony-level behavioral complexity than species with a monomorphic worker caste, as caste morphology apparently provides an additional dimension of behavioral variation that can be controlled by colonies to optimize division of labor<sup>1-4, 22</sup>.

### **Histone deacetylases inhibit foraging and scouting behaviors**

Minors always foraged and scouted more than Majors, regardless of age and social context; this observation is consistent with the idea that Minors and Majors harbor innate, molecularly determined differences that influence behavior. Given results suggesting a functional role for histone acetylation in determining caste-specific traits<sup>16</sup>, we examined whether foraging behavior might be regulated by histone acetylation dynamics controlling gene transcription.

We first measured mRNA abundance in brains of young, age-matched Minors and Majors from the same colony for the five class I and II HDACs encoded in the *C.*

*floridanus* genome. Orthologs of these genes have established roles in neuronal and behavioral plasticity in other insects and mammals <sup>25-27</sup>. Both *Rpd3/Hdac1a* (a putative H3K27ac deacetylase) and *Hdac6* showed caste-specific expression patterns (Student's *t* test,  $P < 0.003$ ).

We confirmed that both *Rpd3* and *Hdac6* transcripts also increased with age in Minors and Majors, using 25 brains evenly sampled from five colonies for each caste and age point ( $n = 100$  brains total; Fig. 3A, 3B). These observations are consistent with specific HDACs influencing foraging behavior, either via age-dependent decreases in histone acetylation or via increased histone acetylation dynamics, as has been observed for *Rpd3* in *Drosophila* <sup>25</sup>.

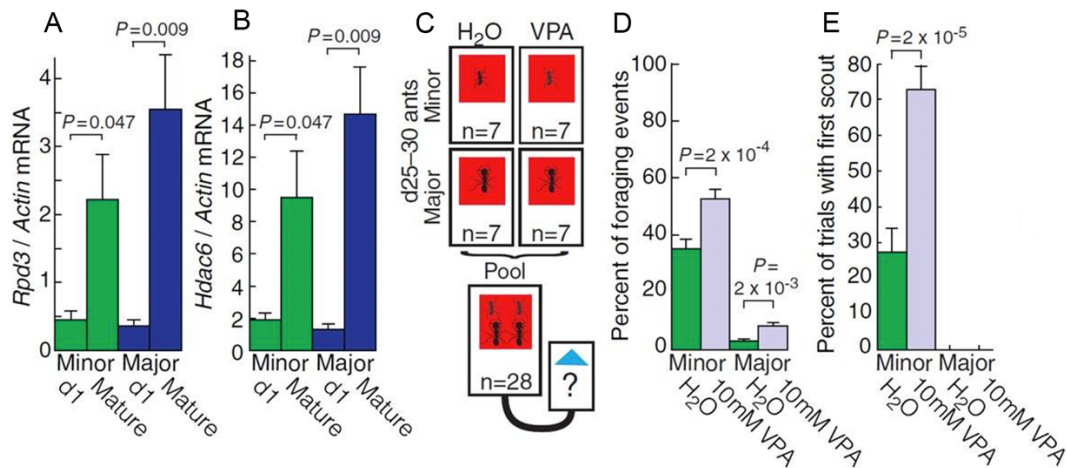


**Fig. 3: HDAC inhibition stimulates foraging and scouting behaviors.**

(A) RT-qPCR analysis of mRNA abundance for *Rpd3* (*Hdac1a*) and (B) *Hdac6* in young (1 day old) and mature (>30 days old) Major and Minor brains. Bars indicate the mean  $\pm$  SE over five colonies, where each measurement represents a pooled sample of five brains ( $n = 100$  brains total). mRNA abundance was normalized against actin. P values were computed by Mann-Whitney U test. (C) Schematic of foraging assay for VPA-treated ants. Cohorts of 28 Minors and Majors, age 25 to 30 days, were fed 20% sugar water with or without 10 mM VPA for 30 days (seven ants in four treatment groups). Ants were then pooled, sugar-starved for 24 hours, and assayed for foraging after attaching a foraging arena. Blue triangle denotes sugar water food source. (D) Average percent of all foraging events performed by untreated or VPA-treated Minors or Majors when pooled as in (C). (E) Average percent of trials in which the first scout that foraged and fed on sugar water had been provided sugar water alone or with VPA.

We then examined foraging and scouting behaviors after inhibiting the activity of class I and II HDACs by feeding workers a small-molecule HDACi, valproic acid (VPA) <sup>28</sup>. As expected <sup>28,29</sup>, VPA treatments increased global levels of H3K27ac when fed to larvae and Minors (Student's *t* test,  $P < 0.02$ ). We fed non-lethal concentrations of 10 mM VPA <sup>28,29</sup> to mixed cohorts

of 25- to 30-day-old Minors and Majors for 30 days. Foraging was assessed after pooling a treated cohort with a corresponding untreated cohort of colony- and age-matched Minors and Majors (Fig. 3C). Both VPA-treated Minors and Majors exhibited significantly more foraging than did controls (Fig. 3D). VPA-treated Minors were also the first to act as scouts by finding food in 73% of trials, whereas Majors never scouted (Fig. 3E). These results indicate that increasing histone acetylation shifts the behavior of both Minors and Majors toward increased foraging and feeding, although Minors remain the predominant foragers and scouts.

To confirm that increases in foraging activity elicited by VPA were due to HDAC inhibition, we used a second HDACi, Trichostatin-A (TSA), which has greater potency (i.e., inhibitory concentration,  $IC_{50}$ ) than VPA, as well as greater specificity toward histone substrates for inhibiting the removal of acetyl groups<sup>28,29</sup>. As with VPA treatments, we assayed foraging using 25- to 30-day-old workers. However, we repeatedly assayed foraging over 42 days (rather than once after 30 days), and we assayed treated and untreated cohorts of Minors separately (rather than mixed) to avoid any potential confounding effects due to social interactions.

In this assay, relative to controls, Minors fed TSA displayed significantly greater foraging activity in a dose-dependent manner (Fig. 4B). TSA also increased the number of scouts (Fig. 4C). Because only a minority of ants fed during a foraging trial, TSA does not appear to cause general locomotor hyperactivity. Furthermore, pharmacological treatment did not affect the correlation between foraging activity and the number of scouts ( $R=0.80$ ) relative to controls ( $R = 0.82$ ; Fig. 2C) nor did it affect the duration of a scout's return to the nest after feeding (expedition time) [Mann-Whitney U test,  $P<0.9$  for TSA versus dimethyl sulfoxide (DMSO)]. Also, TSA-treated Minors showed low mortality over the 42-day treatment course, which suggests that sickness and/or hunger are unlikely explanations for increased foraging and feeding. Hence, we conclude that HDAC activity normally inhibits foraging behavior in workers.

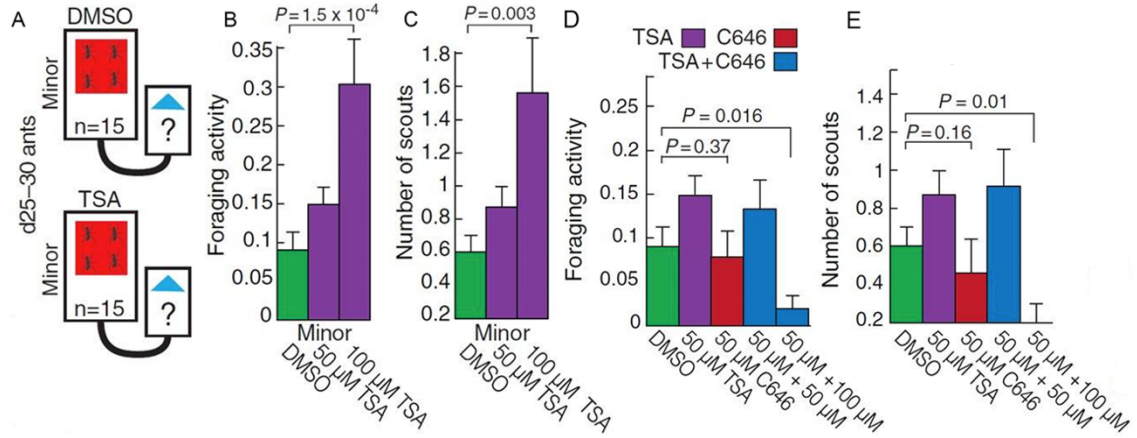


**Fig 4: HDACi stimulates foraging enhancement, CBP HATi represses foraging**  
 (A) Schematic of foraging assay for TSA-treated ants. Cohorts of 15 Minors, age 25 to 30 days, were fed 20% sugar water containing DMSO with or without 50  $\mu\text{M}$  or 100  $\mu\text{M}$  TSA for 42 days. Average foraging activity (B) and number of scouts (C) for DMSO- or TSA-treated Minor cohorts in foraging assay shown in (A). Cohorts were tested weekly over 42 days. Error bars denote SE over six measurements per cohort for 14 (DMSO) or 18 (TSA) independent cohorts from six colonies. P values were computed by Mann-Whitney U test. (D) Average foraging activity  $\pm$  SE and (E) number of scouts  $\pm$  SE for cohorts of 15 Minors isolated at age 25 to 30 days and continuously fed DMSO, 50  $\mu\text{M}$  TSA, 50  $\mu\text{M}$  C646, 50  $\mu\text{M}$  TSA + 50  $\mu\text{M}$  C646, or 50  $\mu\text{M}$  TSA + 100  $\mu\text{M}$  C646 ad libitum in 20% sugar water.

### CBP-dependent histone acetylation regulates foraging and scouting behaviors

Because of the reported correspondence between genomic regions of caste-specific hPTMs and CBP binding<sup>16</sup>, we tested whether the stimulation of foraging behavior by HDAC inhibition depends on stabilization or enhancement of hPTMs acetylated by CBP, such as H3K27ac. We thus used the small molecule C646, a specific inhibitor of CBP's histone acetyltransferase (HAT) activity (HATi) in mammals and insects<sup>30,31</sup>. CBP's mammalian paralog p300 is also targeted by C646, but it is not encoded in the *C. floridanus* genome.

Feeding 25  $\mu\text{M}$  C646 to larvae significantly decreased H3K27ac throughout the genome after global between-sample normalization (Wilcoxon signed-rank test,  $P < 10^{-20}$ ). In particular, C646 treatment significantly altered H3K27ac levels for more than 800 genes [ $\chi^2$  test, false discovery rate (FDR) < 0.05]. Genes affected most by C646 showed significant loss of H3K27ac (Mann-Whitney U test,  $P < 4 \times 10^{-4}$ ). These genes are enriched for a variety of functional terms pertaining to the structure, development, differentiation, and communication of neurons (Fisher's

exact test, FDR < 0.05). This suggests that C646 treatment, despite interfering with a pleiotropic pathway of gene regulation, preferentially inhibits genes with neuronal functions.

To test whether the increased foraging activity of HDACi-treated workers depends on the HAT activity of CBP, we fed 25- to 30-day-old Minors a cocktail of 50  $\mu$ M TSA together with either 50  $\mu$ M or 100  $\mu$ M C646 and assayed foraging behavior as above with TSA alone (Fig. 4D). Treatment with 50  $\mu$ M C646 did not significantly affect foraging or scouting, either alone or in combination with TSA (Fig. 4D, 4E). In contrast, treatment with 100  $\mu$ M C646 essentially blocked all foraging and scouting, despite the presence of TSA at a dosage that stimulated foraging alone (Fig. 4D, 4E). Indeed, delivering 100  $\mu$ M C646 alone was sufficient to inhibit scouting within 14 days of treatment (Mann-Whitney U test,  $P < 0.05$ ). Moreover, C646 had minimal, nonsignificant effects on scout expedition time and mortality, which suggests that it did not affect locomotion or induce severe toxicity. These results imply that HDACi-induced foraging is mediated by histone residues that are acetylated by CBP, such as H3K27ac<sup>32, 33</sup>.

Because foraging activity correlates strongly with the number of scouts, and because scouting is inhibited by C646, we reasoned that CBP may be required to induce workers to become scouts. To examine this, we assayed individually marked 25- to 30-day-old Minors in isolated cohorts. We found that the median duration of individual scouting behavior was 20 days, with some ants consistently scouting for the 49-day duration of the assay (Fig. 5A). Moreover, most of the workers that scouted (66%) emerged in the first 15 days (i.e., were 40 to 45 days old), rather than uniformly over time (Fig. 5B). Therefore, scouts likely represent a persistent behavioral caste expressed by select individuals in *C. floridanus*.

We tested whether the addition of C646 after 14 days of TSA treatment, after most scouts have already emerged (Fig. 5C), affected TSA-dependent increases in scouting and foraging. Indeed, addition of 100  $\mu$ M C646 after 2 weeks of 50  $\mu$ M TSA treatment by feeding failed to reverse increases in foraging and scouting (Fig. 5C, orange versus purple), in contrast to parallel treatment of 50  $\mu$ M TSA together with 100  $\mu$ M C646 (Fig. 5C, orange versus blue). These

results suggest that CBP, via its histone acetylation activity, may serve as a licensing factor to enable the transition of a worker into the scout behavioral caste. Moreover, the fact that the timing of C646 delivery appears to be critical to elicit the behavioral response suggests that loss of foraging is not due to the toxicity of C646 or its nonspecific effects on general locomotion.

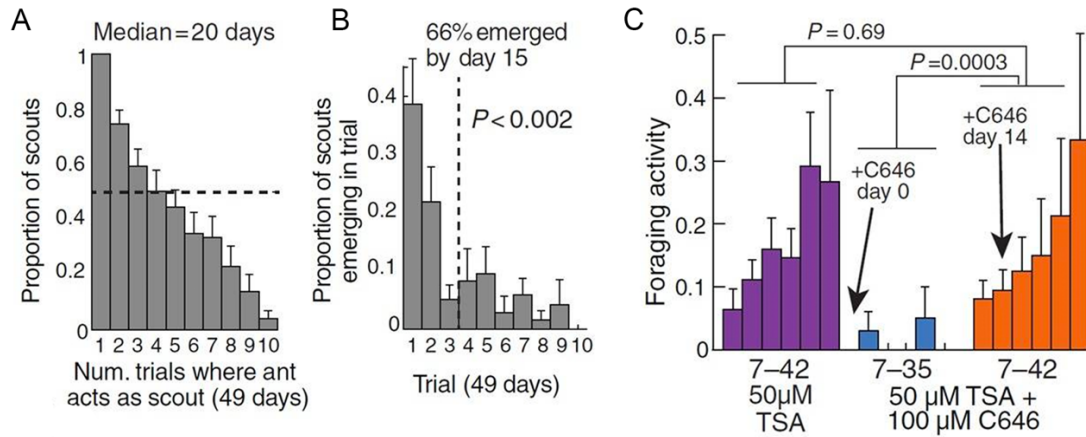


**Fig 5: CBP-dependent acetylation regulates foraging via scout production**

(A) Proportion of Minors that scouted for 1 to 10 consecutive foraging trials over a span of 49 days; an ant that scouted once acted as a scout for a median of 20 days (four trials, indicated by dashed line). (B) Distribution of the number of trials after isolation until an individual first scouted; dashed line indicates 15 days after isolation (three trials). Error bars in (A) and (B) denote SE over seven replicate cohorts of 15 Minors, age 30 to 35 days, from four colonies. P value in (B) is from a  $\chi^2$  test. (C) Average foraging activity  $\pm$  SE for individual trials per treatment group over 42 days. Orange bars represent trials in which C646 was provided starting 14 days after isolation and first administration of TSA; for blue bars, C646 was provided starting immediately upon isolation in parallel with TSA. Cohorts were tested weekly over 42 days. Error bars in (E) denote SE over six measurements per cohort and 14 (green), 6 (red), 18 (purple), 11 (blue), or 8 (orange) independent cohorts sampled from six colonies. P values were estimated by Mann-Whitney U test.

We then examined how the observed changes in behavior after treatment with TSA and C646 are associated with molecular changes. We analyzed genome-wide mRNA expression in individual brains dissected from 21 Minors sampled while feeding on sugar water during a scouting run<sup>19</sup>. Hierarchical clustering analysis of the 250 genes exhibiting greatest differential expression among treatments yielded two clusters of brain samples, a TSA-treated group and a DMSO-treated or TSA + C646-treated group, consistent with our behavioral analyses (Fig. 6C).

In contrast, random gene subsampling and analysis of internal spike-in control transcripts failed to partition samples by treatment group, as expected.

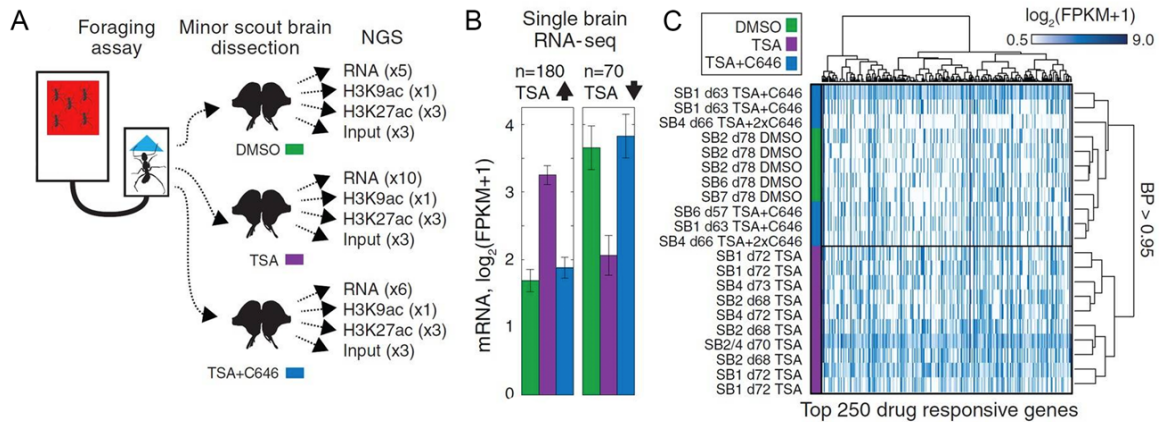


**Figure 6: HAT and HDACi inhibitors alter gene expression in scout brains**

(A) Schematic for genomics analysis. Minor scouts were sampled at the time of feeding in a foraging arena, and their central brains were dissected, homogenized, and analyzed by next-generation sequencing, with replication as indicated. (B) mRNA expression in brains of ~70-day-old Minor scouts for the 250 genes with the greatest alteration between TSA treatment and DMSO or TSA + C646 treatment ( $n = 21$  samples). FPKM denotes fragments per kilobase of transcript per million mapped reads. Left: Average ( $\pm$ SE) mRNA expression of these 250 genes. Right: Hierarchical clustering of samples for the 250 genes, using Mahalanobis distance and Ward's agglomeration criterion. P values were computed by bootstrap (19); BP, bootstrap probability.

Most of the top 250 differentially expressed genes (72%) were up-regulated with TSA (Fig. 6B, left), consistent with an overall increase in histone acetylation due to TSA and overall decrease in CBP-mediated acetylation due to C646. Gene ontology analysis of the 101 genes with significant differential expression (Bonferroni  $P < 0.05$ )<sup>19</sup> revealed enrichment for hormone signaling, dendrite morphogenesis, synaptic transmission, and sphingolipid biosynthesis (Fisher's exact test,  $P < 0.01$ ) as processes responsive to chromatin regulation<sup>25, 33, 34</sup>. These results argue that inhibition of HATs and HDACs by chronic feeding of small-molecule inhibitors may affect the expression of specific genes in the ant central brain.

To assess whether TSA and C646 affect brain gene expression via alterations in chromatin structure, we performed chromatin immunoprecipitation sequencing (ChIP-seq) for H3K27ac and H3K9ac, two hPTMs implicated in neuronal and behavioral plasticity<sup>27,35</sup> using tissue from nine of the scout brains also used for RNA-seq. We normalized these data using input

lysate as well as internal spike-in lysate (ChIP-Rx) from the evolutionarily divergent ant *H. saltator*<sup>12, 19, 36</sup>.

We identified regions of interest (ROIs) that were differentially marked by H3K9ac or H3K27ac between DMSO and TSA treatments (dmROIs). These dmROIs covered 0.33% (H3K9ac) and 1.5% (H3K27ac) of the genome, respectively, and predominantly occurred in noncoding regions (~90%). Notably, dmROIs exhibited both gains and losses in histone acetylation in TSA-treated samples possibly from acclimation to chronic treatment.

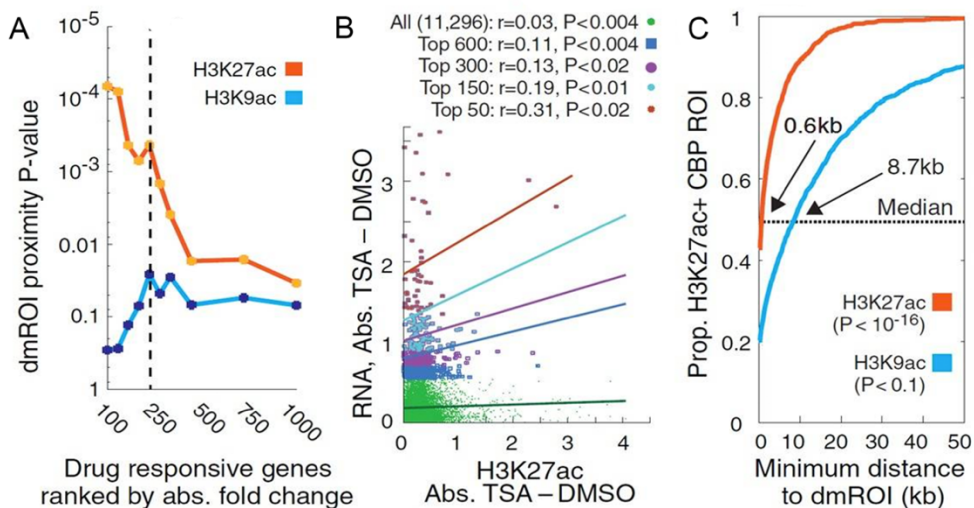


**Figure 7: H3K27ac dmROIs exhibit close proximity to TSS's and CBP binding sites** (A) P values for H3K27ac and H3K9ac dmROIs reflect proximity to gene transcription start sites (TSSs) ranked by absolute differential expression compared to randomly selected genes; P values were computed by Mann-Whitney U test (19). (B) Absolute change in a gene's TSS-proximal H3K27ac dmROI versus absolute change in mRNA level between TSA and DMSO samples, binned by magnitude of differential expression (top 50, 150, 300, and 600 genes). Lines denote linear regression trendlines for each group. Pearson correlation coefficients are shown; P values were computed by Student's t test. (C) Distributions of minimum distance from a dmROI to an H3K27ac-positive CBP binding site for H3K27ac and H3K9ac dmROIs. P values were computed by Mann-Whitney U test with randomly sampled ROI coordinates (n = 250 trials).

We then assessed whether dmROIs occur near differentially expressed genes. Indeed, dmROIs for H3K27ac were significantly enriched among the top 500 differentially expressed genes, with the greatest significance for the top 100 genes, whereas dmROIs for H3K9ac showed no significant enrichment near these genes (Fig. 7A). Furthermore, we found a mild but significant

correlation between the magnitude of a gene's differential expression and the differential enrichment of the nearest H3K27ac dmROI, with correlation coefficients increasing with differential expression ( $0.11 < R < 0.31$ ; Fig. 7B). These results are consistent with a chromatin-based model of gene regulation underpinning foraging behavior.

If CBP mediates the observed, drug-dependent changes in chromatin and gene expression, dmROIs should also cluster near binding sites for CBP<sup>16, 35</sup>. Using a genome-wide annotation of CBP binding sites<sup>16</sup>, we identified 3173 putatively active CBP sites with H3K27ac enrichment. Like dmROIs, these binding sites were also enriched near the top differentially expressed genes (Mann-Whitney U test,  $P < 0.001$  for the top 1000 genes). Furthermore, dmROIs for H3K27ac, but not H3K9ac, were proximal to H3K27ac-positive CBP binding sites (median distance of 0.6 kb versus 8.7 kb from center of CBP site; Fig. 7C). Lastly, 475 H3K27ac dmROIs showed overlap with CBP sites by at least 50%. These data suggest that chronic drug treatment may induce both direct and indirect effects involving multiple histone residues and multiple regulatory factors<sup>30-33</sup>. Taken together, these results are consistent with our prior observation of differential H3K27ac in the brains of Minors and Majors<sup>16</sup> and suggest that CBP may modulate foraging behavior in workers in part by regulating histone acetylation levels at specific genomic loci in the brain.

### **HDAC inhibition induces and sustains Minor-like foraging behavior in Majors**

We next sought to discern why Minors and Majors are differentially predisposed to forage (Fig. 1) and why Majors treated with HDAC inhibitors forage and scout less than Minors. Given that CBP regulates the production of scouts (an age-based caste), we reasoned that differential activity of CBP and HDACs in the brains of young Minors and Majors might likewise establish behavioral states tied to morphological caste.

To evaluate this model, we first identified 160 genes that exhibited significant differential expression by caste in brains of 1-day-old workers from the same colony (Bonferroni  $P < 0.01$ ;

Fig. 8A)<sup>19</sup>. These caste-differential genes pertain to synaptic transmission, synapse structure, and neurotransmitter release (Fisher's exact test, FDR < 0.25). Furthermore, these genes were

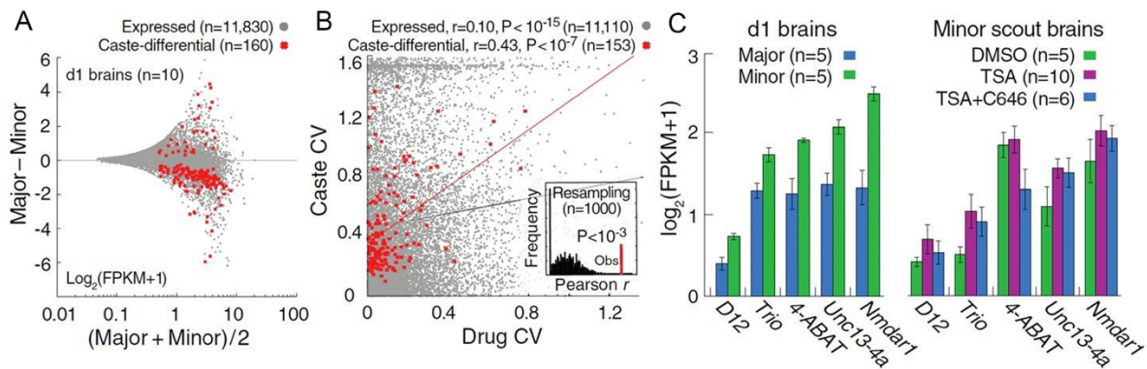


**Figure 8: Caste-specific genes are sensitive to HDACi treatments**

(A) Differential versus average scatterplot comparing mRNA levels for brains dissected from individual 1-day-old Majors and Minors ( $n = 5$  per caste) from one colony. Caste-differential genes were identified by Mann-Whitney U test ( $P < 0.05$ ) and gene-specific SE (Bonferroni  $P < 0.01$ ). (B) Scatterplot comparing coefficients of variation (CVs) in gene expression between drug treatments and caste. Pearson correlation coefficients are shown. Inset shows correlation coefficients for 1000 random sets of 153 genes sampled from 11,110 expressed genes. (C) mRNA levels for select caste-differential genes in 1-day-old worker brains (left) and Minor scout brains (right). Error bars denote SE among biological replicates. 4-ABAT, 4-aminobutyrate aminotransferase; Unc13-4a, mammalian uncoordinated homology 13, 4a ortholog.

particularly responsive to TSA and C646 treatments in mature Minor scout brains

(Student's  $t$  test,  $R = 0.43$ ,  $P < 10^{-7}$ ; Fig. 8B)—a trend also seen for the entire transcriptome

( $R = 0.10$ ,  $P < 10^{-15}$ ) but not for random gene subsets (99.9%; Fig. 8B, inset).

Among these jointly caste- and drug-responsive genes were those encoding D12, a component of the ATAC HAT complex<sup>27</sup>; Rho guanosine triphosphate exchange factor Trio, which regulates dendrite morphogenesis<sup>38</sup>; and *N*-methyl-D-aspartate receptor (NMDAR) 1, which regulates olfactory learning and memory<sup>39</sup> (Fig. 8C). These observations are consistent with a classic response threshold model<sup>10</sup> whereby caste-specific behavioral states are established with chromatin regulatory factors, which suppress behavioral plasticity by regulating genes that modulate the brain's sensitivity to environmental cues, in turn contributing to stable neuroanatomical differences between behavioral castes<sup>40,41</sup>.

Because caste-specific foraging appears to become more pronounced with age (and correspondingly with social experience) (Fig. 9, gray bars), we further hypothesized that Majors may be most sensitive to TSA immediately after eclosion, prior to the establishment of molecular barriers that restrict behavioral plasticity. Unfortunately, 1-day-old workers did not scout after starvation and hence could not receive TSA by feeding. We therefore developed a technique to deliver controlled treatment doses directly to ant brains by micro-injection (Fig. 9). Remarkably, injecting 1  $\mu$ l of 50  $\mu$ M TSA onto newly eclosed Major brains robustly stimulated foraging activity despite the presence of untreated age-, colony-, and group size-matched Minor nestmates.

Over 10 days, Majors injected with TSA upon eclosion consistently foraged more than did Majors injected with DMSO (Mann-Whitney U test,  $P < 6 \times 10^{-6}$ )—and at levels similar to untreated Minor nestmates ( $P < 0.13$ ; Fig. 9). These results suggest that inhibiting HDAC activity in young Majors is sufficient to mitigate chromatin-based barriers that restrict caste-based behavioral plasticity.

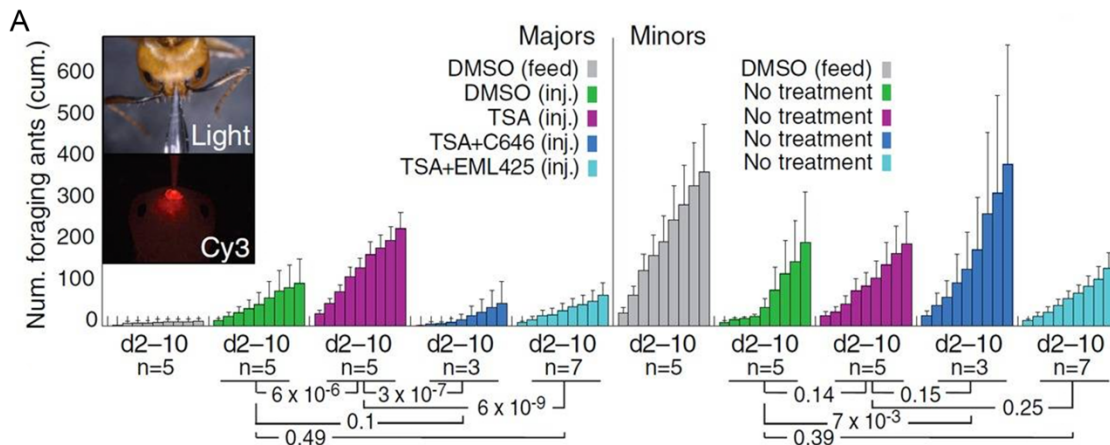


**Figure 9: HDACi injections in newly eclosed Majors induces Minor-like foraging**  
 (A) Cumulative foraging over the course of 9 days for pooled cohorts of Minor and Major nestmates, measured by time-lapse photography every 6 min. Uninjected cohorts were fed 20% sugar water containing 0.5% DMSO. Error bars denote SE over replicate cohorts. See table S5 for colony background and mortality information. Photograph insets depict brain injection procedure.  $P$  values were estimated by Mann-Whitney U test using counts of daily foraging events.

In contrast, Majors injected with 50  $\mu$ M TSA and 100  $\mu$ M C646 largely failed to forage (Fig. 9, dark blue), consistent with the observed effects of these drugs when fed to mature Minors

(Fig. 4D, dark blue). To confirm that suppression of foraging by C646 was not due to off-target effects, we applied a second HAT inhibitor of CBP, EML425, which functions by a different mechanism than C646<sup>42</sup>; again, Majors injected with 50  $\mu$ M TSA and 100  $\mu$ M EML425 exhibited little foraging (Fig. 9, light blue).

We also examined the long-term effects of these brain injections within our starvation-based foraging assay. Remarkably, 30 to 50 days after the single-injection treatments, TSA-injected Majors still displayed significantly increased foraging activity, and with more scouts, than did age- and colony-matched Majors injected with DMSO (Mann-Whitney U test,  $P < 0.05$ ) or TSA + C646 ( $P < 0.01$ ; Fig. 10A). In contrast, untreated Minor nestmates showed no significant differences in foraging among treatment groups (Fig. 10A). Taken together, these findings indicate that CBP is a likely epigenetic factor involved in establishing and maintaining morphological and age-dependent behavioral castes.

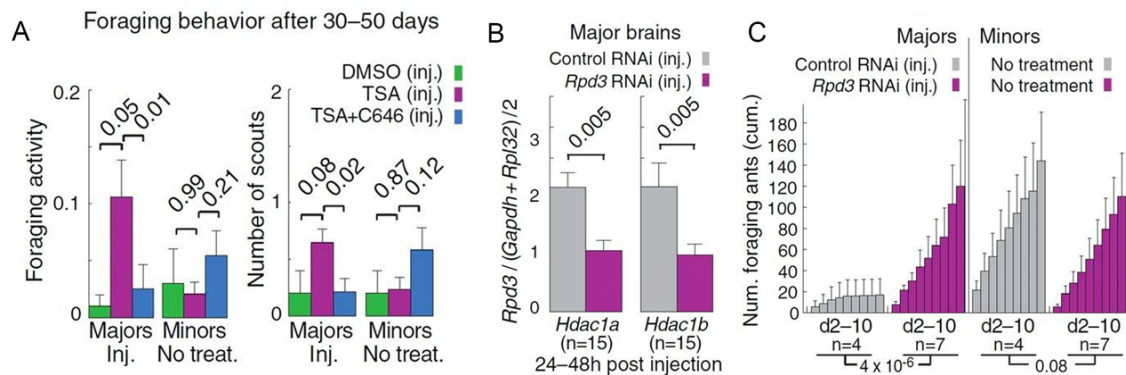


**Figure 10: Stable behavioral reprogramming by HDACi and RNAi targeting RPD3**

(A) Long-term assessment of foraging activity (left) and number of scouts (right) for the same injected Majors and control Minors from Figure 10. (B) RT-qPCR analysis of mRNA abundance for *Rpd3* (*Hdac1a* and *Hdac1b*) in Major brains 24 to 48 hours after injection with nontargeting (control) RNAi or *Rpd3* RNAi. Each bar indicates the mean  $\pm$  SE over measurements from 15 brains. Abundance was normalized against *Gapdh1* and *Rpl32* (C) Cumulative foraging over the course of 10 days for pooled cohorts of Minors and Majors, as in Figure 10.

Finally, we developed and applied a transient RNA interference (RNAi) technique<sup>19</sup> to examine whether Minor-like foraging may be induced in Majors by specifically inhibiting *Rpd3/Hdac1* mRNA. *Rpd3* was selected because it encodes a class I HDAC putatively targeted

by TSA and because its mRNA abundance increased with age in *C. floridanus*. RPD3 also deacetylates residues acetylated by CBP, such as H3K27ac<sup>32</sup>. Injection of 27-nucleotide double-stranded small interfering RNA (siRNA) oligos against the *Rpd3* and *Rpd3*-like transcripts into 1-day-old Major brains led to a factor of 2 reduction in their mRNA levels in the central brain after 24 to 48 hours, relative to injection of nontargeting control double-stranded siRNAs (Fig. 10B). Moreover, *Rpd3* RNAi induced Minor-like foraging in injected Majors (Fig. 10C) This result suggests that RPD3 normally acts to repress foraging in *C. floridanus* workers by removing acetyl groups from histones catalyzed by CBP.

Our examination of foraging behavior as a caste-specific trait in the ant *C. floridanus* sheds light on a fundamental question in sociobiology regarding molecular determinants of division of labor in eusocial insects<sup>1</sup>. Whereas recent studies have brought increasing attention to the role of genetic variation in caste specification<sup>2,8,9,43</sup>, our findings implicate the histone-modifying enzymes RPD3/HDAC1 and CBP as licensing and reprogramming factors underlying morphology and age-dependent social behaviors, hence revealing a key role for chromatin-based regulation of behavioral castes. *C. floridanus* colonies express two distinct morphological worker castes, Minors and Majors, and our results show that Minors perform the majority of foraging and scouting for a colony (Fig. 1). HDACi-induced changes in CBP-dependent histone acetylation in the brains of mature Minors reinforce and accentuate foraging and scouting<sup>3</sup>. In scouting ants, these behavioral changes correspond to altered transcript abundance of select neuronal genes with specific roles in synaptic transmission and olfactory learning, and to changes in histone acetylation that occur near CBP binding sites proximal to these genes.

Remarkably, the delivery of a single dose of HDACi or RNAi against *Rpd3* in Major brains immediately after pupal eclosion is sufficient to overcome the intrinsic molecular barriers that normally inhibit Major foraging and scouting. Hence, regulation of caste-specific social behaviors involves an epigenomic landscape that remains plastic for a period of time after eclosion. This

malleability appears to permit drug-and RNAi-mediated up-regulation of genes that are inherently expressed at lower levels in Majors, resulting in “transdifferentiation” between behavioral castes.

Epigenetic control over behavioral castes, and thus division of labor, may allow colonies to adapt dynamically to drastic ecological changes within their lifetime—for example, in response to prolonged famine or colony predation, which can alter caste ratios<sup>13</sup>. Hence, our findings may be broadly relevant to other eusocial insects that display age-based or caste-based division of labor. Further, our results suggest that CBP and HDACs might help to establish complex social interactions for other invertebrate, vertebrate, and mammalian species, in which these conserved enzymes are known to play critical roles in the regulation of behavioral plasticity as well as in learning and memory<sup>27-29,44,45</sup>. Finally, our ability to alter a canonical altruistic behavior in a truly social organism by experimental perturbation of a single gene suggests that the application of increasingly versatile reverse genetic approaches in eusocial insects will allow us to expose the general organizational principles underlying complex social systems<sup>10</sup>.

## **Materials and Methods**

### **Ant colonies and husbandry**

Mature, queen-right colonies of *C. floridanus* and *C. tortuganus* were used in this study, collected as foundresses from Long Key and Sugar Loaf Key in the Florida Keys, USA, in 2007 and 2011. Colonies were maintained in a sealed environmental growth chamber at constant temperature (25°C) and humidity (50%) under a 12:12 light: dark cycle. Colonies were fed twice weekly with excess supplies of water, 20% sugar water (sucrose cane sugar), and Bhatkar-Whitcomb diet<sup>46</sup>.

### **Caste and age identification**

Adult morphological caste was identified by body size and head width. For calibration, head width and scape (basal antennal segment) length (a proxy for body size) were measured using a digital micrometer (Fisher Scientific FB70252) and stereo-microscope (Nikon SMZ-1500)

for 377 workers. A worker was considered a Major if her head width exceeded 2.25 mm and a Minor if under 1.75 mm. Age was determined by marking gasters of 1-day-old callows with enamel paint. One-day-old ants were identified by their location among brood in the nest, their general behavior, and their light cuticle coloration (compared to a reference panel of ants aged from pupation through 30 days).

### **Foraging assays and analyses**

Three assays were used for analysis of foraging behavior. In the whole-colony foraging assay, a foraging arena was attached to a mature (7.5-year-old) queen-right colony containing more than 4000 workers. Petri dishes containing 15 ml each of pure water ( $\times 2$ ) or 20% sugar water ( $\times 2$ ) were placed in the arena. The arena was photographed every 3 min continuously for periods of 24 hours. For each photograph, the time of day and number of Majors and Minors feeding from water and sugar water dishes were recorded.

In the piggyback foraging assay, worker cohorts were isolated from single colonies (with specified caste, age, and number) and placed into a “piggyback” nest box. A 1.5-ml Eppendorf tube containing 20% sugar water was placed in the arena on the wall opposite the arena entrance. The arena was photographed every 6 min continuously for periods of 24 hours over the course of 10 days. The time and caste of each ant that fully entered into the foraging arena was recorded and analyzed blindly. Idle ants that spent more than 30 min in the arena without feeding on sugar or departing from the foraging arena were not counted.

In the starvation-induced foraging assay, worker cohorts were isolated from single colonies as above and placed into “standard” 195c nest boxes. Seven larvae (instar 2 to 4) were included to facilitate acclimation to the new nest. A 1.5-ml Eppendorf microcentrifuge tube containing 20% sugar water was provided and replaced weekly. Twenty-four hours prior to assay, the tube of sugar water was replaced with a 1.5-ml tube containing ultrapure water filtered by Milli-Q (EMD Millipore). At assay time (14:00 to 17:00 hours), a foraging arena was attached to the 195c nest box, and a half weigh boat containing 500  $\mu$ l of 20% sugar water was placed within

the arena at the far side relative to the tube leading to the nest. Video recordings were made for each foraging trial lasting 70 to 75 min and were analyzed blindly.

Time and caste of each ant that entered the foraging arena from the nest and fed on (i.e., contacted and consumed) sugar water for at least 10 s (one feeding event) were recorded. An ant must have returned to the nest, then reentered the foraging arena and refeed to be counted again. Also, the time that the first feeding ant (a scout) returned to the nest (by descending beneath a piece of red acetate film covering a nest cavity) was recorded, as well as the number of scouts, defined as the number of individual ants feeding before the first scout returned to the nest. Scout expedition time was computed as the difference between the time the first scout returned to the nest and the time that she began to feed on sugar water. Quantitation of each foraging trial video recording was used to estimate a foraging activity statistic that summarized the foraging plus feeding rate of a worker cohort. This statistic was computed as the number of scouts plus the number of additional feeding events occurring within the first 20 min after the first scout's return to the nest.

### **Reverse transcription quantitative polymerase chain reaction (RT-qPCR) sample preparation and analyses**

Individual brains dissected from 1-day-old ants were rinsed in sterile phosphate-buffered saline solution (PBS) and transferred to 1.5-ml microcentrifuge tubes containing 500  $\mu$ l of ice-cooled PBS. Brain tissue was dissociated by sonication using a Diagenode Bioruptor Standard device for 30 s on low power. Total RNA was purified from individual brains by phenol:chloroform extraction and purification using RNase-free Agencourt AMPure XP beads (Beckman Coulter). cDNA was produced from total RNA using SuperScript III Reverse Transcriptase (Invitrogen). Abundance of specific mRNA transcripts was estimated using Power SYBR Green PCR Master Mix (Life Technologies) on a Real Time qPCR machine (Applied Biosystems 7900HT). Relative transcript abundance was estimated using the delta Ct method <sup>19</sup>.

### **Chromatin immunoprecipitation**

Chromatin lysate and subsequent immunoprecipitated double-stranded DNA (dsDNA) were prepared using antibodies recognizing H3K9ac (Active Motif 39137, Lot 102), H3K27ac (Abcam ab4729, Lot GR132150-4), and total H3 (Abcam ab1791, Lot GR135488-1) by processing larvae or adult ants as described <sup>16, 19</sup>.

### **Foraging assays for pharmacologically treated ants**

Analysis of VPA (Calbiochem) was performed using the starvation-induced foraging assay. For a single foraging trial, four groups of seven Minor or Major 25- to 30-day-old ants (age-matched within 72 hours) were isolated from a queen-right colony and placed into 28c nest boxes (seven ants in each of four boxes). VPA was dissolved in liquid Bhatkar (or no VPA as control) to final desired concentration and replaced daily for 32 to 42 days (depending on number of starvation days). After 32 days of treatment, all 28 ants were pooled into a common 195c nest box containing seven larvae (instar 2 to 4). The ants were starved with water for 24 hours, then assayed for foraging by attaching a 79c foraging arena and recording the time of every foraging and feeding event for each individual ant. If a cohort failed to exhibit a single feeding event within an hour of assay, the foraging arena was detached and the ants were starved for another 24 hours, for a maximum of 10 days. In the rare case of multiple feeding events by the same individual ant, only the first feeding event was recorded.

For TSA and C646 treatments, foraging assays were conducted using cohorts of 15 workers of the same age (within 48 hours) and colony. No larvae were provided, as the isolated ants were kept in the same 195c nest box for the duration of the trial. Pharmacological small molecules TSA (Sigma-Aldrich) and C646 (Calbiochem) were dissolved in DMSO and then in 20% sugar water to the desired final concentration. Ants were permitted to drink this solution ad libitum. Fresh aliquots were prepared from stock every 48 hours. During 24-hour starvation periods, fresh aliquots were prepared by dissolving a compound into water; otherwise, aliquots were dissolved in 20% sugar water. Each cohort was assayed for foraging activity 7, 14, 21, 28,

35, and 42 days after isolation, unless indicated otherwise. Foraging activity, number of scouts, and expedition time were computed as described above.

### **Preparation of RNA-seq libraries**

Whole brains were dissected from individual mature Minor scouts fed DMSO, 50  $\mu$ M TSA, or 50  $\mu$ M TSA with either 50  $\mu$ M or 100  $\mu$ M C646 for 45 days. Scouts were identified, sampled, and frozen on dry ice while feeding on sugar water after foraging, during a starvation-induced foraging assay. Each dissected brain was rinsed in PBS and transferred to a 1.5-ml microcentrifuge tube containing 100  $\mu$ l of prechilled PBS (on ice). Brain tissue was dissociated using a Diagenode Bioruptor Standard device for 30 s on low power. A 15- $\mu$ l aliquot representing 15% of cells in a single brain [estimated to be 20,000 to 25,000 cells <sup>47</sup>] was taken for RNA-seq; this represents a sufficient sampling of cells to recapitulate whole-brain transcriptome patterns and allows remaining cells to be processed for ChIP-seq.

Total RNA was purified by phenol:chloroform extraction and purification using RNase-free Agencourt AMPure XP beads (Beckman Coulter). 1  $\mu$ l of ERCC RNA Spike-In Mix (Ambion) was added to each 15- $\mu$ l aliquot of total RNA to facilitate transcript-level normalization relative to cell number and to control for technical variation during library preparation. The mRNA fraction of RNA was purified by selection for polyadenylated transcripts using oligo(dT)25 Dynabeads (Invitrogen) as described <sup>48</sup>, and RNA fragmentation was performed for 8 min at 94°C. cDNA was produced from total RNA using SuperScript III Reverse Transcriptase (Invitrogen), and second-strand synthesis was performed using deoxyuridine triphosphate (dUTP) to preserve strand specificity <sup>48</sup>. Strand-specific RNA-seq libraries were produced for these dUTP-incorporated dsDNA libraries after one round of linear amplification <sup>19</sup>.

RNA-seq libraries from individual 1-day-old Minor and Major brains were processed as above, except that whole brains were dissected from 10 1-day-old Minors and Majors sampled from the same colony at the same time and the same location in the nest. All 10 brains were

dissected in a single session; all RNA-seq libraries were prepared from the entire brain samples as a single batch; all libraries were bar-coded and sequenced on the same flowcell.

All libraries were prepared using the NEB NextUltra DNA Library Prep Kit for Illumina (New England BioLabs) and were amplified by PCR for 15 cycles, purified using Agencourt Ampure XP beads, and quantified by Qubit 2.0 Fluorometer (Invitrogen) and Kapa qPCR (Kapa Biosystems). Libraries were sequenced on an Illumina NextSeq 500 Desktop Sequencer.

### **Preparation of ChIP-seq libraries**

ChIP was performed on individual scout brains using 45  $\mu$ l of remaining cell material (60,000 to 75,000 cells) for a subset of the same brains used for RNA-seq (above). Chromatin was prepared as described <sup>16</sup>, except that brain tissue was cross-linked with formaldehyde for 5 min. Before immunoprecipitation, cross-linked chromatin prepared from pools of heads and thoraces from 1-day-old workers of the evolutionarily divergent ant *Harpegnathos saltator* was added to a final concentration of 2.5% by volume based on Qubit protein quantitation [ChIP-Rx (36)]. After mixing *C. floridanus* (75  $\mu$ g/IP) and *H. saltator* (1.88  $\mu$ g/IP) chromatin, immunoprecipitation was performed as described <sup>16</sup> using 1  $\mu$ g of antibody for H3K27ac or H3K9ac. dsDNA was purified from ChIP material as described <sup>16</sup>, and ChIP-seq libraries were prepared using the NEB NextUltra DNA Library Prep Kit for Illumina. Libraries were amplified by PCR for 15 cycles, purified using Agencourt Ampure XP beads, quantified by Qubit and Kapa qPCR, and sequenced on an Illumina NextSeq 500 Desktop Sequencer.

### **Analysis of RNA-seq and ChIP-seq data**

Sequenced reads were aligned to a diploid version of the *C. floridanus* reference genome v3.0 <sup>12</sup> after incorporating single-nucleotide polymorphisms (SNPs). This diploid reference was first split into two pseudo-haplotypes by randomly partitioning the two alleles at each SNP into two haploid genome sequences. Mapping was performed against each reference haplotype using Glimmr <sup>16</sup>, with calls to Bowtie2 <sup>49</sup> with options (`--end-to-end--very-sensitive`) and allowing each read to display valid alignment for up to 10 distinct genomic locations (`-k 10`). Mapped reads were

merged into a single alignment file by retaining the alignments for a given read that contained fewer mismatches to the particular reference haplotype. For RNA-seq, remaining unmapped reads were also aligned to a reference transcriptome containing full-length transcripts for annotated genes. Remaining unmapped reads were trimmed in an iterative manner from full-length 75-nt reads to 55-nt reads to 35-nt reads, where the 10 outer bases on either end of the read were removed at each step. Analysis of RNA-seq and CHIP-seq data are described in <sup>19</sup>.

### **Brain injection procedure**

Before eclosion, Major and Minor pupae were removed from their natal colony and reared in smaller nests by 15 adult Minors. In 24-hour intervals, newly eclosed callows were removed from rearing nests and organized into age-matched treatment groups containing 10 Majors and 10 Minors. Individuals were isolated in 1.5-ml microcentrifuge tubes and cooled on ice for up to 5 min until sedated. Major workers were moved to an ice-cooled silicone platform, and their cuticles were superficially perforated at the target injection site using a sterilized steel pin (Minutae, Sphinx). Immediately after perforation, a borosilicate glass needle filled with injection material was directed to the injection site using a robotic arm (Patchman N2, Eppendorf) and the needle tip was placed just beneath the surface of the cuticle to avoid damage to underlying tissue. A Femtojet microinjector (Eppendorf) delivered 1  $\mu$ l of injection material to the injection site. After injection, individuals were given 1 hour to recover before being assessed for morbidity and mortality. Successful injections were pooled in groups of 10 with age-matched Minors and placed into the test arena for behavioral analysis.

### **RNAi-mediated mRNA knockdown and analysis**

Individual Major brains were injected with a 1- $\mu$ l pool of 1  $\mu$ M each of two different 27-nt double-stranded siRNAs targeting *Rpd3* (Cflo\_10463) and *Rpd3-like* (Cflo\_10465) (*Rpd3* RNAi) or a 1- $\mu$ l pool of 1  $\mu$ M each of two different nontargeting control double-stranded siRNAs (Control RNAi) (19). Individuals were killed 24 or 48 hours after injection. cDNA libraries were prepared from individual dissected brains as described above. RT-qPCR was performed as described

above, using primers specific to Cflo\_10463 and Cflo\_10465 and to *Gapdh1* and *Rpl32* mRNAs (table S2). Quantitation was performed using the median quantity estimated based on fivefold dilution series of each primer. *Rpd3* quantities were normalized to the average of *Gapdh1* and *Rpl32* quantities as controls. *P* values were calculated by Mann-Whitney U test.

### **Brain injection piggyback foraging assay**

Cohorts of 10 Majors and 10 Minors, all 1 day old, were sampled from a single queen-right colony. Only Majors received brain injections with a fixed delivery volume of 1  $\mu$ l, containing 0.5% DMSO, 50  $\mu$ M TSA, or 50  $\mu$ M TSA with 100  $\mu$ M C646. For RNAi, Majors were injected with pools of 1  $\mu$ M 27-nt duplex RNA oligos (RPD3 or nontargeting controls). All injections were performed between 15:00 and 17:00 hours. After injection, Majors were placed with their Minor nestmates into a piggyback nest box with foraging arena containing a microcentrifuge tube with 1 ml of 20% sugar water. The arena was photographed every 6 min for 10 days; recorded photographs were analyzed blindly as described above.

## Chapter 2 Bibliography

1. Hölldobler B, Wilson EO. *The Ants*. Belknap/Harvard Univ. Press; Cambridge, MA: 1990.
2. Robinson GE. Regulation of division of labor in insect societies. *Annu. Rev. Entomol.* 1992;37:637–665. doi: 10.1146/annurev.en.37.010192.003225; pmid: 1539941.
3. Wilson EO. Behavioral discretization and the number of castes in an ant species. *Behav. Ecol. Sociobiol.* 1976;1:141–154. doi: 10.1007/BF00299195.
4. Fjerdingstad EJ, Crozier RH. The evolution of worker caste diversity in social insects. *Am. Nat.* 2006;167:390–400. doi: 10.1086/499545; pmid: 16673347.
5. Tschinkel WR. *The Fire Ants*. Belknap/Harvard Univ. Press; Cambridge, MA: 2013.
6. Lucas C, Sokolowski MB. Molecular basis for changes in behavioral state in ant social behaviors. *Proc. Natl. Acad. Sci. U.S.A.* 2009;106:6351–6356. doi: 10.1073/pnas.0809463106; pmid: 19332792.
7. Dulac C. Brain function and chromatin plasticity. *Nature.* 2010;465:728–735. doi: 10.1038/nature09231; pmid: 20535202.
8. Robinson GE, Grozinger CM, Whitfield CW. Sociogenomics: Social life in molecular terms. *Nat. Rev. Genet.* 2005;6:257–270. doi: 10.1038/nrg1575; pmid: 15761469.
9. Smith CR, Toth AL, Suarez AV, Robinson GE. Genetic and genomic analyses of the division of labour in insect societies. *Nat. Rev. Genet.* 2008;9:735–748. doi: 10.1038/nrg2429; pmid: 18802413.
10. Yan H, et al. Eusocial insects as emerging models for behavioural epigenetics. *Nat. Rev. Genet.* 2014;15:677–688. doi: 10.1038/nrg3787; pmid: 25200663.
11. Kucharski R, Maleszka J, Foret S, Maleszka R. Nutritional control of reproductive status in honeybees via DNA methylation. *Science.* 2008;319:1827–1830. doi: 10.1126/science.1153069; pmid: 18339900.
12. Bonasio R, et al. Genomic comparison of the ants *Camponotus floridanus* and *Harpegnathos saltator*. *Science.* 2010;329:1068–1071. doi: 10.1126/science.1192428; pmid: 20798317.
13. Herb BR, et al. Reversible switching between epigenetic states in honeybee behavioral subcastes. *Nat. Neurosci.* 2012;15:1371–1373. doi: 10.1038/nn.3218; pmid: 22983211.
14. Bonasio R, et al. Genome-wide and caste-specific DNA methylomes of the ants *Camponotus floridanus* and *Harpegnathos saltator*. *Curr. Biol.* 2012;22:1755–1764. doi: 10.1016/j.cub.2012.07.042; pmid: 22885060.
15. Alvarado S, Rajakumar R, Abouheif E, Szyf M. Epigenetic variation in the *Egfr* gene generates quantitative variation in a complex trait in ants. *Nat. Commun.* 2015;6:6513. doi: 10.1038/ncomms7513; pmid: 25758336.

16. Simola DF, et al. A chromatin link to caste identity in the carpenter ant *Camponotus floridanus*. *Genome Res.* 2013;23:486–496. doi: 10.1101/gr.148361.112; pmid: 23212948.
17. Gadau J, Heinze J, Hölldobler B, Schmid M. Population and colony structure of the carpenter ant *Camponotus floridanus*. *Mol. Ecol.* 1996;5:785–792. doi: 10.1111/j.1365-294X.1996.tb00374.x; pmid: 8981768.
18. Spannhoff A, et al. Histone deacetylase inhibitor activity in royal jelly might facilitate caste switching in bees. *EMBO Rep.* 2011;12:238–243. doi: 10.1038/embor.2011.9; pmid: 21331099.
19. See [supplementary materials](#) in *Science aac6633* Online.
20. Calabi P, Traniello JFA. Behavioral flexibility in age castes of the ant *Pheidole dentata*. *J. Insect Behav.* 1989;2:663–677. doi: 10.1007/BF01065785.
21. Liang ZS, et al. Molecular determinants of scouting behavior in honey bees. *Science.* 2012;335:1225–1228. doi: 10.1126/science.1213962; pmid: 22403390.
22. Mersch DP, Crespi A, Keller L. Tracking individuals shows spatial fidelity is a key regulator of ant social organization. *Science.* 2013;340:1090–1093. pmid: 23599264.
23. Hölldobler B. Recruitment behavior in *Camponotus socius* (Hym. Formicidae) *Z. Vgl. Physiol.* 1971;75:123–142.
24. Stroeymeyt N, Franks NR, Giurfa M. Knowledgeable individuals lead collective decisions in ants. *J. Exp. Biol.* 2011;214:3046–3054. doi: 10.1242/jeb.059188; pmid: 21865517.
25. Fitzsimons HL, Scott MJ. Genetic modulation of Rpd3 expression impairs long-term courtship memory in *Drosophila*. *PLOS ONE.* 2011;6:e29171. doi: 10.1371/journal.pone.0029171; pmid: 22195015.
26. Fischer A, Sananbenesi F, Wang X, Dobbin M, Tsai L-H. Recovery of learning and memory is associated with chromatin remodelling. *Nature.* 2007;447:178–182. doi: 10.1038/nature05772; pmid: 17468743.
27. Vecsey CG, et al. Histone deacetylase inhibitors enhance memory and synaptic plasticity via CREB:CBP-dependent transcriptional activation. *J. Neurosci.* 2007;27:6128–6140. doi: 10.1523/JNEUROSCI.0296-07.2007; pmid: 17553985.
28. Göttlicher M, et al. Valproic acid defines a novel class of HDAC inhibitors inducing differentiation of transformed cells. *EMBO J.* 2001;20:6969–6978. doi: 10.1093/emboj/20.24.6969; pmid: 11742974.
29. Cho Y, Griswold A, Campbell C, Min K-T. Individual histone deacetylases in *Drosophila* modulate transcription of distinct genes. *Genomics.* 2005;86:606–617. doi: 10.1016/j.ygeno.2005.07.007; pmid: 16137856.

30. Bowers EM, et al. Virtual ligand screening of the p300/CBP histone acetyltransferase: Identification of a selective small molecule inhibitor. *Chem. Biol.* 2010;17:471–482. doi: 10.1016/j.chembiol.2010.03.006; pmid: 20534345.
31. Crump NT, et al. Dynamic acetylation of all lysine-4 trimethylated histone H3 is evolutionarily conserved and mediated by p300/CBP. *Proc. Natl. Acad. Sci. U.S.A.* 2011;108:7814–7819. doi: 10.1073/pnas.1100099108; pmid: 21518915.
32. Tie F, et al. CBP-mediated acetylation of histone H3 lysine 27 antagonizes *Drosophila* Polycomb silencing. *Development.* 2009;136:3131–3141. doi: 10.1242/dev.037127; pmid: 19700617.
33. Jin Q, et al. Distinct roles of GCN5/PCAF-mediated H3K9ac and CBP/p300-mediated H3K18/27ac in nuclear receptor transactivation. *EMBO J.* 2011;30:249–262. doi: 10.1038/emboj.2010.318; pmid: 21131905.
34. Schrader L, Simola DF, Heinze J, Oettler J. Sphingolipids, transcription factors, and conserved toolkit genes: Developmental plasticity in the ant *Cardiocondyla obscurior*. *Mol. Biol. Evol.* 2015;32:1474–1486. doi: 10.1093/molbev/msv039; pmid: 25725431.
35. Malik AN, et al. Genome-wide identification and characterization of functional neuronal activity-dependent enhancers. *Nat. Neurosci.* 2014;17:1330–1339. doi: 10.1038/nn.3808; pmid: 25195102.
36. Orlando DA, et al. Quantitative ChIP-Seq normalization reveals global modulation of the epigenome. *Cell Rep.* 2014;9:1163–1170. pmid: 25437568.
37. Suganuma T, et al. ATAC is a double histone acetyltransferase complex that stimulates nucleosome sliding. *Nat. Struct. Mol. Biol.* 2008;15:364–372. doi: 10.1038/nsmb.1397; pmid: 18327268.
38. Iyer SC, et al. The RhoGEF trio functions in sculpting class specific dendrite morphogenesis in *Drosophila* sensory neurons. *PLOS ONE.* 2012;7:e33634. doi: 10.1371/journal.pone.0033634; pmid: 22442703.
39. Xia S, et al. NMDA receptors mediate olfactory learning and memory in *Drosophila*. *Curr. Biol.* 2005;15:603–615. doi: 10.1016/j.cub.2005.02.059; pmid: 15823532.
40. Gronenberg W, Heeren S, Hölldobler B. Age-dependent and task-related morphological changes in the brain and the mushroom bodies of the ant *Camponotus floridanus*. *J. Exp. Biol.* 1996;199:2011–2019. pmid: 9319922.
41. Withers GS, Fahrbach SE, Robinson GE. Selective neuroanatomical plasticity and division of labour in the honeybee. *Nature.* 1993;364:238–240. doi: 10.1038/364238a0; pmid: 8321320.
42. Milite C, et al. A novel cell-permeable, selective, and noncompetitive inhibitor of KAT3 histone acetyltransferases from a combined molecular pruning/classical isosterism approach. *J. Med. Chem.* 2015;58:2779–2798. doi: 10.1021/jm5019687; pmid: 25730130.

43. Wang J, et al. A Y-like social chromosome causes alternative colony organization in fire ants. *Nature*. 2013;493:664–668. doi: 10.1038/nature11832; pmid: 23334415.
44. Korzus E, Rosenfeld MG, Mayford M. CBP histone acetyltransferase activity is a critical component of memory consolidation. *Neuron*. 2004;42:961–972. doi: 10.1016/j.neuron.2004.06.002; pmid: 15207240.
45. Alarcón JM, et al. Chromatin acetylation, memory, and LTP are impaired in CBP<sup>+/-</sup> mice: A model for the cognitive deficit in Rubinstein-Taybi syndrome and its amelioration. *Neuron*. 2004;42:947–959. doi: 10.1016/j.neuron.2004.05.021; pmid: 15207239.
46. Bhatkar A, Whitcomb WH. Artificial diet for rearing various species of ants. *Fla. Entomol.* 1970;53:229–232. doi: 10.2307/3493193.
47. Ehmer B, Gronenberg W. Mushroom body volumes and visual interneurons in ants: Comparison between sexes and castes. *J. Comp. Neurol.* 2004;469:198–213. doi: 10.1002/cne.11014; pmid: 14694534.
48. Zhong S, Joung J-G, Zheng Y, Chen Y.-r., Liu B, Shao Y, Xiang JZ, Fei Z, Giovannoni JJ. *Cold Spring Harb. Protoc.* 2011. High-throughput Illumina strand-specific RNA sequencing library preparation. 10.1101/pdb.prot5652.
49. Langmead B, Salzberg SL. Fast gapped-read alignment with Bowtie 2. *Nat. Methods*. 2012;9:357–359. doi: 10.1038/nmeth.1923; pmid: 22388286.

## **CHAPTER 3: Behavioral reprogramming by HDACi causes a targeted transcriptional response during a critical period of epigenetic sensitivity.**

### **Background**

Eusocial insect colonies exhibit sophisticated division of labor (DoL) strategies that assign behavioral repertoires to distinct groups of individuals, called castes<sup>1</sup>. All eusocial species display reproductive division of labor (i.e. separation of queen and worker caste duties), and some species, including the Formicine ant *Camponotus floridanus* (*Cflo*), express two or more non-reproductive worker castes<sup>2,3</sup>. These sterile worker castes are morphologically and behaviorally distinct in *Cflo*, and are often referred to as 'Majors' and 'Minors' due to their striking differences in size<sup>4</sup>. Castes, represented by morphological or behavioral specialists, are understood to arise during larval development or at adulthood through the interaction of endogenous and exogenous cues, highlighting the importance of epigenetic gene regulation in the expression of caste identity<sup>2,4,6</sup>. Despite broad interest in regulators of caste determination and identity, few specific molecular pathways governing stable epigenetic differences between castes have been identified.

Juvenile hormone (JH) is a well-characterized exogenous cue that has been shown to influence insect development overall and caste identity specifically in *Formicidae*<sup>6-9</sup>. Brood caring workers (i.e. nurses) tailor their behavior to different larval stages<sup>10</sup>, and are thought to supply quantitative differences in JH to each larva. Elevated JH delays larval molting, thereby extending growth in a particular larval stage, and putatively altering gene expression networks<sup>11</sup>. This prolonged growth phase gives rise to enlarged anatomical features in individuals with higher JH, and strikingly, JH levels have been experimentally shown to influence elaboration of caste-specific morphology in ants<sup>9</sup>. Additionally, JH elevation is known in honey bee to precede the behavioral transition from nursing to foraging, demonstrating JH's role in adult behavioral plasticity<sup>12</sup>. JH signaling is directly<sup>13</sup> and indirectly<sup>14</sup> antagonized by the insect molting hormone 20-hydroxyecdysone (e.g. ecdysone, Ec), which activates molting and is thus a key regulator of

the timing of developmental checkpoints. JH and Ec are adept regulators of morphological and behavioral phenotypes in adult ants, and are therefore attractive targets of epigenetic regulation for trait plasticity in reprogramming. However, insights into how these modulatory pathways interact with features of the epigenome to influence behaviors have remained elusive.

We have shown that foraging behavior, a putative behavioral target of JH signaling, is a strongly Minor-biased trait in *Cflo* that varies in intensity with respect to aging (i.e. age polyethism) and morphology (i.e. caste identity)<sup>4</sup>. Additionally, we have demonstrated a link between caste identity and histone post-translational modifications (hPTMs), wherein caste-specific patterns of histone H3 lysine 27 acetylation (H3K27ac) are predictive of gene expression and RNA PolIII binding differences between castes<sup>15</sup>. Furthermore, we have demonstrated that histone deacetylase inhibitor (HDACi) treatments in newly eclosed Majors are sufficient to reprogram Major foraging to resemble Minor-like foraging<sup>4</sup>. These observations indicate a role for epigenetic function, and dynamic histone acetylation in particular, in behavioral caste identity in *Cflo*<sup>4,15,16</sup>.

We hypothesized that behavioral programming results from transcriptional control of caste-specific gene networks in the brain, and predicted that neuroepigenetic factors involved in cell identity and neurotransmitter signaling likely underlie behavioral reprogramming by HDACi. To test these predictions in the current study, we performed an unbiased screen of transcriptional activity (e.g. RNA-seq) in Major and Minor brains during a time course of early adult maturation (d0-d10) to detect caste-biased patterns of gene expression. We find transcriptional evidence for opposing JH and Ec signaling between castes and behavioral evidence for a critical period, or 'window' of sensitivity to epigenetic reprogramming in juvenile Majors. We characterize a targeted transcriptional response to HDACi that implicates members of the REST/CoREST corepressor complex, as well as tramtrack, (*ttk*, the functional homolog of REST in insects) which recruits the CoREST complex to DNA binding sites, as candidate epigenetic mechanisms underlying altered JH signaling, and thus foraging behavior, in reprogrammed Majors.

## Caste identity and early maturation stimulate transcriptional change in worker brains

We conducted a genome-wide comparison of transcriptional activity in brains of Major and Minor workers at three timepoints during the first ten days of adult maturation (Fig. 1A). Individuals from each caste were aged 0, 5, or 10 days in their maternal nest before single brains were dissected and processed for mRNA-sequencing (Fig. 1B). Using a maximum likelihood estimation (MLE) design with Caste and Age factors in the R package DESeq2<sup>17</sup>, we tested for genes that are differentially expressed by castes throughout the period of early adult maturation.

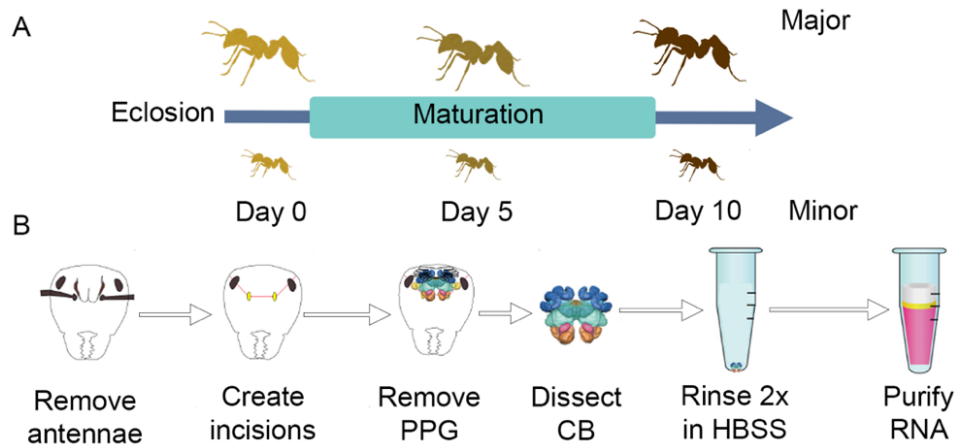


**Figure 1: Schematic of cohorts evaluated for caste-DEGs and dissection method**

(A) Individual Major and Minor workers were paint marked on the day of eclosion and aged in nest for 0, 5, or 10 days. (B) On collection day, marked ants were removed from the nest and placed on ice for <5 minutes before dissection. Antennae are removed and incisions are made along the side of the head. After removing cuticle and the post-pharyngeal gland, optic lobes are severed and the central brain is cleaned of trachea and non-neuronal tissues, rinsed 2x in cold 1x HBSS, and transferred to phenol:chloroform for RNA isolation. Post-pharyngeal gland (PPG), central brain (CB), Hank's balanced salt solution (HBSS, Sigma-Aldrich)

The caste-specific model, which controls for differences caused by age (caste DEGs) detected 167 differentially expressed genes (DEGs; Maximum Likelihood Estimation, FDR<0.05, Fig. 2). Of these, 134 DEGs are upregulated in Major and 34 DEGs are upregulated in Minor (Fig. 2). A large number of DEGs ( $p_{adj}<.05 = 7,367$ ) were identified in our test for age-related changes among d0, d5, and d10 brains of both castes (age DEGs). This indicates both castes undergo substantial transcriptional changes in the brain during this maturation period. The large number of DEGs changing during maturation from d0-d10 led us to conclude that gene regulatory

mechanisms underlying the transition from callow (d0) to mature (d10) adult (i.e. age polyethism) have broad transcriptional impacts in brain tissues. Therefore, in our test controlling for age (caste DEGs), we have identified reproducibly caste-specific DEGs during this period of maturation, which are thus candidate factors underlying differences in behavior between castes.

DEGs in each caste were analyzed for gene ontology (GO) with a classic Fisher design (FDR<0.01) in the R package TopGO<sup>18</sup>, and redundant terms were collapsed with REVIGO (Resnick semantic similarity allowed = 0.7)<sup>19</sup>. 134 significant Major DEGs are enriched for 19 GO terms, including negative regulation of neuronal apoptosis (GO:0043524), negative regulation of cell growth (GO:0030308), *de novo* protein folding (GO:0006458), and others. TopGO analysis of 34 Minor DEGs reveals 4 significantly enriched terms: gamma-aminobutyric acid (GABA) signaling (GO:0007214), chloride transport (GO:0006821), regulation of heart rate (GO:0002027), and bombesin receptor signaling (GO:0031989); 3 of the 34 DEGs are GABA-related. Thus,

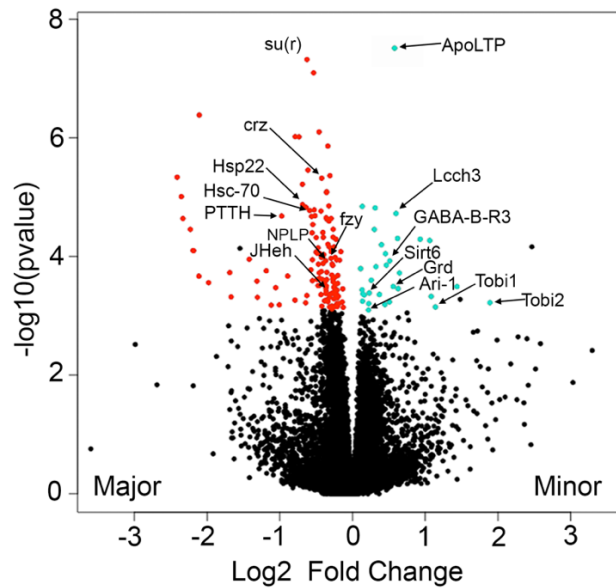


**Figure 2: Volcano plot of caste-specific DEGs**

Plot of Log<sub>2</sub>Fold Change by -log<sub>10</sub>(pvalue) for all expressed genes detected in untreated samples. Colored dots represent genes above the significant threshold (DESeq2, MLE, FDR<0.05) in Majors (left, red dots, n=134) and Minors (right, teal dots, n=34).

controlling for the effects of age on transcription, we find Major DEGs overall are enriched for neuronal cell cycle regulation, and Minor DEGs are enriched for GABA signaling. Together, these

results suggest distinct gene regulatory programs in Majors and Minors influence differences in the structure and function of the brain at adulthood.

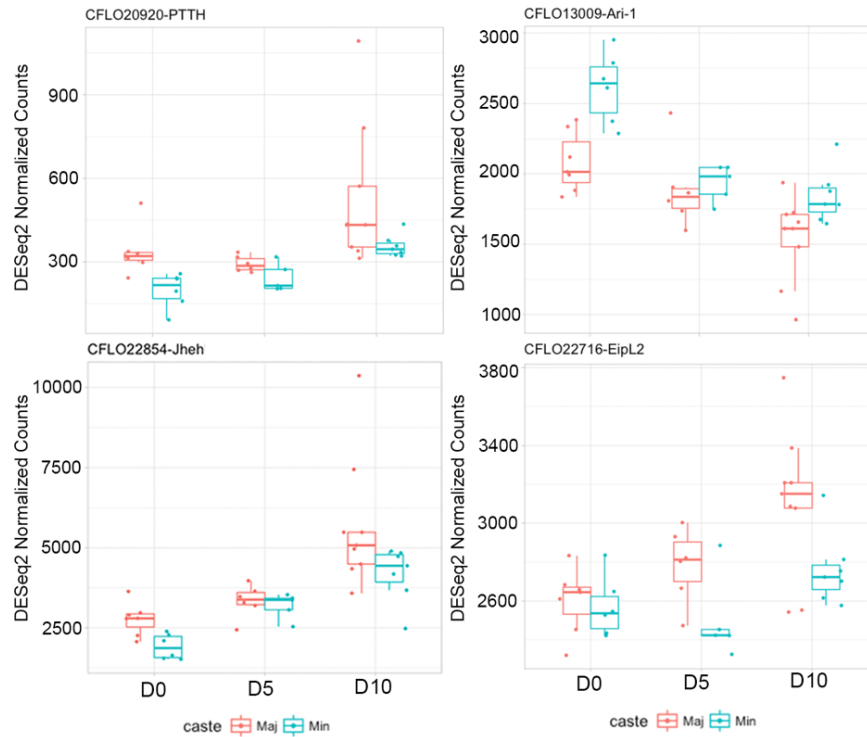


**Figure 3: Gene plots of caste-specific DEGs related to JH and ecdysone signaling** Normalized counts of caste-specific DEGs PTTH (top left), Ari-1(top right),Jheh(bottom left) and EipL2(bottom left). DEGs are plotted by caste (Major, red; Minor, teal) and age (x-axis) over the first 10 days after eclosion.

### Ecdysteroid factors are differentially expressed in *Cflo* worker brains by caste

Prothoracicotropic hormone (PTTH, CFLO20920), encodes a steroid hormone neuropeptide that is a central factor in the balance of JH and Ec levels<sup>20</sup>. PTTH activation stimulates Ec release by the prothoracic gland (PG), inducing ecdysis and facilitating transitions between larval stages<sup>21</sup>. We find average PTTH expression is elevated in Majors and, surprisingly, both castes exhibit increased PTTH levels during maturation, with notable upregulation in d10 Majors (Fig. 3, top left). This is indicative of a post-developmental role for PTTH in the brain, and supports the hypothesis that the balance of JH and E signaling regulates behavioral differences in *Cflo* workers. Altered JH/Ec regulation between castes is further

supported by a Minor-upregulated ecdysteroid factor, Ariadne-1 (Ari-1, CFLO13009), which encodes a Really Interesting New Gene (RING) domain ubiquitin E3 ligase (RING E3 Ligase)<sup>22</sup>. RING E3 ligases are emerging as key epigenetic factors controlling cell proliferation<sup>23,24</sup> neuronal development<sup>22,25,26</sup> and have established roles in cancers<sup>23,27</sup>. Ari-1 specifically targets the main isoform of the ecdysone receptor (EcR-A) and ubiquitinates it for proteasomal destruction<sup>28</sup>. In *Dmel*, elevated levels of Ari-1 suppress expression of EcR-A, ultraspiracle (USP), and ecdysone inducible proteins Eip74EF, Eip78C, and Eip75B<sup>28</sup>. In *Cflo*, Ari-1 (CFLO13009) is highly expressed in young Minors, and remains upregulated in Minors as levels decline after eclosion in both castes (Fig. 3, top right). Strikingly, ecdysone inducible proteins Eip74EF (CFLO19624), Eip75B (CFLO17720), and EipL2 (CFLO22716, Fig. 3, bottom right) exhibit a similar expression pattern to PTTH, being much higher in Majors, and an antagonistic pattern to Ari-1 levels, mimicking observed responses to Ari-1 in *Dmel*<sup>28</sup>.

An additional key differentially expressed JH/Ec factor is juvenile hormone epoxide hydrolase (JHeh, CFLO22854, Fig. 3, bottom left), which along with juvenile hormone esterase (JHe, CFLO15397) are the only known JH-metabolizing enzymes<sup>29</sup>. JHeh is upregulated in Major brains, arguing for both indirect (via PTTH/Ecdysone) and direct (via JH metabolism) antagonism of JH in Majors. Taken together, concomitant upregulation of JH antagonists (PTTH, JHeh) in Majors and a JH agonist (Ari-1) in Minors suggests a key role for ecdysteroid and JH signaling in the programming of caste-specific foraging behavior.

Based on our observations of caste-specific expression of JH and Ec factors, we predict a model (Fig. 4) in which neurosecretory cells in Major brains secrete elevated PTTH, signaling more Ec release from PG cells and propagating the Ec signal in Majors, while JHeh keeps Major JH low (Fig. 4, left). In contrast, Minor PTTH secretion is low, leading to lower Ec release by PG cells. Downstream Ec signaling is further diminished in Minors by Ari-1 targeting to EcR, and along with simultaneous low JHeh elevates JH in Minors (Fig. 4, right). In summary, high JH and low Ec likely encourage precocious nest exit and foraging behavior in Minors, whereas low JH

and high Ec inhibit these behaviors in Majors. Thus, our findings support an important role for steroid hormones in regulating caste-specific differences in *Cflo* foraging behavior.

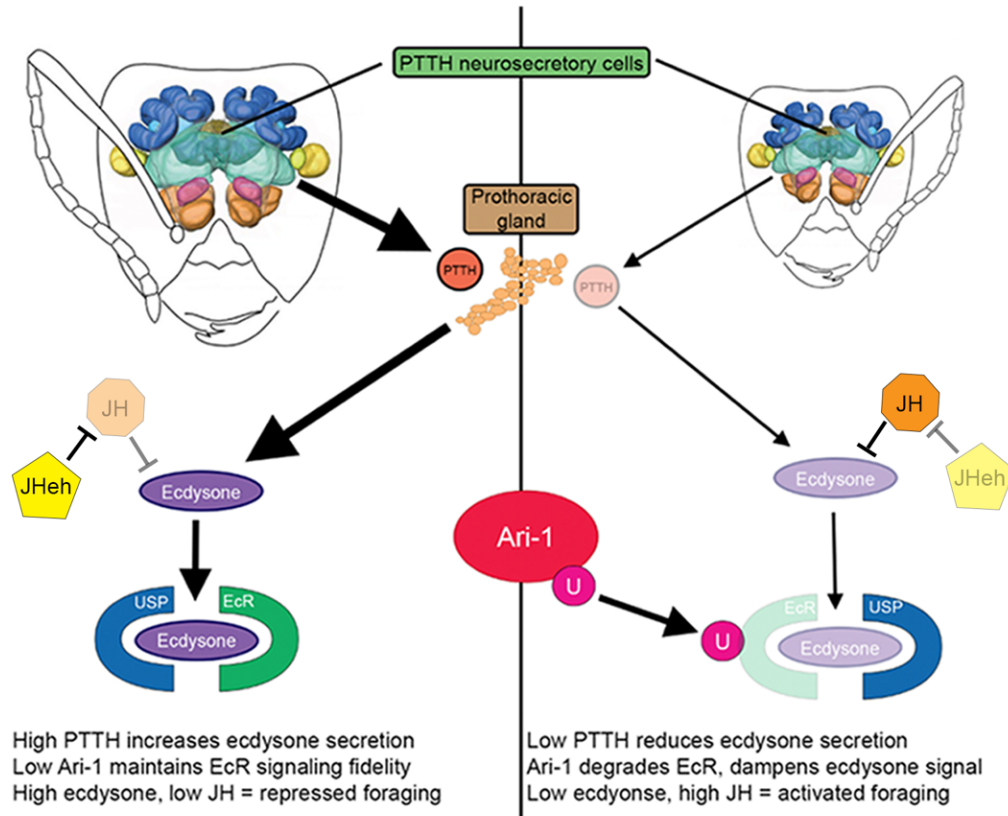


**Figure 4: Model of innate PTTH and Ari-1 mediated regulation of ecdysone and JH**  
 Our results suggest neurosecretory cells in the brain (top, green) secrete more PTTH in Majors (left side) than Minors (right side) to the PG. Elevated PTTH in Majors causes greater ecdysone release than in Minors. Increased JHeh (yellow) in Majors inhibits JH signaling (orange), thereby increasing ecdysone action (purple), which binds the ecdysone receptor (EcR) and ultraspiracle (USP) to program downstream gene function. Lower JHeh in Minors oppositely elevates JH, thereby further inhibiting ecdysone in Minors. Finally, ubiquitination of EcR (magenta U) by the Minor-upregulated E3 ligase Ari-1 (red oval) further dampens downstream ecdysone signaling.

### GABA signaling factors related to *Dmel* feeding behavior are upregulated in Minors

GABA is the most highly enriched GO category for genes upregulated in Minors, and 3 of 34 (8.8%) Minor DEGs encode GABA signaling factors. Ligand-gated chloride channel homolog 3 (Lcch3, CFLO21694) and glycine receptor (Grd, CFLO21733) form heteromultimeric channels that function as GABA-gated cation channels in insect brains<sup>30</sup>. Lcch3 and Grd are upregulated

in Minor brains (Fig. 5, top row), and surprisingly these genes exhibit dissimilar dynamics during maturation, suggesting they are under different forms of transcriptional control. Grd has a second paralog in *Cflo*, (*Grd2*, CFLO15205) and importantly *Grd*, *Grd2*, and GABA-B receptor 3 (GABA-B-R3, CFLO18545) are upregulated in Minor and follow consistent expression dynamics, whereas GABA-B-R1 expression dynamics track with *Lcch3*. GABA-B-R2 expression is similar to *Grd*/GABA-B-R3, but this receptor is not differentially expressed by caste, suggesting only certain GABA-B receptors contribute to behavioral caste identity. These results are relevant to differences in foraging activity, because GABA is known to regulate appetite and feeding behavior in species from invertebrates to mammals<sup>31, 32</sup>. Thus, variable GABA signaling between castes indicates that appetite and feeding stimuli may contribute to division of labor in *Cflo*.

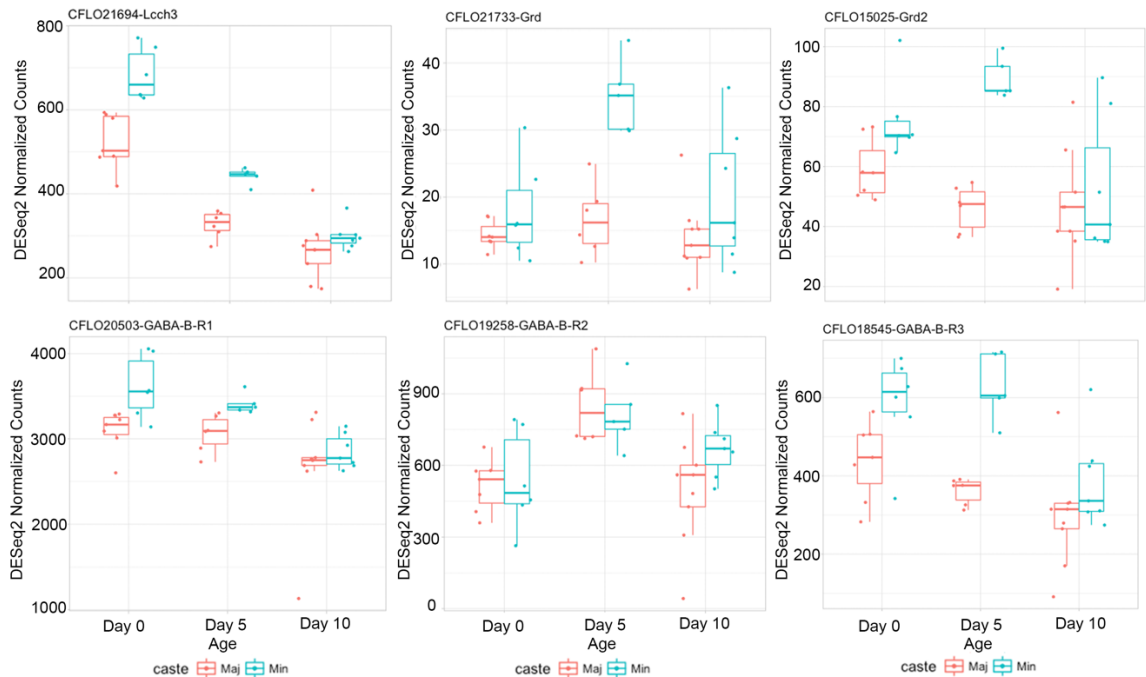


**Figure 5: Minor DEGs are enriched for GABA signaling factors**

Top row: Gene plots of Minor-specific DEGs *Lcch3* (top left), *Grd1* (top center), *Grd2* (top right). Bottom row: Gene plots of three GABA-B receptor subunits encoded in the *Cflo* genome. GABA-B-R3 (bottom right) is also a Minor-specific DEG. Genes are plotted by caste (Major, red; Minor, teal) and age (x-axis) in the first 10 days after eclosion.

## Mediators of heterochromatin and euchromatin indicate a period of epigenetic plasticity during maturation

We examined the transcriptional profiles of heterochromatin and euchromatin regulators, to determine whether epigenetic features of the genome undergo caste and age dependent responses. Whereas we did not detect caste-specific expression, we observed significant age-dependent changes in certain classes of epigenetic factors. We detected changes in Transcriptional activators (HATs, HMTs), transcriptional silencers (DNMTs, HDACs, HMTs) and heterochromatin proteins (HP1/Cbx family). We find both of the HP1 orthologs in *Cflo* are higher in d10 Majors, and notably we find that HP1 $\alpha$  (HP1, CFLO11228) drops at d5, and is then reactivated at day 10, perhaps indicating de-repression after d5 (Fig. 6, top left). The putative *de novo* DNA methyltransferase in *Cflo* (DNMT3, CFLO27010), exhibits progressive increases in expression throughout maturation in Majors, but is stably expressed throughout d0-d10 in Minors (Fig. 6, top right), suggesting alternate *de novo* DNA methylation may occur in each caste.

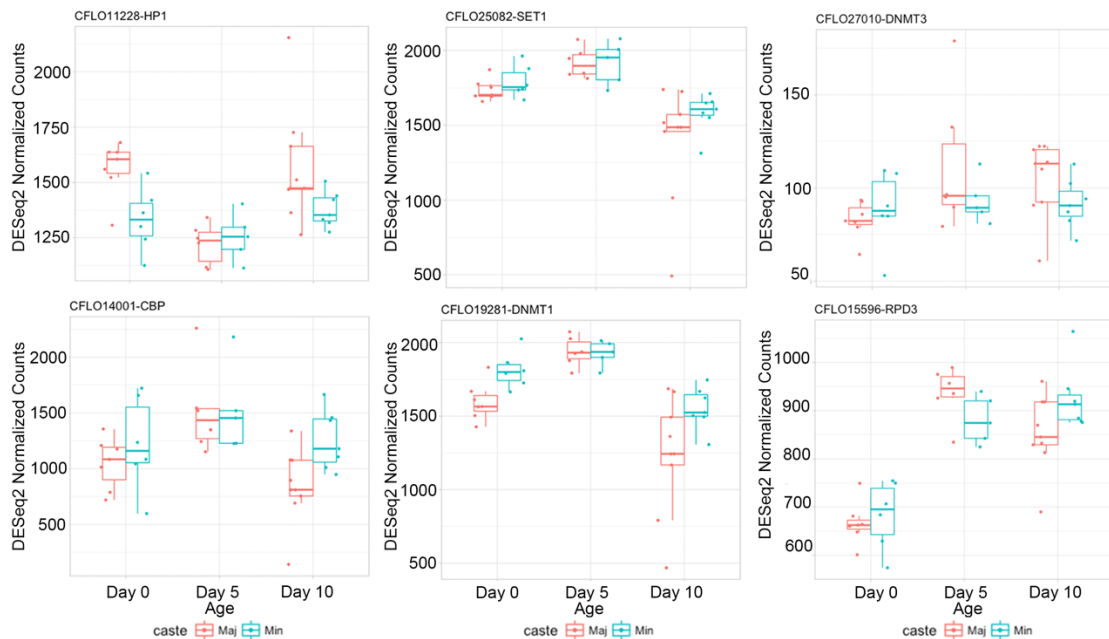


**Figure 6: Markers of euchromatin indicate a period of plasticity in d5 *Cflo* workers**

Normalized counts of heterochromatic marker HP-1 (top left) drop in d5, notably in Majors. Histone modifiers SET1 (top middle), CBP (bottom left) are slightly elevated in d5. *De novo* DNA methyltransferase DNMT3 is stable in Minors, but rises progressively in Majors, though this difference between castes is non-significant (top right). Maintenance DNA methyltransferase DNMT1 is also elevated in d5 (bottom middle), and RPD3 is lowly expressed in early life, but is

elevated starting in d5 (bottom right). Genes are plotted by caste (Major, red; Minor, teal) and age (x-axis) over the first 10 days after eclosion.

Previous reports indicate a relationship between DNMT3, DNA-methylation, and caste identity in honeybee<sup>33</sup>, and our results hint at the possibility of a difference in DNMT3 expression between *Cflo* castes, though this difference is non-significant in our data. DNMT1 (CFLO19281), binds hemi-methylated DNA and maintains fidelity of DNA methylation during DNA replication. DNMT1 is elevated in both castes at d5 before becoming repressed at d10 (Fig. 6, bottom right). DNMT1 is an essential component of a DNA replication complex<sup>34</sup>, and thus increased DNMT1 during d5 may indicate a period of enhanced cell proliferation.

Two important histone modifying enzymes regulating chromatin structure are the H3K27ac HAT CREB binding protein (CBP, CFLO14001) and the putative H3K27 HDAC in *Cflo*, histone deacetylase 1 (HDAC1/RPD3, CFLO15597)<sup>4</sup>. CBP expression is elevated at d5 (Fig. 6, bottom middle), and RPD3 expression is low at d0, before rising in d5 and d10 (Fig. 6, bottom right). This indicates H2K27ac may be globally enriched early in d0-5, likely conferring chromatin openness and transcriptional activation. Additionally, the histone lysine methyltransferase SET1 (CFLO25082) is high in day 0 and day 5, but drops at day 10 (Fig. 6, top middle). SET1 is a catalytic component of the COMPASS complex, and functions by methylating histone 3 lysine 4 (H3K4me3), a marker of active and poised promoters<sup>35,36</sup>.

Taken together, these results indicate low levels of DNA methylating factors and repressive factors in d0 brains may induce a transcriptionally active environment. In the intermediate stage of maturation, at d5, we observe a prominent drop in HP1, and an increase in SET1 and CBP expression. This indicates a continued activating chromatin environment at d5, in which hPTMs by SET1 and CBP provide an open chromatin environment. By day 10, HP1 and RPD3 expression rise, likely signaling the establishment of a more static heterochromatic epigenome at this stage. Thus, we hypothesize that the key epigenetic changes during maturation reflect a potential period of epigenetic plasticity at d5.

## A time course of pharmacologic treatments in Majors indicates a critical period for behavioral reprogramming in early development

Based on our previous behavioral and transcriptional evidence discussed in Chapter 2 and investigated above, we predicted a critical period or ‘window’ of sensitivity to HDACi exists in *Cflo* Majors. We hypothesized young individuals (d0-d5) are characterized by transcriptionally active euchromatin and are thus behaviorally sensitive to HDACi, whereas mature adults (d10) express signs of heterochromatin and are therefore behaviorally resistant to HDACi. To test these hypotheses, we aged Major and Minor workers in their maternal nest for 0, 5, or 10 days after eclosion, and injected groups of 10 Majors with either control or HDACi (Fig. 7, panels 1-4). 10 treated Majors were mixed with age-matched groups of 10 untreated Minors (Fig. 7, panel 5) and placed in nest boxes containing a nest area and an external foraging arena (Fig. 7, panel 6), and foraging activity was observed for 240 consecutive hours (10 day/night cycles) after injection.

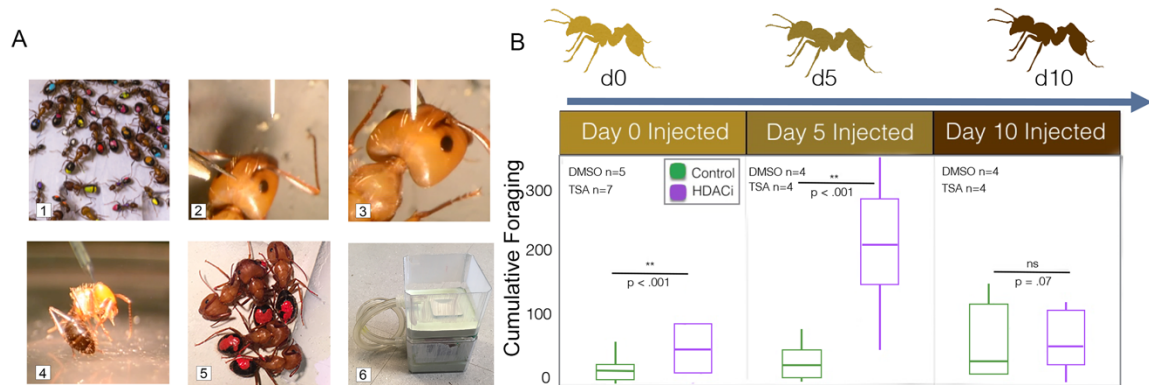


**Figure 7: A time course of HDACi injections reveals a ‘window’ of behavioral reprogramming**

(A) Setup for HDACi brain injection and foraging analysis. (1) Majors and Minors are paint marked upon eclosion and returned to the nest. On injection day, groups of 20 Majors and Minors are placed on ice, and (2) Major cuticles are pierced with a steel pin to create a shallow opening before (3) a borosilicate glass needle containing injection material is placed at the opening. (4) Majors are injected with 1ul of HDACi (Trichostatin-A) or control (DMSO), and (5) are allowed to recover for 5 minutes after injection. (6) Groups of 10 injected Majors are mixed with 10 untreated age-matched Minors in a nest area (bottom) connected to an external foraging arena by a 1ft length of tubing. (B) Major foraging behavior was observed over 10 days after injection. Day 0 injections result in a mild but significant (Mann-Whitney U,  $P < 0.05$ ) increase in foraging, whereas Day 5 injections result in a dramatic increase in foraging (center, Mann-Whitney U,  $P < 0.05$ ). Day 10 Majors do not exhibit significant differences in foraging after HDACi injection.

Major foraging behavior was induced in HDACi treated Majors at d0 compared with control injections (Mann-U,  $pval < 0.001$ ,  $N = 5$ ) (Fig. 7, right), replicating our previous results discussed in Chapter 2. Strikingly, we detected a dramatic enhancement of foraging activity in Majors injected at d5 (Mann-U,  $pval < 0.001$ ,  $N = 4$ ), whereas d10 Majors showed no significant change in foraging (Mann-U,  $pval = 0.07$ ,  $N = 4$ ). These observations suggest d5 individuals experience greater sensitivity to HDACi treatments, consistent with predictions from transcriptional results in untreated samples discussed above. Together, these observations support a model for behavioral reprogramming in which d0-d5 Majors exist in a behaviorally sensitive epigenetic state, and a subsequent loss of plasticity during maturation results in a behaviorally stable state at d10. We sought to understand this critical period of sensitivity from both transcriptional and epigenetic standpoints, and thus we pursued mRNA-seq and ChIP-seq in HDACi- and control-treated Majors.

### **HDACi treatments induce rapid transcriptional change in d5 Major brains**

TSA and other class I/II HDAC inhibitors are known to cause transcriptional activation, largely due to their ability to block the removal of activating acetylation, including H3K27ac marks. TSA has a reportedly short half-life of ~6-40 minutes before inactivation<sup>37-39</sup>. However, we observe prolonged changes in reprogrammed Major foraging behavior for 35+ days after injection<sup>4</sup>, discussed in Chapter 2. Thus, to understand the dynamic effects of HDACi on transcription after treatment, we conducted a time course of d5 and d10 Major injections with control or HDACi, and returned treated individuals to their maternal nest for 1h or 3h before dissection. We then prepared RNA-seq libraries from individual brains, to test for DEGs arising between control and treatment groups 1h and 3h after injection, as well as in the combined 1h+3h dataset.

We observed a rapid and consistent transcriptional response to HDACi in d5 Major brains. HDACi affects a greater number of genes after 1h (308 DEGs,  $FDR < 0.05$ ) than 3h (72 DEGs,  $FDR < 0.05$ ), likely reflecting the rapid metabolism of TSA *in vivo*. 83% of DEGs are upregulated in the combined 1h+3h dataset (Fig. 8A), and overall approximately 2% of all protein

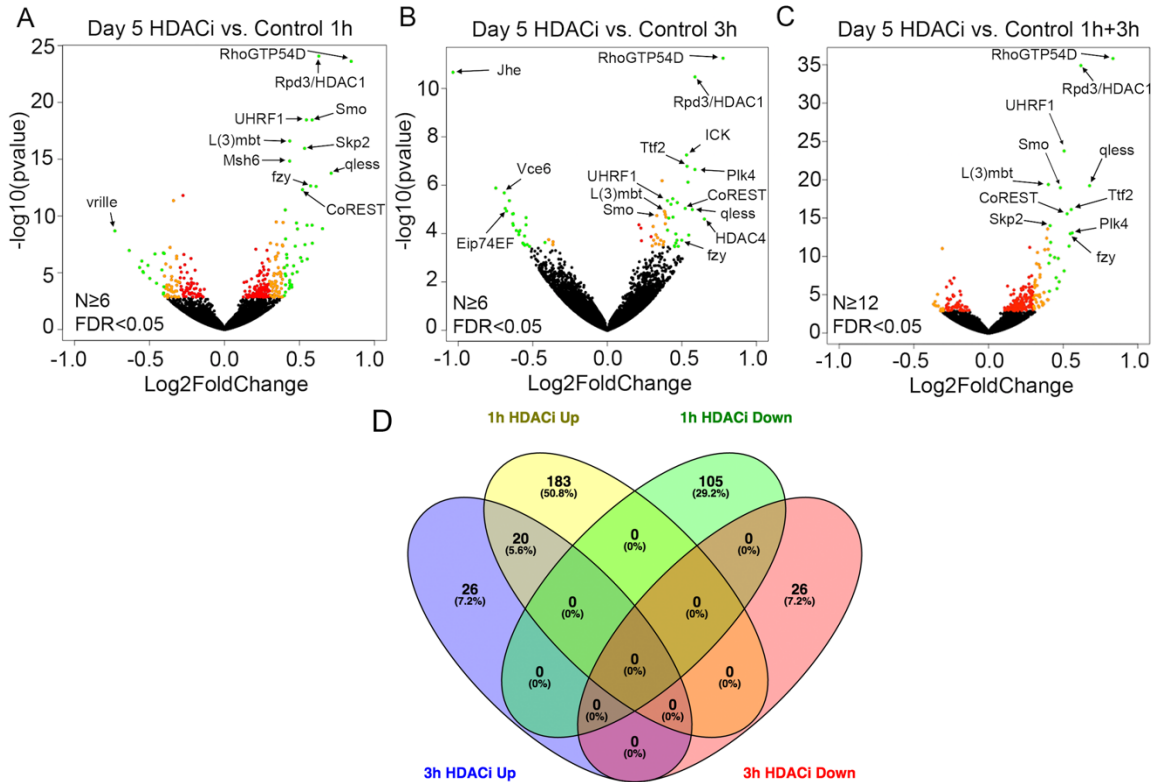


**Figure 8: HDACi induces targeted transcriptional activation in d5 Major brains**

Log2FoldChange vs.  $-\log_{10}(\text{pvalue})$  for all detected genes in 1 hour (A), 3 hour (B), and combined 1h+3h data. DEGs with  $\text{FDR} < 0.05$  are colored. Green represents HDACi DEGs with  $\text{L2FC} > 0.4$ , orange represents DEGs with  $0.4 > \text{L2FC} > 0.3$ , red dots are DEGs with  $\text{L2FC} < 0.3$ . (B) Venn diagram of overlapping DEGs between 1h and 3h HDACi induced (HDACi Up) and HDACi repressed (HDACi Down) gene lists.

coding genes ( $380 \sim 17,061$ )<sup>15</sup> are sensitive to HDACi injections, indicating HDACi causes a rapid pulse of targeted transcriptional activation. This activating effect is consistent between timepoints: we find 7 DEGs (21.2%) appear in the top 20 genes ranked by p-value at both timepoints (Fig. 9A, red boxes). Further, among all 229 upregulated DEGs, 8.7% are detected in both 1h and 3h samples (Fig. 8, bottom, blue and yellow). By comparison, none of the 131 downregulated DEGs were shared in both timepoints (Fig. 8, bottom, red and green), suggesting gene silencing effects of HDACi occur less systematically than gene activation, perhaps due to dysregulation of downstream targets by HDACi activated genes. Together, these results are consistent with observed effects in other models (e.g. a short pulse of transcriptional activation), and confirms TSA causes rapid and targeted transcriptional changes in day 5 Major brains.

**A Top 20 1h HDACi activated DEGs Top 20 3h HDACi activated DEGs**

GeneID	baseMean	L2FC	padj	Gene ID	baseMean	L2FC	padj
CFLO15597-RA	952.6834	0.6287	8.6E-21	CFLO18970-RA	93.7614	0.7772	5.8E-08
CFLO18970-RA	107.0892	0.8449	1.3E-20	CFLO15597-RA	886.9364	0.5887	1.1E-07
CFLO20056-RA	366.4146	0.5462	8.9E-16	CFLO13338-RA	175.1883	0.5319	1.5E-04
CFLO17965-RA	354.6512	0.5844	8.9E-16	CFLO21746-RA	175.2745	0.5353	3.4E-04
CFLO16321-RA	1335.0794	0.4353	5.1E-14	CFLO18095-RA	116.7779	0.5883	3.9E-04
CFLO14056-RA	255.3096	0.5346	1.9E-13	CFLO18893-RA	1660.7206	0.3676	9.6E-04
CFLO19675-RA	516.5837	0.4348	2.1E-12	CFLO14105-RA	197.0625	0.5415	9.6E-04
CFLO18584-RA	81.9799	0.7116	2.2E-11	CFLO15348-RA	733.3107	0.4393	3.4E-03
CFLO18428-RA	129.5781	0.5744	2.6E-10	CFLO16565-RA	291.2795	0.4041	3.5E-03
CFLO15431-RA	123.9444	0.6108	2.6E-10	CFLO21625-RA	320.2151	0.4700	3.9E-03
CFLO15400-RA	405.6420	0.5204	4.5E-10	CFLO20056-RA	342.6221	0.4274	4.2E-03
CFLO14459-RA	353.4475	0.4053	2.1E-08	CFLO15400-RA	375.8306	0.5225	5.6E-03
CFLO15173-RA	578.9532	0.3452	2.3E-07	CFLO18584-RA	72.7612	0.5706	5.8E-03
CFLO16565-RA	331.0186	0.3910	2.4E-07	CFLO15212-RA	374.5501	0.3831	6.2E-03
CFLO20013-RA	190.7162	0.4802	2.5E-07	CFLO15618-RA	1485.9124	0.3865	6.3E-03
CFLO21746-RA	195.7893	0.5506	3.5E-07	CFLO14016-RA	305.0678	0.3882	6.9E-03
CFLO14260-RA	96.4118	0.5840	3.5E-07	CFLO20882-RA	406.8402	0.3327	7.5E-03
CFLO22723-RA	49.3494	0.6539	6.8E-07	CFLO16287-RA	427.5229	0.3944	8.0E-03
CFLO22463-RA	180.9004	0.4867	6.8E-07	CFLO22701-RA	1393.2590	0.4413	8.0E-03
CFLO16209-RA	296.6074	0.4077	4.6E-06	CFLO13963-RA	304.4064	0.4126	8.1E-03

**B**

Top 10 GO terms - All upregulated DEGs

GO.ID	Term	Annot.	Sig.	Exp.	classicFisher
GO:0007049	cell cycle	278	21	4.33	1.30E-09
GO:0006260	DNA replication	96	13	1.5	2.30E-09
GO:0006270	DNA replication initiation	9	5	0.14	1.00E-07
GO:0051276	chromosome organization	213	16	3.32	1.60E-07
GO:0000278	mitotic cell cycle	165	14	2.57	2.30E-07
GO:0022402	cell cycle process	219	16	3.41	2.40E-07
GO:0006261	DNA-dependent DNA replication	31	7	0.48	3.60E-07
GO:0034645	cellular macromolecule biosynthetic process	1432	45	22.33	7.40E-07
GO:0006277	DNA amplification	6	4	0.09	8.20E-07
GO:0016070	RNA metabolic process	969	35	15.11	9.10E-07

Top 10 GO terms - 1h+3h Overlap DEGs

GO.ID	Term	Annot.	Sig.	Exp.	classicFisher
GO:0016575	histone deacetylation	6	3	0.03	1.30E-06
GO:0006476	protein deacetylation	12	3	0.05	1.40E-05
GO:0035601	protein deacylation	14	3	0.06	2.40E-05
GO:0098732	macromolecule deacylation	14	3	0.06	2.40E-05
GO:0007455	eye-antennal disc morphogenesis	15	2	0.06	0.0017
GO:0012501	programmed cell death	133	4	0.56	0.0022
GO:0008219	cell death	139	4	0.58	0.0025
GO:0007143	female meiotic division	19	2	0.08	0.0028
GO:0016569	covalent chromatin modification	68	3	0.29	0.0028
GO:0016570	histone modification	68	3	0.29	0.0028

**Figure 9: Top 20 HDACi upregulated DEGs and associated GO terms**

(A) Top 20 DEGs by pvalue in 1h (left) and 3h (right) comparisons. Red boxes indicate 7 upregulated DEGs overlapping 1h and 3h tests. (B) Top 10 GO terms from topGO of all HDACi upregulated DEGs (top) and 20 DEGs that are upregulated in 1h and 3h comparisons (bottom).

We identified orthologous genes with a reciprocal best hit approach, and used topGO to assign groups of DEGs to biological processes. 1h upregulated DEGs are enriched for cell cycle

regulation, chromatin modification, and DNA replication GO terms (Fig. 9B, top), indicating HDACi rapidly alters chromatin, and suggesting reprogramming may occur through alterations in proliferation and/or differentiation of neural cells. The 20 overlapping DEGs between 1h and 3h are highly enriched for GO terms specifying histone deacetylation and covalent histone modification (Fig. 9B, bottom). Taken together, these results indicate a multifaceted transcriptional response underlies reprogramming, involving DNA replication, chromatin organization, and cell cycle factors.

### **E3 ubiquitin ligases with RING-domain cofactors are induced by HDACi**

We detected HDACi-induced upregulation of E3 ligases that function in multi-subunit complexes with RING domain-containing E3 Ligases (Fig. 10, top row). Fizzy (*fzy*, CFLO18428) is a homolog of CDC20, a key regulator of cell cycle, and functions in a regulatory complex with a RING domain E3 ligase<sup>40</sup>. Skp2 (CFLO16778) is also an E3 ligase that regulates cell cycle progression, and interacts with *fzy*/CDC20<sup>41</sup>, suggesting HDACi induction of E3 ligases may alter neural stem cell maintenance and/or proliferation programs. UHRF1 is activated by HDACi, and encodes a RING E3 ligase thought to function in part as a bridging mechanism between DNA-methylation and histone modifications<sup>42-44</sup>. This result is notable, because it represents the first time to our knowledge that UHRF-1 has been identified downstream of HDACi, and may signal additional layers of epigenetic crosstalk between histone modifying enzymes and other forms of epigenetic control. All three of these E3 ligases are dramatically induced by HDACi at 1h, and remain elevated at 3h (Fig 10, top row, 1h green, 3h blue). Thus, E3 ligases, and notably UHRF-1, are attractive candidates in the reprogramming phenotype (see Chapter 4), and may serve to prolong the stability of reprogramming beyond the short half-life of TSA *in vivo*.

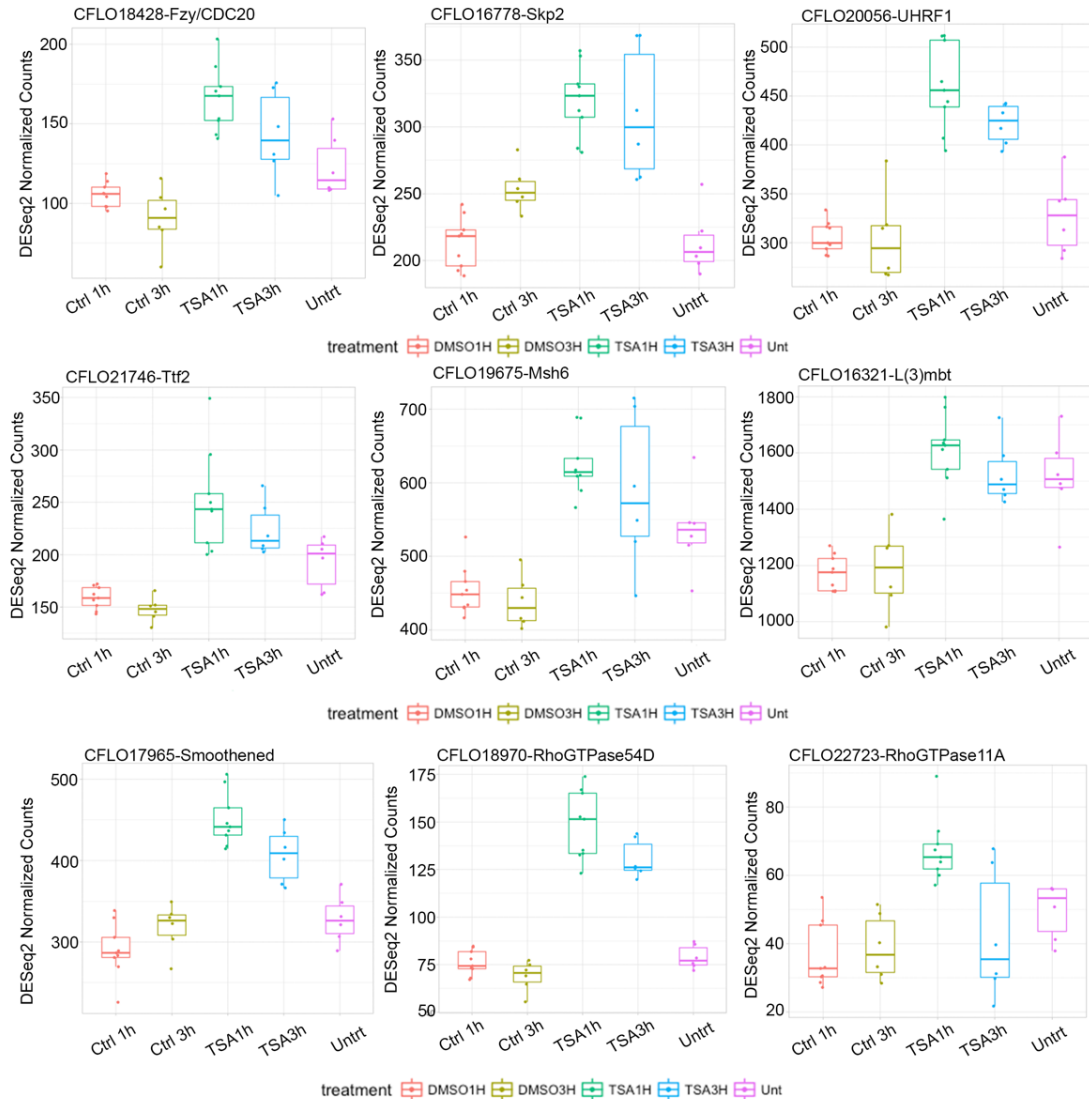


**Figure 10: Gene plots of HDACi induced DEGs with untreated d5 Major data.**

Normalized counts from DESeq2 of 9 HDACi DEGs from 1h and 3h incubations with either HDACi (100 $\mu$ M TSA) or Control (0.05% DMSO). Red boxplots indicate 1h control, yellow indicates 3h control, green represents 1h HDACi, blue represents 3h HDACi, and purple represents uninjected control. Top row: HDACi induced E3 ligases. Middle row: HDACi induced chromatin modifiers. Bottom row: HDACi induced sonic hedgehog (shh) pathway member Smoothened (left) and RhoGTPases (middle, right).

### Chromatin modifiers are induced by HDACi

Ttf2, msh6, and l(3)mbt are HDACi induced chromatin associated factors (Fig. 10, middle row). Transcription termination factor 2 (ttf2, i.e. lodestar) encodes a SWI2/SNF2-related DNA dependent ATPase with RNA PolIII termination activity<sup>45</sup>. Little is known about ttf2 (CFLO21746), but it has been shown to interact with Cdc5L, a positive regulator of G2/M cell cycle transition<sup>46</sup>.

Upregulated mitotic exit factors such as *ttf2* in the brain argue HDACi may lead to changes in progenitor and differentiated cell populations. Notably, *ttf2* has been previously reported as an HDACi inducible gene by SAHA treatment<sup>47</sup>, which inhibits HDACs in classes I, II, and IV<sup>48</sup>. Our *in vivo* observations in insects highlight the evolutionarily conserved sensitivity of *ttf2* to HDACi, and suggest SWI/SNF ATP-dependent chromatin remodeling is a downstream effect of HDACi.

Msh6 is a DNA mismatch repair factor which is recruited to chromatin during G1 and early S phase. Mismatch repair in eukaryotes involves 3 proteins, Msh2, Msh3, and Msh6. Msh2-Msh6 forms the main mismatch recognition complex, and Msh6 contains a PWWP domain which specifically recognizes H3K36me3 sites and is recruited to chromatin to facilitate rapid identification of DNA mismatches and recruitment of the mismatch repair complex<sup>49</sup>. Thus, Msh6 is an additional chromatin binding protein related to cell cycle progression that is activated by HDACi, highlighting the centrality of this process in our results. Msh6 is upregulated at 1h (Fig. 10, center, green), and exhibits lower levels by 3h (Fig. 10, center, blue), suggesting HDACi activates a complement of chromatin associated cell-cycle machinery immediately after treatment.

L(3)mbt is a chromatin binding protein that acts in the LINT repressive complex with Lint-1 and CoREST<sup>50</sup>. L(3)mbt is upregulated in HDACi compared to control (Fig. 8, top row), but interestingly HDACi levels are comparable with untreated samples, whereas the control conditions indicate repression of this gene (Fig. 9, middle right). Importantly, we see elevated CoREST expression in HDACi treatments (see next section), and hence it is possible that the L(3)mbt:Lint-1:CoRest complex stabilizes L(3)mbt expression under stress. Interestingly, this may be the first report linking HDACi to L(3)mbt/LINT activation, as previous reports suggest the LINT complex binds and represses targets genes that are not under HDAC control, and TSA did not induce L(3)mbt in previous studies<sup>50,51</sup>. Alternatively, L(3)mbt stimulation may be an downstream effect of HDACi, perhaps due to CoREST elevation, which may stimulate its cofactors, including L(3)mbt and Lint-1.

Together, these findings indicate that HDACi stimulates a range of chromatin mediating factors that operate in related cellular pathways. Importantly, many of the chromatin pathways

detected in this analysis are related to transactivation, proliferation, and differentiation in neural cell types. This argues that reprogramming of Majors likely alters behavioral identity as well as cell type identity.

### **HDACi induced Rho GTPases indicate non-canonical Shh/Smoothened activation**

Neuronal differentiation results from a stepwise process beginning with migration from progenitor cells, and continues with growth and progressive connectivity with other neurons<sup>52, 53</sup>. Rho family GTPases have specialized roles in dendritic arborization<sup>54</sup>, axon pathfinding<sup>55</sup>, and neurite differentiation<sup>56</sup>, and are central signaling factors in neural structure and function. Importantly, the top upregulated gene at both 1h and 3h after HDACi encodes a Rho GTPase, (RhoGAP54D, CFLO18970, Fig. 8 top row; Fig. 10 bottom row) and an additional Rho family member (RhoGAP102A, CFLO22723) is dramatically upregulated at 1h, signaling that Major brain structure may be altered through Rho GTPase function. Importantly for this hypothesis, we also detect upregulation of the Hedgehog (Hh) co-receptor *Smoothened* (*Smo*, CFLO17965, Fig. 10, bottom left). *Smo* is a seven transmembrane protein and an integral cell surface receptor in a non-canonical sonic hedgehog (*shh*) signaling pathway involved in neuronal differentiation<sup>57-59</sup>. Previous reports indicate that *Smo* is essential in embryonic and neuronal development<sup>60</sup>, and is coactivated with Rho GTPases<sup>61</sup>, leading to altered structure and function in developing brains. Induction of this signaling pathway by HDACi indicates that changes in *Smo* and Rho signaling may underlie important aspects of foraging reprogramming.

### **The insect CoREST repressive complex is activated by HDACi in d5 Majors**

The RE1-silencing transcription factor, REST (aka NRSF) is a transcriptional repressor and master regulator of neurogenesis<sup>62-64</sup>. REST functions through recognition and binding of genomic neuron-restrictive silencer elements (NRSEs), thereby silencing neuronal gene expression in non-neuronal tissues<sup>63</sup>. REST is abundant in undifferentiated neuronal

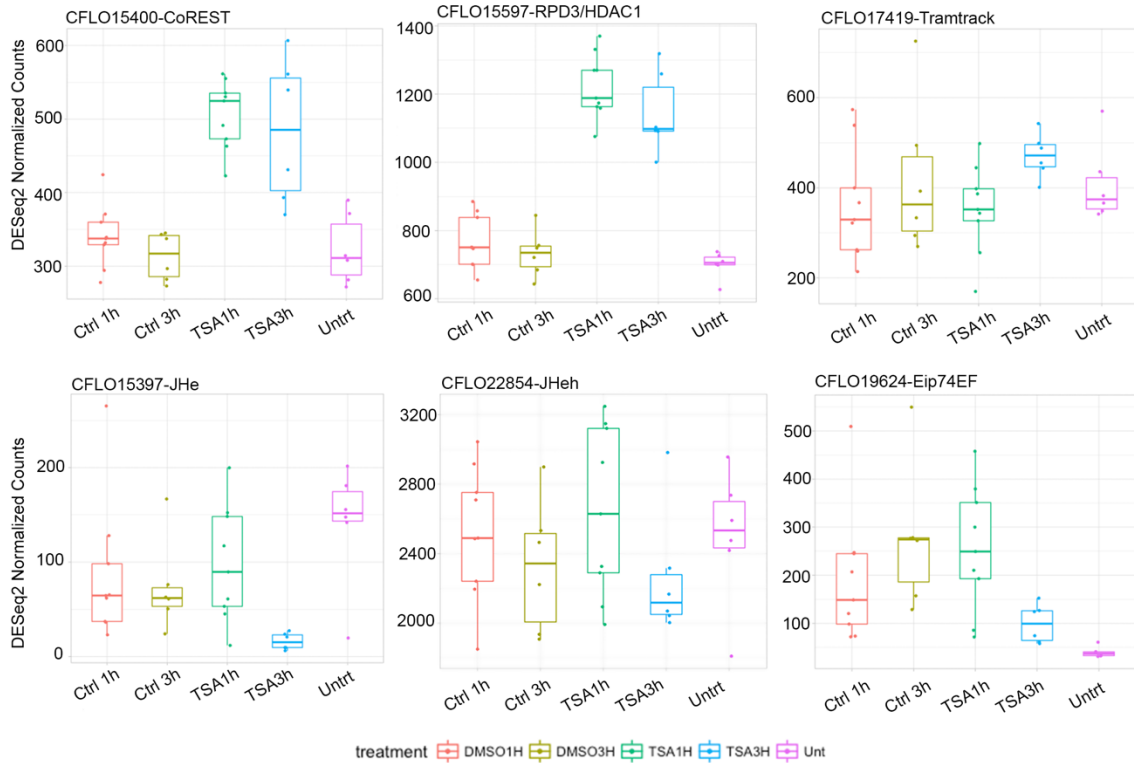


**Figure 11: HDACi activates CoREST complex members, and represses JH signaling**  
 Top row: Normalized counts of HDACi upregulated DEGs CoREST (top left) and RPD3 (top middle), alongside their DNA-binding cofactor tramtrack (ttk, top right). Ttk is not a DEG at FDR<0.05, but ttk expression moderately elevated at 3h. Bottom row: HDACi downregulated DEGs JHe (bottom left), JHeh (bottom middle), and Eip74EF. Notably, downregulation of these JH antagonists corresponds with activation of ttk at 3h, signaling they are potential downstream targets of CoREST repression.

progenitors, and REST expression strongly correlates with longevity and cognitive function in humans<sup>65</sup>. When bound to NRSEs, REST functions as a modulatory scaffold for dynamic recruitment of its cofactor complex, including its primary cofactor CoREST, as well as chromatin modifying factors RPD3, LSD1, and other cofactors in a context-dependent manner<sup>66</sup>. CoREST also has established functions in transcriptional control during transdifferentiation of epithelial to mesenchymal cells. In this context, CoREST forms a multiunit complex with PRC2, LSD1, HDAC1, and HDAC2, demonstrating the potential for CoREST and its chromatin modifying cofactors in stimulating cellular transdifferentiation in different cellular contexts<sup>67</sup>. Additionally, CoREST can interact with I(3)mbt and Lint-1, as previously noted<sup>50</sup>.

Two members of the REST corepressor complex, RPD3 and CoREST, are consistently among the top HDACi activated genes 1h and 3h after HDACi (Fig. 11, top row). While REST does not exist in insects, the functionally analogous DNA-binding partner tramtrack (ttk), which recruits CoREST in insects<sup>68</sup>, is elevated 3h after injection (Fig. 11, top right). LSD1 expression is consistent across treatments, but previous reports indicate CoREST recruitment can scaffold LSD1 and protect it from degradation<sup>69</sup>. Thus, we find multiple members of the mature CoREST repressive complex (ttk, CoREST, RPD3) are activated by HDACi in this system, strongly arguing CoREST activation is a reproducible consequence of HDACi.

### **Two antagonists of JH function, JHe and JHeH, are silenced by HDACi**

Despite the broadly upregulating effects of HDACi in Majors, 17% of DEGs are downregulated in the 1h+3h dataset, suggesting either some activated genes engage in downstream repressive gene regulation, or HDACi has direct repressive effects in this system, which is unlikely. We hypothesized that activation of the CoREST repressive complex is a potential mechanism by which HDACi may indirectly suppress genes. A key finding for our overall model is the observation that JHe and JHeh are transcriptionally repressed 3h after treatment (Fig. 11, bottom row). JHe and JHeh are the sole enzymes in insects which catabolize JH, and decreased JHe/JHeh expression is expected to activate JH signaling. Thus, silencing of JH antagonists by HDACi is predicted to increase JH levels in reprogrammed Majors, leading to activation of foraging behavior. We hypothesize that reduction of chromatin activation (including histone acetylation) upstream of JH and ecdysteroid gene promoters by CoREST is a potential epigenetic mechanism regulating caste-specific behaviors. In this paradigm, we predict HDACi activates RPD3, CoREST, and ttk expression while active. Once the effect of HDACi has diminished (e.g. 3h condition), RPD3-containing complexes become catalytically active, causing downstream silencing. Importantly for this hypothesis, we see JHe and JHeh repression only in the 3h HDACi incubations.

## Induction of the CoREST complex is not observed in mature (d10) Majors

Day 10 Majors were behaviorally insensitive to HDACi treatment (Fig. 7B, right). To determine how transcriptional activity is altered by HDACi in d10 Major brains, we injected d10 Majors and prepared RNA-seq libraries 1h and 3h after treatment, as before. We observed 5 DEGs resulting from HDACi after 3h in d10 brains, one putatively uncharacterized protein (PUP) after 1h, and one PUP in the combined 1h+3h dataset (Fig. 12). Importantly, none of the d10 HDACi genes overlap with the set of d5 HDACi-induced genes, and we do not observe significant upregulation of RPD3 or other CoREST complex members. Therefore, we conclude that the consistent induction of CoREST and its functional partners observed at d5 does not occur at d10, and overall there are exceedingly few HDACi-sensitive DEGs at d10. This suggests an altered epigenetic environment in d10 blocks behavioral transdifferentiation caused by HDACi. This remarkable change in sensitivity to HDACi could be caused by the establishment of a more repressive chromatin state in Major worker brains during maturation at d10. One possibility is that genome-wide accumulation of H3K27me3 towards the end of maturation may block the effects of HDACi by removing H3K27ac targets upstream of foraging-related genes. To address this hypothesis, we conducted native ChIP-seq (NChIP) on individual HDACi-treated *Cflo* brains 1h and 3h after injection and probed for changes in H3K27ac and H3K27me3.

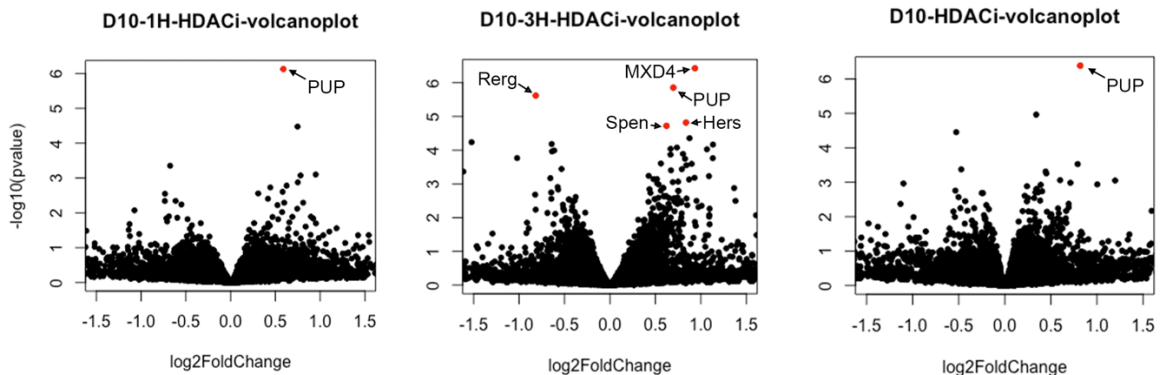


**Figure 12: HDACi treatments in behaviorally resistant day 10 Majors do not induce consistent transcriptional changes in the brain.**

Volcano plots of log<sub>2</sub>foldchange vs. -log<sub>10</sub>(pvalue) for all detected genes in comparisons of HDACi vs. control treated day 10 Major brains 1 hour (left) 3 hours (middle) and in the combined 1h + 3h dataset. Red dots indicate DEGs (DESeq2, MLE, FDR<0.05).

*Note: ChIP-seq data are in progress, and thus some analyses are preliminary. Please advise key tests needed to finalize results in this section as warranted.*

### **Global and targeted changes in H3K27ac, but not H3K27me3, due to HDACi**

We injected Majors with HDACi or control for 1h and 3h and prepared ChIP-seq libraries enriched for H3K27ac and H3K27me3 from individual ant brains. We detected differentially bound regions (DBRs) with a peak calling prioritization pipeline tool (PePr)<sup>70</sup> between DMSO and TSA samples 1h and 3h after treatment. This analysis revealed an expected increase in H3K27ac enrichment (DBRs=7,679, FDR<0.05) in d5 HDACi treated samples compared with DMSO controls. 1h H3K27ac enrichment was higher than in 3h samples (DBRs=407, FDR<0.05), indicating a transient global effect of HDACi on patterns of H3K27ac, similar to observations of transcription above. We did not detect a striking change in H3K27me3 resulting from HDACi, as just 95 DBRs were detected 1h after treatment, and 10 DBRs after 3h.

Despite a minimal transcriptional effect of HDACi in d10 Majors, ChIP-seq samples in d10 Majors reflect a similar pattern to d5: H3K27ac changes are strongest at 1h (DBRs = 9,185, FDR<0.05) and begin to diminish after 3h (DBRs = 2,439, FDR<0.05). To confirm the global changes in H3K27ac and H3K27me3, we included chromatin from a related species (*Hsal*) and used ChIP-Rx normalization methods<sup>71</sup> to estimate relative hPTM changes between samples. In d5 brains we detect a 1.5-fold increase in H3K27ac enrichment in HDACi samples (ChIP-RX DMSO/TSA ratio = 1.56) and in d10 brains we detect a 1.6-fold increase (ChIP-RX DMSO/TSA ratio = 1.66). Interestingly, whereas d10 acetylation is enriched after 1h, it has little sustained effect (3h DMSO/TSA ratio = 1.07), suggesting the lack of consistent transcriptional differences may result from decreased stability of HDACi's acetylating effect at d10.

H3K27me3 samples do not exhibit a similar induction following HDACi, as expected. In d5 and d10, there was a similarly weak effect of HDACi on H3K27me3 enrichment (DMSO/TSA = 1.08; DMSO/TSA = 1.02). To assess the relationship between transcriptional and hPTM changes resulting from HDACi treatment, we calculated correlation coefficients for these two datasets. The most highly correlated samples are the d5 1h+3h datasets from ChIP-seq and RNA-seq

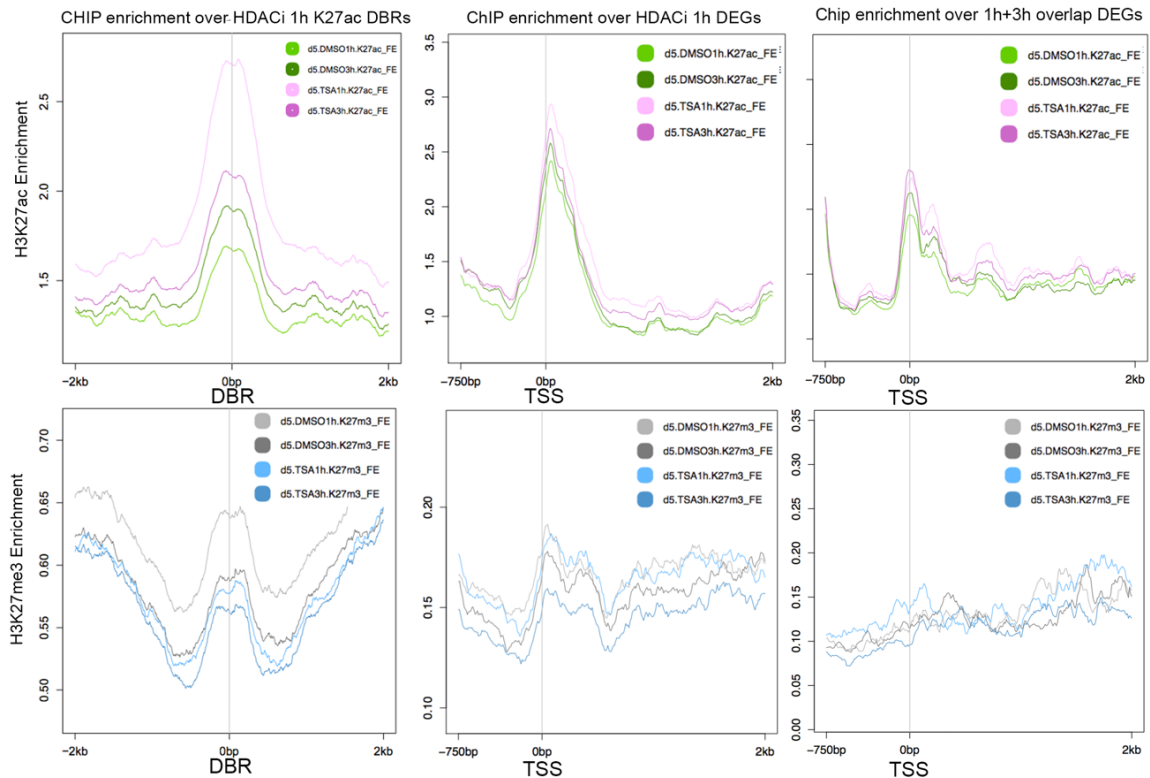


**Figure 13: H3K27ac, but not H3K27me3 is enriched by HDACi globally and at DEGs.** Metaplots for ChIP enrichment of H3K27ac (top row) and H3K27me3 (bottom row) signal over all significant 1h HDACi K27ac DBRs (left column, diffbind). Light pink represents 1h HDACi (TSA) enrichment, purple indicates 3h HDACi, light green indicates 1h control (DMSO), and dark green represents 3h control. K27ac enrichment is enhanced at the averaged TSS of 229 1h HDACi induced DEGs (middle, top), but K27me3 does not show a consistent pattern by treatment type (middle, bottom, blue HDACi vs. grey control). Averaging over TSS's for the 20 overlapping 1h and 3h DEGs, we find a modest trend of elevated K27ac directly over and after the TSS. H3K27me3 is very lowly enriched at TSS's of overlap DEGs (bottom right).

( $\rho = 0.45$ ). This indicates that changes in H3K27ac are positively correlated with transcriptional effects of HDACi, and suggests that DEGs detected by RNA-seq are likely downstream of chromatin changes in H3K27ac enrichment. We detect weaker correlation between H3K27ac and transcription in d10 1h+3h samples ( $\rho = 0.271$ ), further suggesting that transcriptional effects of HDACi in d10 brains are less influenced by changes in H3K27ac.

### HDACi response genes gain H3K27ac peaks upstream of TSS after treatment

We compared ChIP-Rx normalized Native ChIP-seq samples in HDACi and control treated single brains, and detected global increases in H3K27ac enrichment 1h after HDACi

treatment (Fig. 13, top left, purple). 1h increases in H3K27ac are strongest (Fig. 13, top left, pink vs. light green), and by 3h H3K27ac begins to return towards baseline levels. H3K27me3 enrichment does not show consistent changes at HDACi sensitive H3K27 peaks, suggesting HDACi does not cause off-target effects on non-acetylated histones. We next analyzed H3K27ac and H3K27me3 enrichment over TSS's of HDACi induced DEGs (Fig. 13, middle top). This analysis revealed a similar trend, in which the greatest H3K27ac enrichment is observed at 1h, and remains elevated, but returns towards baseline levels after 3h. As expected, we did not detect consistent changes in H3K27me3 near HDACi DEGs (Fig. 13, middle bottom). Finally, we looked specifically at the 20 genes which are upregulated 1h and 3h after HDACi, and detected enriched H3K27ac signal at these genes (Fig. 13, top left, pink and purple). These results suggest different genomic locations experience 'decay' of the HDACi effect at different rates. In other words, some H3K27ac gains are quickly lost, but others appear to stabilize in 3h conditions. This stabilization could occur through alternative activity of histone modifiers, or could reflect differences in chromatin structure at transient vs. stable H3K27ac DBR sites.

Looking at individual genes, we detected significant DBRs upstream of our top upregulated DEGs. As previously noted, RPD3 is one of the top DEGs, and also has a large DBR (red bars) indicating H3K27ac gain in 1h HDACi (TSA vs. DMSO; Fig. 14, top). CoREST is also decorated with increased H3K27ac upstream of its transcription start site (Fig. 14, second from top) in HDACi samples, indicating transcriptional activation and H3K27ac enrichment at these genes are regulated by HDACs. One possibility is that RPD3's HDAC activity targets its own TSS/enhancer in normal conditions, and that blocking RPD3's catalytic activity by HDACi yields an 'always on' feedback loop of RPD3 activation (see Ch. 4). We also compared Chip-seq tracks near genes that are transcriptionally repressed by HDACi. While we did not detect significant DBRs in these regions, we do observe anecdotally enriched H3K27ac regions (red arrows) in the control samples upstream of JHe (Fig. 14, second from bottom) and JHeh (Fig. 14, bottom). Thus, transcriptional repression of these genes is reflected by lowered histone acetylation. It is notable that we observe reduced acetylation at JHe and JHeh, which are important regulators of

behavior that may interact with naturally occurring histone deacetylase inhibitors (e.g. 10HDA) in royal jelly. Thus, our results suggest JH and Ec signaling may be intrinsically related to HDAC and HAT function in eusocial insect species. Our results raise a number of questions about the transcriptional and epigenetic responses conferred by HDACi. treatment. In particular, the role of

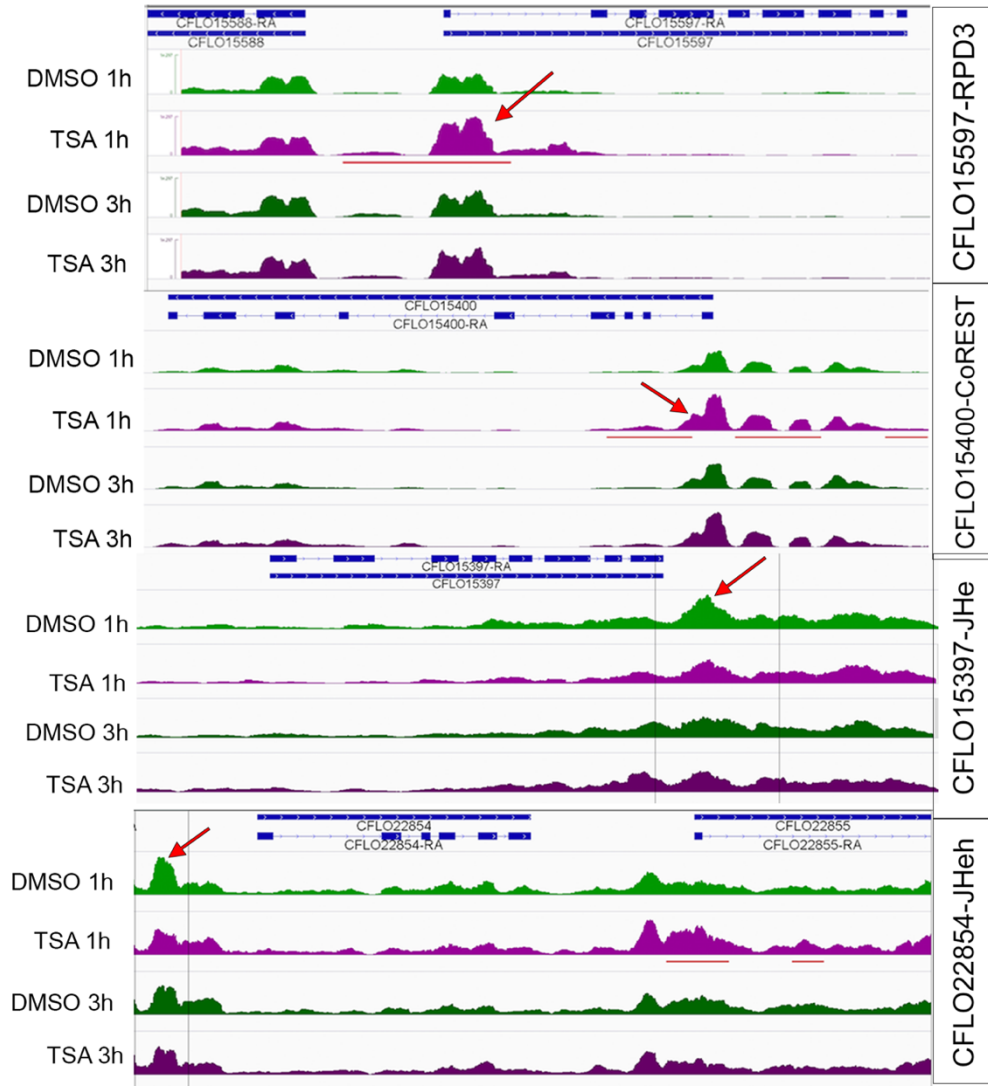


**Figure 14 HDACi induces de novo H3K27ac peaks upstream of top HDACi DEGs.** Browser view of H3K27ac enrichment after HDACi (purple) or Control (green) injections at HDACi induced (RPD3, CoREST) and HDACi repressed (JHe, JHeh) genes. Dark colors represent 3h treatment incubations, light colors represent 1h incubations.

CoREST and RPD3 in repressing JHe and JHeh is a promising candidate pathway underlying behavioral reprogramming, and we are now exploring CoREST binding by ChIP-seq. RING domain E3 ubiquitin ligases and their cofactors appear to function naturally in caste identity and behavior (e.g. Ari-1), and are induced by HDACi (e.g. UHRF-1). Thus, how these factors function in epigenetic control of foraging behavior is a fascinating question to pursue. Also, the auto-regulation of RPD3 expression by HDACs is a novel observation which may contribute to understanding of how RPD3 is regulated, and why it is activated by HDACi in this context.

## Discussion

We sought to understand how behavioral reprogramming is achieved by epigenetic treatments at the transcriptional level. We detected robustly caste-specific DEGs, and determined that JH and Ec signaling are key pathways regulating caste-specific differences in the brain. We detected a transcriptional signature of relaxed chromatin structure at d5, and treated Major workers with HDACi in a time course of early maturation. We detected a 'window' of sensitivity to behavioral reprogramming in d0-d5 that closes by d10. To address transcriptional changes underlying behavioral reprogramming, we prepared HDACi and control treated brains for RNA-seq, and detected a consistent and targeted transcriptional effect. Notably, we detected enhanced expression of E3 ligases, chromatin modifying proteins, and multiple members of the CoREST complex (e.g. RPD3, CoREST, ttk). Interestingly, 17% of DEGs were downregulated, and the intensity of downregulation (e.g. L2FC) was greater in 3h downregulated DEGs compared to 1h downregulated DEGs. Based on this evidence, we propose a model (Fig. 15) in which activation of repressive CoREST complex members may functionally activate JH signaling in reprogrammed Majors by repressing JH antagonists JHe, JHeh. JH signaling is known to activate foraging behavior in eusocial insects, and thus stable repression of JHe and JHeh by CoREST is a plausible pathway governing behavioral reprogramming by HDACi in *Cflo* Majors. Broadly, these results indicate epigenetic factors, such as RPD3, CoREST, and others are intimately involved in the induction and stabilization of caste-specific pathways. Importantly, we

detected differential regulation of a well-characterized steroid hormone pathway (e.g. JH/Ec). Thus, in this thesis work, we provide evidence for epigenetic control of behavioral identity and division of labor in ants, and establish *Cflo* caste identity as a model for behavioral epigenetics.

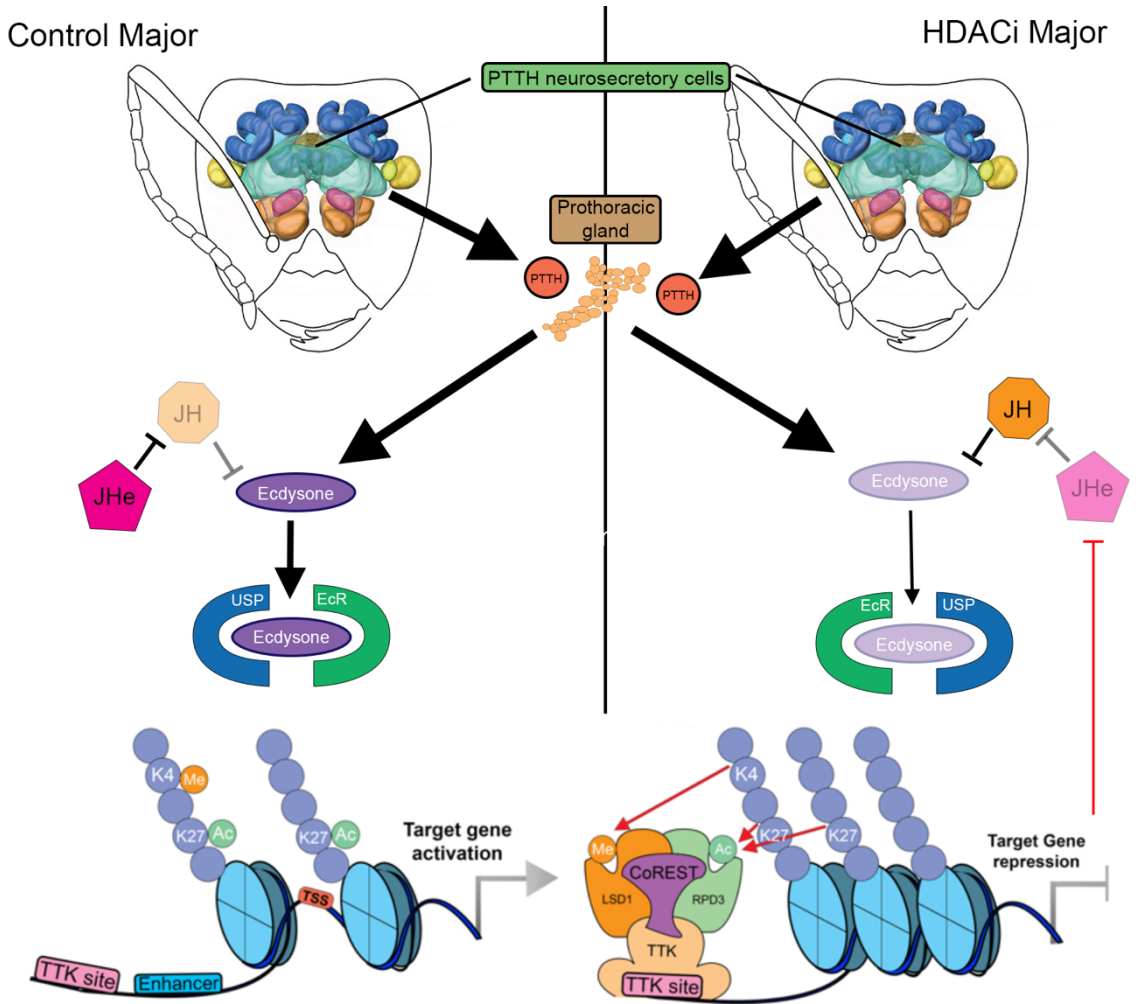


**Figure 15: Model for HDACi mediated repression of JHe by assembly of CoREST repressive complex members.**

In control Majors, JH is repressed by high JHe, thereby increasing ecdysone signalling and likely inhibiting foraging. (left side, orange octagon and magenta pentagon). *ttk* DNA binding sites are not bound, and H3K4 monomethylation (K4me, orange circle) and H3K27 acetylation (K27ac, green circle) maintain a relaxed euchromatic state that exposes TSS's (red rectangle) for target genes (e.g. *Jhe*), allowing transcriptional activation. Upon HDACi treatment (right side), activation of RPD3, CoREST, and *ttk* allows the assembly of the CoREST repressive complex (bottom right). RPD3 deacetylates H3K27ac targets upstream of target genes, and LSD1 demethylates enhancers, leading to establishment of a repressive heterochromatic state that blocks access to enhancers and TSS's of target genes. In the case of *JHe*, this repression is expected to lead to increased foraging behavior. (right side, red line indicating CoREST repression of *JHe*).

## **Materials and Methods**

### **Ant collection and husbandry**

Mated queens were collected from their nests in the Florida Keys in October and November of 2016. Mature colonies are kept in 270C Tupperware boxes with latching lids. Dental plaster is poured into nest boxes and allowed to harden and cure before ants are introduced. Boxes are treated with Fluon to prevent escape. Humidity is kept at 65% and temperature is constant at 40C with 12h/12h light/dark cycle. Colonies are fed sugar water and water ad libitum, and are provided with Bhatkar-Whitcombe diet and frozen superworm pieces twice per week.

### **Caste and age determination**

All workers used in this study were extracted from Queen-right natal nests. On the day of eclosion, callow workers are exceptionally light in color and exhibit callow-like behaviors. Major and Minor workers are identified based on morphological features described in detail in Chapter 2. Cohorts of callows which eclosed within 24 hours of one-another were removed from the nest and marked with a small dot of colored enamel paint on their gasters. After the paint dries (~5 min) they were returned to their natal nest. On the day of experimentation, painted individuals of known age were extracted from the nest based on paint color.

### **Untreated Cflo collection and dissection**

Untreated individuals were sampled from three colonies from unique collection sites in the Florida Keys to ensure genetic diversity among test colonies. Individual ants from three colonies were removed from the nest and painted as described above. Once paint marked, ants were returned to their maternal nest and reared under normal conditions for 5 or 10 days. On collection dates individuals were removed from the nest between 11:00-13:00, placed on ice until immobile, then transferred to a silicone (Sylgard, Dow Corning) dissection dish. Using forceps, we removed the antennae and then created an incision linking the two antennal pores. We then made two incisions from the antennal pores to the posterior of the head case midway between the dorsal-ventral and medial axes. The cuticle is then lifted up and removed, exposing the post-

pharyngeal gland (PPG), which is removed by grasping the base of the gland with forceps. We then separate the optic lobes from the central body (CB) and gently transfer the CB to a cold 25 $\mu$ L droplet of 1X HBSS. The brain is then 'cleaned' of vascular tissue and fat body contents. However, since fat body may infiltrate the CB to an extent, efforts to remove fat body did not supersede maintaining integrity of the dissected brain tissues. Once these tissues were removed, the brain was rinsed in a second 25 $\mu$ L droplet of cold 1X HBSS and transferred to 10 $\mu$ L of 1X HBSS in a pre-labelled 1.5mL microcentrifuge tube. The tube was then submerged in liquid Nitrogen and transferred directly into a -80C freezer.

### **mRNA-seq sample preparation**

Frozen brains in 10 $\mu$ L 1X HBSS were removed from the freezer and combined with cold (4°C) Trizol for 5 minutes on a rotating rack in a 4°C cold room, resulting in cell lysis and RNA stabilization via intercalation and RNase inhibition of Trizol. This solution was mixed with chloroform and nucleic acids were separated into a supernatant by ultracentrifugation. The nucleic acids were precipitated in cold isopropanol and washed in 70% and then 80% ethanol. Dried pellets were resuspended in the presence of DNases (Turbo DNase, Invitrogen) to digest genomic DNA. After digestion samples were placed in Trizol for a second round of nucleic acid precipitation, this time purifying total RNA in the eluate. Eluted total RNA was quantified by Qubit and quality of total RNA was inspected by BioAnalyzer. Total RNA samples were subjected to Poly A+ selection to purify and enrich mRNAs in the sample using the NEB Poly A+ selection module. mRNA libraries were generated from purified Poly A+ samples using the NEB Next Ultra II Directional mRNA-seq Kit and multiplexed for sequencing on an Illumina NextSeq500 platform.

### **RNA-seq analysis pipeline**

Bcl2fastq was used to demultiplex barcoded reads into individual samples. We aligned reads to the OGS v 3.3 *Camponotus* genome with RNASSTAR using a two-pass alignment strategy. In the first pass alignment, splice junctions were calculated for all samples and compiled in a splice junction data frame. Samples were then-realigned in a second pass alignment

command including splice site information. Bamfiles were processed with samtools, and loaded into FeatureCounts to generate raw count files. Raw counts were loaded into DESeq2 in R.

Untreated samples were combined into a single data frame and analyzed using a likelihood ratio test (LRT) to isolate transcriptional differences due to caste identity independent of age (e.g. expression =  $\text{Beta}(\text{Caste}) + \text{Beta}(\text{Age}) + (\text{Caste}) * (\text{Age})$ , reduced =  $\sim \text{Age}$ ), and vice versa (e.g. expression =  $\text{Beta}(\text{Caste}) + \text{Beta}(\text{Age}) + (\text{Caste}) * (\text{Age})$ , reduced =  $\sim \text{Caste}$ ). The interaction term ( $\text{Caste} * \text{Age}$ ) of this linear model was also analyzed for genes under different dynamics due to maturation in each caste. Replicates were combined and tested via Maximum Likelihood Estimation (MLE) comparisons. We tested individual timepoints, (e.g. DMSO 1h vs. TSA 1h; DMSO 3h vs. TSA 3h) and also combined all control and HDACi samples into a single comparison (1h+3h combined).

## **Injections**

Individual ants were removed from their nest and paint marked to track age. On the appropriate day, individuals were removed from the nest and placed on ice for 5 minutes or until anesthetized, whichever came first. Anesthetized ants were moved to a silicon injection surface under a Nikon SMZ 1000 dissecting microscope. A pin affixed to the end of a toothpick was used to create a small, shallow puncture in the cuticle along the sagittal plane of the head, just dorsal to the antennal pores and ventral to the eyes to avoid puncturing the post-pharyngeal glands. After perforation, a borosilicate glass needle loaded with injection material is positioned in the puncture using an Eppendorf InjectMan 2 system. Once the needle has penetrated the cuticle, a foot pedal is depressed causing an Eppendorf FemtoJet to release a controlled dose of injection material. Once 1ul has been injected, individuals are transferred to a 29C nest box for recovery for 5 minutes and, if necessary, marked before being returned to their maternal nest.

## **Foraging behavior analysis**

After recovery from injection, groups of 10 HDACi or control treated Majors were combined with 10 age-matched Minor workers and placed in 29C boxes with plaster floors

including a nest impression covered in red acetate to simulate a dark nest environment. 2ft lengths of tubing connect the nest box to an external foraging arena containing a depression for a plastic weigh boat. Weigh boats were filled with 20% sugar water and were the sole source of food. Pure water was supplied *ad libitum* in the nest box. Foraging activity was recorded using a Nikon D600 fired via remote timer every 6 minutes for the duration of the 10 day assay post-injection (240 hours, 2,400 total observations per nest).

### **Preparation of ChIP-seq samples**

For Native ChIP-seq, single ant brains were dissected into 10uL HBSS supplemented with protease inhibitors and the histone deacetylase inhibitor Na-butyrate (5mM final). Samples were kept on ice until proceeding to ChIP. For each batch of samples, a single *Harpegnathos saltator* brain was dissected for ChIP-RX spike-in.

### **Native ChIP-seq sample preparation**

Native ChIP was performed as in Brind'Amour et al. <sup>72</sup> with several modifications. Briefly, HBSS was removed from ant brains, which were promptly immersed in 20uL of EZ nuclei isolation buffer (Sigma: NUC101-1KT). Samples were incubated on ice for 10 minutes, followed by homogenization using a chilled insulin syringe. To this, MNase master mix was added containing 10X MNase buffer (NEB), DTT (2mM final), and MNase (2U\*uL<sup>-1</sup> final), and digestion was carried out at 37C for 10 minutes. Following digestion, reactions were halted with EDTA (10mM final), Triton-X and Na-deoxycholate were used to lyse nuclei (0.1% final), and approximately 5% *Harpegnathos saltator* chromatin was added for RX normalization. Following chromatin solubilization and pre-clearing, 30uL (~10%) of lysate was saved as input control. Lysate was then split and incubated overnight with antibodies conjugated to protein A and G beads. Following washes, chromatin was eluted from beads by incubating 2x with elution buffer (1% SDS, 50mM Tris-HCl, 10mM EDTA) at 65C for 1h, followed by Phenol Chloroform extraction and Ethanol DNA precipitation. Samples were subjected to a second round of purification using

Ampure XP beads (2x), and sequencing libraries were prepared using the NEB Ultra II DNA library preparation kit (NEB: E7645L).

### ChIP-seq analysis pipeline

Sequencing reads were trimmed for quality and adapter contamination using trimmomatic<sup>73</sup> followed by alignment to a composite *Hsal+Cflo* reference genome using bowtie2<sup>74</sup> (settings: --local -X 1000). Peaks were called with macs2 in paired-end mode<sup>75</sup> (BAMPE). Differential peak calling was performed using the replicate aware software PePr (settings: --normalization intergroup --threshold 1e-4 -f bampe --diff --peaktype sharp --keep-max-dup 2) and Diffbind<sup>76</sup>. For Diffbind analyses the program DESeq2<sup>17</sup> was used for significance testing, using a blocking factor (batch for all single-timepoint TSA vs DMSO tests, hours-post-injection when combining injection timepoints). Differential peaks were linked to genes using a custom perl script. Metaplots were produced using seqplots. Tracks were produced using macs2 input-subtracted bedgraphs (macs2 bdgcmp) converted to bigwig files (bedGraphToBigWig).

### Chapter 3 Bibliography

1. Hölldobler, Bert, and Edward O. Wilson. *The ants*. Harvard University Press, 1990.
2. Wheeler, Diana E. "The developmental basis of worker caste polymorphism in ants." *The American Naturalist* 138.5 (1991): 1218-1238.
3. Wilson, Edward O. "The origin and evolution of polymorphism in ants." *The Quarterly Review of Biology* 28.2 (1953): 136-156.
4. Simola, Daniel F., et al. "Epigenetic (re) programming of caste-specific behavior in the ant *Camponotus floridanus*." *Science* 351.6268 (2016): aac6633.
5. Yan, Hua, et al. "Eusocial insects as emerging models for behavioural epigenetics." *Nature Reviews Genetics* 15.10 (2014): 677.
6. Wheeler, Diana E., and H. Frederik Nijhout. "Soldier determination in ants: new role for juvenile hormone." *Science* 213.4505 (1981): 361-363.

7. Jindra, Marek, Subba R. Palli, and Lynn M. Riddiford. "The juvenile hormone signaling pathway in insect development." *Annual review of entomology* 58 (2013): 181-204.
8. Penick, Clint A., Steven S. Prager, and Jürgen Liebig. "Juvenile hormone induces queen development in late-stage larvae of the ant *Harpegnathos saltator*." *Journal of insect physiology* 58.12 (2012): 1643-1649.
9. Rajakumar, Rajendhran, et al. "Ancestral developmental potential facilitates parallel evolution in ants." *Science* 335.6064 (2012): 79-82.
10. Walsh, Justin T., et al. "Ant nurse workers exhibit behavioural and transcriptomic signatures of specialization on larval stage." *Animal Behaviour* 141 (2018): 161-169.
11. Linksvayer, Timothy A., et al. "Developmental evolution in social insects: regulatory networks from genes to societies." *Journal of Experimental Zoology Part B: Molecular and Developmental Evolution* 318.3 (2012): 159-169.
12. Robinson, Gene E. "Regulation of honey bee age polyethism by juvenile hormone." *Behavioral Ecology and Sociobiology* 20.5 (1987): 329-338.
13. Liu, Suning, et al. "Antagonistic actions of juvenile hormone and 20-hydroxyecdysone within the ring gland determine developmental transitions in *Drosophila*." *Proceedings of the National Academy of Sciences* 115.1 (2018): 139-144.
14. Li, Kang, Qiang-Qiang Jia, and Sheng Li. "Juvenile hormone signaling—a mini review." *Insect science* (2018).
15. Simola, Daniel F., et al. "A chromatin link to caste identity in the carpenter ant *Camponotus floridanus*." *Genome Research* (2012): gr-148361.
16. Yan, Hua, et al. "Eusocial insects as emerging models for behavioural epigenetics." *Nature Reviews Genetics* 15.10 (2014): 677.
17. Love, Michael I., Wolfgang Huber, and Simon Anders. "Moderated estimation of fold change and dispersion for RNA-seq data with DESeq2." *Genome biology* 15.12 (2014): 550.
18. Alexa, Adrian, and Jorg Rahnenfuhrer. "topGO: enrichment analysis for gene ontology." *R package version 2.0* (2010).
19. Supek, Fran, et al. "REVIGO summarizes and visualizes long lists of gene ontology terms." *PloS one* 6.7 (2011): e21800.
20. Konogami, Tadafumi, Kazuki Saito, and Hiroshi Kataoka. "Prothoracicotropic Hormone." *Handbook of Hormones*. 2015. 407-e55.
21. Yamanaka, Naoki, Kim F. Rewitz, and Michael B. O'Connor. "Ecdysone control of developmental transitions: lessons from *Drosophila* research." *Annual review of entomology* 58 (2013): 497-516.

22. Aguilera, Miguel, et al. "Ariadne-1: a vital *Drosophila* gene is required in development and defines a new conserved family of ring-finger proteins." *Genetics* 155.3 (2000): 1231-1244.
23. Jenkins, Yonchu, et al. "Critical role of the ubiquitin ligase activity of UHRF1, a nuclear RING finger protein, in tumor cell growth." *Molecular biology of the cell* 16.12 (2005): 5621-5629.
24. Espinosa, Alexander, et al. "The Sjögren's syndrome-associated autoantigen Ro52 is an E3 ligase that regulates proliferation and cell death." *The Journal of Immunology* 176.10 (2006): 6277-6285.
25. Upadhyay, Arun, et al. "E3 ubiquitin ligases neurobiological mechanisms: development to degeneration." *Frontiers in molecular neuroscience* 10 (2017): 151.
26. Kuo, Chay T., et al. "Identification of E2/E3 ubiquitinating enzymes and caspase activity regulating *Drosophila* sensory neuron dendrite pruning." *Neuron* 51.3 (2006): 283-290.
27. Ashraf, Waseem, et al. "The epigenetic integrator UHRF1: on the road to become a universal biomarker for cancer." *Oncotarget* 8.31 (2017): 51946.
28. Gradilla, Ana-Citlali, Alicia Mansilla, and Alberto Ferrús. "Isoform-specific Regulation of a Steroid Hormone Nuclear Receptor by an E3 Ubiquitin Ligase in *D. melanogaster*." *Genetics* (2011): genetics-111.
29. Khlebodarova, T. M., et al. "A comparative analysis of juvenile hormone metabolizing enzymes in two species of *Drosophila* during development." *Insect biochemistry and molecular biology* 26.8-9 (1996): 829-835.
30. Gisselmann, Günter, et al. "*Drosophila melanogaster* GRD and LCCH3 subunits form heteromultimeric GABA-gated cation channels." *British journal of pharmacology* 142.3 (2004): 409-413.
31. Cheung, Samantha K., and Kristin Scott. "GABAA receptor-expressing neurons promote consumption in *Drosophila melanogaster*." *PloS one* 12.3 (2017): e0175177.
32. Delgado, Teresa Cardoso. "Glutamate and GABA in appetite regulation." *Frontiers in endocrinology* 4 (2013): 103.
33. Kucharski, Robert, et al. "Nutritional control of reproductive status in honeybees via DNA methylation." *Science* 319.5871 (2008): 1827-1830.
34. Vertino, Paula M., et al. "DNMT1 is a component of a multiprotein DNA replication complex." *Cell cycle* 1.6 (2002): 416-423.
35. Hon, Gary C., R. David Hawkins, and Bing Ren. "Predictive chromatin signatures in the mammalian genome." *Human molecular genetics* 18.R2 (2009): R195-R201.
36. Ng, Huck Hui, et al. "Targeted recruitment of Set1 histone methylase by elongating Pol II provides a localized mark and memory of recent transcriptional activity." *Molecular cell* 11.3 (2003): 709-719.

37. Elaut, G., et al. "Major phase I biotransformation pathways of Trichostatin a in rat hepatocytes and in rat and human liver microsomes." *Drug metabolism and disposition* 30.12 (2002): 1320-1328.
38. Sanderson, Lisa, et al. "Plasma pharmacokinetics and metabolism of the histone deacetylase inhibitor trichostatin a after intraperitoneal administration to mice." *Drug metabolism and disposition* (2004).
39. Elaut, G., et al. "A metabolic screening study of trichostatin A (TSA) and TSA-like histone deacetylase inhibitors in rat and human primary hepatocyte cultures." *Journal of Pharmacology and Experimental Therapeutics* 321.1 (2007): 400-408.
40. Lorca, Thierry, et al. "Fizzy is required for activation of the APC/cyclosome in *Xenopus* egg extracts." *The EMBO journal* 17.13 (1998): 3565-3575.
41. Bashir, Tarig, et al. "Control of the SCF Skp2–Cks1 ubiquitin ligase by the APC/C Cdh1 ubiquitin ligase." *Nature* 428.6979 (2004): 190.
42. Unoki, Motoko, Julie Brunet, and Marc Mousli. "Drug discovery targeting epigenetic codes: the great potential of UHRF1, which links DNA methylation and histone modifications, as a drug target in cancers and toxoplasmosis." *Biochemical pharmacology* 78.10 (2009): 1279-1288.
43. Hashimoto, Hideharu, et al. "UHRF1, a modular multi-domain protein, regulates replication-coupled crosstalk between DNA methylation and histone modifications." *Epigenetics* 4.1 (2009): 8-14.
44. Rothbart, Scott B., et al. "Association of UHRF1 with methylated H3K9 directs the maintenance of DNA methylation." *Nature Structural and Molecular Biology* 19.11 (2012): 1155.
45. Smith, Edwin, and Ali Shilatifard. "Transcriptional elongation checkpoint control in development and disease." *Genes & development* 27.10 (2013): 1079-1088.
46. Jiang, Yan, et al. "Involvement of transcription termination factor 2 in mitotic repression of transcription elongation." *Molecular cell* 14.3 (2004): 375-386.
47. Baldan, Federica, et al. "Synergy between HDAC and PARP inhibitors on proliferation of a human anaplastic thyroid cancer-derived cell line." *International journal of endocrinology* 2015 (2015).
48. Zhao, Lan, et al. "Histone deacetylation inhibition in pulmonary hypertension: therapeutic potential of valproic acid (VPA) and suberoylanilide hydroxamic acid (SAHA)." *Circulation* (2012): CIRCULATIONAHA-112.
49. Li, Feng, et al. "The histone mark H3K36me3 regulates human DNA mismatch repair through its interaction with MutS $\alpha$ ." *Cell* 153.3 (2013): 590-600.
50. Meier, Karin, et al. "LINT, a novel dL (3) mbt-containing complex, represses malignant brain tumour signature genes." *PLoS genetics* 8.5 (2012): e1002676.

51. Boccuni, Piernicola, et al. "The human L (3) MBT polycomb group protein is a transcriptional repressor and interacts physically and functionally with TEL (ETV6)." *Journal of Biological Chemistry* 278.17 (2003): 15412-15420.
52. Menezes, Joao RL, et al. "The division of neuronal progenitor cells during migration in the neonatal mammalian forebrain." *Molecular and Cellular Neuroscience* 6.6 (1995): 496-508.
53. Matsuzawa, Mieko, et al. "Directional neurite outgrowth and axonal differentiation of embryonic hippocampal neurons are promoted by a neurite outgrowth domain of the B2-chain of laminin." *International journal of developmental neuroscience* 14.3 (1996): 283-295.
54. Murakoshi, Hideji, Hong Wang, and Ryohei Yasuda. "Local, persistent activation of Rho GTPases during plasticity of single dendritic spines." *Nature* 472.7341 (2011): 100.
55. Hall, Alan, and Giovanna Lalli. "Rho and Ras GTPases in axon growth, guidance, and branching." *Cold Spring Harbor perspectives in biology* (2010): a001818.
56. Yamada, Tomohiro, et al. "RA-RhoGAP: Rap-activated Rho GTPase-activating protein implicated in neurite outgrowth through Rho." *Journal of Biological Chemistry* (2005).
57. Kasai, Kenji, et al. "The G12 family of heterotrimeric G proteins and Rho GTPase mediate Sonic hedgehog signalling." *Genes to Cells* 9.1 (2004): 49-58.
58. Jenkins, Dagan. "Hedgehog signalling: emerging evidence for non-canonical pathways." *Cellular signalling* 21.7 (2009): 1023-1034.
59. Teperino, Raffaele, et al. "Canonical and non-canonical Hedgehog signalling and the control of metabolism." *Seminars in cell & developmental biology*. Vol. 33. Academic Press, 2014.
60. Varga, Zoltán M., et al. "Zebrafish smoothed functions in ventral neural tube specification and axon tract formation." *Development* 128.18 (2001): 3497-3509.
61. Chen, James K., et al. "Small molecule modulation of Smoothed activity." *Proceedings of the National Academy of Sciences* 99.22 (2002): 14071-14076.
62. Lunyak, Victoria V., and Michael G. Rosenfeld. "No rest for REST: REST/NRSF regulation of neurogenesis." *Cell* 121.4 (2005): 499-501.
63. Gao, Zhengliang, et al. "The master negative regulator REST/NRSF controls adult neurogenesis by restraining the neurogenic program in quiescent stem cells." *Journal of Neuroscience* 31.26 (2011): 9772-9786.
64. Ballas, Nurit, and Gail Mandel. "The many faces of REST oversee epigenetic programming of neuronal genes." *Current opinion in neurobiology* 15.5 (2005): 500-506.
65. Lu, Tao, et al. "REST and stress resistance in ageing and Alzheimer's disease." *Nature* 507.7493 (2014): 448.

66. Cunliffe, Vincent T. "Eloquent silence: developmental functions of Class I histone deacetylases." *Current opinion in genetics & development* 18.5 (2008): 404-410.
67. Roche, Joëlle, Robert M. Gemmill, and Harry A. Drabkin. "Epigenetic Regulation of the Epithelial to Mesenchymal Transition in Lung Cancer." *Cancers* 9.7 (2017): 72.
68. Dallman, Julia E., et al. "A conserved role but different partners for the transcriptional corepressor CoREST in fly and mammalian nervous system formation." *Journal of Neuroscience* 24.32 (2004): 7186-7193.
69. Shi, Yu-Jiang, et al. "Regulation of LSD1 histone demethylase activity by its associated factors." *Molecular cell* 19.6 (2005): 857-864.
70. Zhang, Yanxiao, et al. "PePr: a peak-calling prioritization pipeline to identify consistent or differential peaks from replicated ChIP-Seq data." *Bioinformatics* 30.18 (2014): 2568-2575.
71. Orlando, David A., et al. "Quantitative ChIP-Seq normalization reveals global modulation of the epigenome." *Cell reports* 9.3 (2014): 1163-1170.
72. Brind'Amour, Julie, et al. "An ultra-low-input native ChIP-seq protocol for genome-wide profiling of rare cell populations." *Nature communications* 6 (2015): 6033.
73. Bolger, Anthony M., Marc Lohse, and Bjoern Usadel. "Trimmomatic: a flexible trimmer for Illumina sequence data." *Bioinformatics* 30.15 (2014): 2114-2120.
74. Langmead, Ben, and Steven L. Salzberg. "Fast gapped-read alignment with Bowtie 2." *Nature methods* 9.4 (2012): 357.
75. Feng, Jianxing, et al. "Identifying ChIP-seq enrichment using MACS." *Nature protocols* 7.9 (2012): 1728.
76. Stark, Rory, and Gordon Brown. "DiffBind: differential binding analysis of ChIP-Seq peak data." *R package version* 100 (2011): 4-3.

## Chapter 4: Discussion

### Histone acetylation dynamics influence caste identity and behavior

We have established that histone post-translational modifications (hPTMs) are important epigenetic mechanisms regulating transcriptional differences between morphological and behavioral castes in the ant *Camponotus floridanus* (*Cflo*)<sup>1,2</sup>. An epigenomics survey of hPTMs in *Cflo* worker castes detected caste-specific patterns of histone H3, lysine 27 acetylation (H3K27ac) prominently among a number of hPTMs altered between castes<sup>1</sup>. Importantly, these hPTMs correlated with caste-specific patterns of transcription. In addition to morphological differences between castes, we observed biases in foraging behavior. Minors forage significantly more than Majors in a variety of contexts<sup>2</sup>. We asked whether histone acetylation in neurological tissues regulates caste-specific behaviors. To address this question, we manipulated the activity of histone modifying enzymes by treating ants with histone deacetylase inhibitors (HDACi) and histone acetyltransferase inhibitors (HATi). We found that HDACi increased foraging and scouting, and co-treatment of HDACi and HATi blocked this increase in foraging<sup>2</sup>. Of great interest, we did not detect significant increases in Major foraging behavior after HDACi in adults.

We thus hypothesized that epigenetic systems contributing to caste differentiation may be stabilized at maturity compared to juveniles, and developed methods to treat d0-d1 (i.e. callow) workers with precise treatment doses. We injected callow Majors with HDACi within their heads, and then observed a persistent increase in Minor-like foraging behavior in treated Majors. Minor-like foraging was maintained for >30 days after injection, suggesting that HDACi injection into callow Majors caused a form of stable behavioral 'reprogramming'<sup>2</sup>. Co-treatment of HDACi plus HATi blocked this effect, arguing foraging is downstream of changes in histone acetylation, and is regulated by HAT and HDAC enzymes. Importantly, HATi treatment specifically inhibited the catalytic HAT domain of the co-activator CREB Binding Protein (CBP). CBP and its target modification, H3K27ac, have established functions in learning and memory, and therefore our

observation of HATi dependent changes in foraging suggest that dynamic H3K27ac downstream of CBP may contribute to caste-specific behavioral control.

Based on these observations, we predicted that caste-specific differences in transcription and epigenetic function are linked to processes establishing caste-identity and maturation. To examine this, we characterized naturally occurring differences in transcription during early maturation using a time-course of RNA-seq. This analysis revealed opposing JH and Ec factors (e.g. PTTH, Ari-1) that are differentially regulated in the brain of Major and Minor castes. We also detected caste-specific expression of JH/Ec factors, neurotransmitter receptors, circadian clock genes, heat shock proteins, and other factors relevant to caste-specific phenotypes from behavior to longevity (details in Ch. 3).

### **Ecdysteroid and JH signaling is linked to HDAC function**

Invertebrate and vertebrate species rely on steroid hormones to regulate transitions from juvenile states to maturation.<sup>7</sup> In holometabolous insects (i.e. those with complete metamorphosis), once growth in a particular larval stage has reached a critical threshold, JH levels decline and PTTH secretory neurons are activated<sup>8</sup>. PTTH activation stimulates ecdysone release by the PG, thereby inducing ecdysis and transition to the next larval stage<sup>9</sup>. JH is directly and indirectly antagonized by ecdysone<sup>10</sup>, and thus our observation that PTTH is upregulated in Majors indicates variable JH levels may influence *Cflo* foraging.

Additionally, a role for PTTH in light avoidance has been established in *Dmel*<sup>11</sup>, which may indicate that JH level and light avoidance are potentially cooperative response thresholds downstream of PTTH that suppress Major foraging in *Cflo*. In this model, attention to foraging stimuli (e.g. trail pheromone, scout recruitment) is accompanied by JH activation in Minors, but is blocked by PTTH in Majors. PTTH concurrently increases light avoidance, thereby influencing Majors to remain in the subterranean nest environment. In this way, multiple response thresholds may cooperate in the sophisticated control of caste-specific behaviors exhibited in *Cflo*<sup>12</sup>.

## **Minor GABA and Grd expansion supports GABA role in DoL**

In our analyses of innate transcriptional differences between Major and Minor brains in early maturation, we detected significant enrichment of DEGs and GO terms related to GABA signaling in Minors. These results are relevant to differences in foraging activity, because GABA and glutamate are known to regulate appetite and feeding behavior from invertebrates to mammals <sup>13,14</sup>.

Further, GABAergic neuron activity is associated with foraging behavior in honey bee <sup>15</sup>, and GABA stimulation induces feeding behavior in Mollusca <sup>16</sup>. Thus, we predict that increased GABA signaling in Minor brains may serve to alter 'appetite' or desire to engage in foraging behavior.

Strikingly, we detected a significantly upregulated paralog of the GABA receptor subunit (e.g. *Grd*, *Grd2*) in *Cflo*, which is not found in *Dmel* <sup>17</sup>. This suggests ants possess a second copy of *Grd*, which may have evolved novel function contributing to caste-specific patterns of foraging behavior. An important follow up to this observation will be an analysis of *Grd* and *Grd2* receptor subunits in eusocial vs. solitary insects. We predict the expansion of GABA receptor subunits may correspond with evolution of eusocial behaviors. Further, as Queens do not forage at all, we predict that a comparison of Major, Minor, and Queen GABA expression will exhibit significant differences between reproductive and worker castes.

## **Caste DEGs have established function in circadian clock regulation**

Naturally occurring ecdysteroid hormone rhythms during insect development have been well-documented, and PTTH is emerging as a central factor controlling circadian rhythm in adult insects <sup>18</sup>. PTTH has been linked to signaling between central clock (sLN<sub>v</sub>) neurons in the brain and peripheral clock (PG) neurons in the prothoracic gland of *Dmel*. sLN<sub>v</sub> neurons project to PTTH neurons and secrete sNPF, which activates PTTH signaling to the PG, resulting in ecdysone release and molting. Importantly, the specific relevance of circadian *Dmel* orthologs in *Cflo* rhythmic behaviors has been demonstrated at the neurobiological level <sup>19</sup>. Minors exhibit

rhythmic free running locomotion in constant darkness, and expression of the circadian gene PERIOD (PER) oscillates in central clock neurons on a light/dark cycle.

Our observations suggest differential expression of PTTH in Major and Minor brains may set up a form of 'molecular heterochrony', or separation of the timing of transcriptional cascades between castes. Foraging is a strongly circadian behavior in *Cflo*, and circadian clock pathways are known to influence a number of downstream targets. Thus alternative circadian cycles in Major and Minor workers may represent an additional layer of molecular control over foraging behavior, and highlight ways in which molecular heterochrony may induce DoL in *Cflo*. One way to experimentally address this possibility in follow up studies is to capture circadian differences between castes by sampling brains for RNA-seq in a time course across a 24 hour day/night cycle in day 0, day 5, and day 10 workers. However, because the relevance of clock genes like PERIOD have been established in *Cflo*, another approach will be to design qPCR primers against established circadian genes and probe for caste-specific molecular heterochrony.

### **Neuropeptides corazonin and neuroparsin antagonize vitellogenin in non-reproductive workers**

The neuropeptide *corazonin* (*crz*) has been identified as a regulator of behavioral caste identity in the ant *Harpegnathos saltator* (*Hsal*)<sup>20</sup>. *Hsal* hunts live prey, and *crz* expression is upregulated in hunting workers, who exhibit low *vitellogenin* (*vg*) levels. Workers in this species are facultatively sterile, and when they transition to their reproductively active state (known as gamergates), hunting behavior and *crz* levels fall and *vg* levels rise in the brain. An additional neuropeptide, neuroparsin (NPLP), is tied to expression of the corazonin receptor in *Hsal*, and is known to antagonize *vg* levels in other invertebrates<sup>21</sup>. Both *crz* and *NPLP* are upregulated in *Cflo* Majors (Ch. 3, Fig. 1E), indicating neuropeptide differences influence neuronal signaling between castes. *Cflo* does not hunt live prey, but Majors are often called 'soldiers' due to their vigilance in detecting and attacking nest intruders. Elevated *crz* and *NPLP* levels in the brain may therefore contribute to nest defense in Majors, which anecdotally shares behavioral elements with hunting, such as aggression.

We find further support for a conserved antagonistic relationship between *vg* and *crz*/*NPLP* in the Minor DEG apolipoprotein lipid transfer particle (*apoLTP*, CFLO18090, Ch. 3, Fig. 1E). *ApoLTP* is a haemolymph lipid carrier which contains a *vitellogenin* open beta sheet domain (lipovitellin-1), that may be cleaved to produce *vg* precursors<sup>22,23</sup>. Interestingly, *apoLTP* expression is the most significantly upregulated DEG in Minors. The observed pattern of *apoLTP* expression during maturation is similar to vitellogenin-1 (*vg*, CFLO22478), and is inversely related to *crz* and *NPLP* levels, supporting the established model for these neuropeptides as antagonists of *vg* expression. Our findings expand this model into sterile dimorphic worker castes, and indicate non-reproductive behaviors are also influenced by interactions among *crz*, *NPLP*, and *vg*. Thus, *crz*, *NPLP*, and *apoLTP* may comprise an additional neuropeptide pathway contributing to DoL between *Cflo* worker castes.

### **Elevated heat shock protein in Majors signals a role in caste longevity**

Maximum lifespan is one of the most dramatic phenotypic differences found among *Cflo* individuals within a colony. Whereas mated queens have survived longer than 10 years in the laboratory, Majors typically live no longer than 18 months, and Minors rarely live longer than 9 months. Despite these striking differences in maximum lifespan, little is known about how aging and lifespan are alternatively regulated among Queen, Major, and Minor phenotypic states. One hypothesis is that baseline levels of anti-aging factors are different between castes, setting up differences in the biological clock of aging. Heat shock proteins (HSPs) and their partners are notable in the context of aging, because they enhance protein homeostasis and reduce the occurrence of misfolded proteins under stress, including age related stressors<sup>24</sup>. HSPs have previously been identified as important regulators of aging, and deficiencies in these proteins lead to premature aging and senescence phenotypes in insect models<sup>25</sup>.

We observe upregulated heat shock protein 22 (*Hsp22*, CFLO16301, *padj*<0.01), heat shock protein 60 (*Hsp60*, CFLO13180, *padj*<.05) and heat shock protein cognate 70-1 (*Hsc70-1*, CFLO23110, *padj*<0.01) in the long-lived Major worker caste (Ch. 3, Fig. 1E). In light of the

established role for Hsps in stress resilience, these results suggest Majors may be buffered against stressors, including aging, at the proteomic level. Notably, whereas *Hsp22* and *Hsc70-1* begin lowly expressed and rise during maturation, *Hsp60* levels begin high in Major at da0, supporting the hypothesis that baseline levels of HSPs are distinct in castes regardless of age.

### **DEGs in untreated samples indicate targeted transcriptional differences in behaviorally relevant pathways between castes.**

Together, our findings in untreated Major and Minor workers indicate gene regulatory differences during development initiate alternative transcriptional programs. Importantly, we have found persistent caste-specific difference at adulthood, suggesting epigenetic and transcriptional differences are 'set up' during larval and pupal development, and continue to modulate caste identity in adulthood. In some ways, these results contradict the prevailing hypothesis that neurologic systems are mature at eclosion in insects, and raises the possibility that the early stages of adulthood represent a period of enhanced transcriptional (and therefore behavioral) plasticity. Indeed, our findings in HDACi treated Majors support a model in which d0-d5 individuals exist in a period of epigenetic malleability, whereas d10 individuals have a characteristically stable epigenetic status.

### **One Really Interesting New Gene to rule them all**

E3 ligases, and RING-domain containing E3 ligases in particular, have gained attention in recent years as regulators of intracellular protein levels. A number of epigenetic factors have demonstrated E3 ligating activity (e.g. LSD2) or have RING E3 ligase cofactors (e.g. DNMT1)<sup>28</sup>. Fizzy (*fzy*) is an E3 ligase orthologous to mammalian cell division cycle protein 20 (Cdc20). Along with Cdh-1, Cdc20/*fzy* is a central regulatory subunit of the anaphase promoting complex (APC), which also contains RING domain E3 ligase APC11<sup>29</sup>. In the context of APC, *fzy* association (Cdc20-APC) activates substrate specificity and catalytic function of APC<sup>30</sup>. During mammalian cell cycle progression, mitotic exit is induced by Cdc20-APC dependent cyclin B1 degradation,

suggesting APC interaction with Fzy's mammalian homolog is essential for processes regulating the timing of development.

Recent evidence suggests Cdc20-APC promotes self-renewal and invasiveness of human glioblastomas<sup>31</sup>, signifying the importance of *fzy* in orchestrating neural cell identity and proliferation. *Fzy* is lowly expressed in untreated d0 workers, and is upregulated during maturation in both castes, signaling a role in adult nervous system development and function. Further, *fzy* is the sole caste-specific DEG that is also induced by HDACi (Fig. 3A, 3B), strongly advocating the importance of this gene and E3 ligases overall in programming DoL. A diverse set of nervous tissue functions are associated with APC, notably the regulation of synaptic connectivity and plasticity in developing and mature brains<sup>32</sup>. Our findings raise the possibility that E3 ligases and *fzy* in particular alter CNS structure and function both naturally between *Cflo* castes, and during behavioral reprogramming.

We observed in HDACi treatment, activation of S-phase kinase associated protein 2 (*Skp2*, CFLO14056, Fig. 3A, 3B), and non-significant but consistent upregulation of *Skp2*'s cofactor, *Cks1* (CFLO27000). *Skp2* is also found in a multi-subunit complex containing a RING E3 ligase (*Rbx1*) and is a substrate targeting factor in CUL1-*Rbx1*-*Skp1*-F-box<sup>*Skp2*</sup> (SCF) complexes<sup>33</sup>. *Skp2* is a direct target of activated APC, and has been the focus of much interest due to its oncogenic activity in humans and established function during neuronal differentiation in the mammalian cortex<sup>34,35</sup>. In insects, *Skp2* has been shown to target *Dacapo* (*Dap*), the *Dmel* homologue of cyclin-dependent kinase inhibitors (p21/p27/p57), for ubiquitination, and is therefore a positive regulator of cell cycle progression<sup>36</sup>. While *Skp2* function in cell cycle has been extensively studied, its role in differentiation in the nervous system is less understood. *Skp2* is involved in regulating differentiation of primary neurons in *Xenopus*: depletion of *Skp2* results in generation of extra primary neurons, whereas *Skp2* overexpression reduces the number of primary neurons formed<sup>37</sup>. Thus, *Skp2* upregulation may block neural progenitor cell maintenance programs and activate neuronal differentiation pathways.

An additional upregulated DEG encoding a RING domain-containing E3 Ligase is Ubiquitin-like containing PHD and RING finger domains 1 (UHRF1, CFLO20095; Ch. 3, Fig 3A, 3B). This protein binds to hemi-methylated DNA during S-phase and recruits DNMT1 to maintain DNA-methylation fidelity<sup>38</sup>. UHRF1 is also a key epigenetic regulator of histone post-translational modifications, and contains five established domains, including a tandem tudor domain (TTD) which binds H3K9me3, and a plant homeodomain (PHD) that binds the tail of histone H3<sup>39</sup>. In this way, UHRF1 is considered a key factor linking DNA methylation and histone modifications.

In untreated *Cflo*, UHRF1 exhibits an overlapping expression pattern similar to DNMT1, in that it is lowly expressed in d0 individuals, upregulated at d5, and then repressed in d10. As we have previously noted, this may signal increased epigenetic plasticity in day 5 individuals, and overall these data suggest UHRF1, and RING domain E3 ligases in general, have important roles in regulation of chromatin structure and neuronal cell identity in juvenile *Cflo* brains. Additionally, to our knowledge this is the first experimental evidence linking UHRF-1 to DNA methylation agents in insects, perhaps due to the lack of DNA methylation machinery in *Drosophila*. Together, these results highlight the emerging importance of E3 ligases in epigenetic control, argue that E3 ligases interact with HDAC machinery, and link DNA methylation factors to the epigenetic bridging capabilities of UHRF-1 in insects.

### **Manipulation of HDAC function reprograms behavior and transcription**

We observed reprogramming of foraging behavior in callow Majors, but did not detect reprogramming in adult Majors after HDACi. Thus, we hypothesized that the earliest stages of adult life (i.e. post-eclosion) represent a period of epigenetic and behavioral plasticity, which ends later in life to facilitate the rigid behavioral caste-identity characteristic of *Cflo*. To survey behavioral sensitivity to HDACi in early life we injected d0, d5, and d10 Major workers with HDACi and observed their foraging behavior. We detected a modest but significant foraging enhancement in d0 Majors, replicating our published results. Strikingly, we observed a dramatic increase in foraging activity in d5 Majors, and a non-significant change in foraging in d10 Majors.

Thus, we hypothesized the window of behavioral reprogramming confers susceptibility in d0-d5 Majors, and block susceptibility after d10.

We sought to understand the transcriptional and epigenetic dynamics caused by HDACi in reprogramming, and thus prepared HDACi-injected d5 Majors for RNA-seq and ChIP-seq. We observed a rapid, targeted, and robust transcriptional response to HDACi in d5 Majors, and did not detect a strong differential transcriptional response in d10 Majors. D5 Majors exhibited reproducible transcriptional induction of several RING-E3 ligases, chromatin modifying proteins, and cell cycle factors.

### **Current model for stable reprogramming of foraging behavior by HDACi**

Our findings indicate stable reprogramming of foraging behavior is achieved for >30 days after treatment with HDACi in d0 callow Major workers. This result is striking considering the relatively short half-life of HDACi treatments *in vivo*, and suggests that epigenetic factors induced by HDACi may form stable feedback loops of gene activation or repression which serve to extend behavioral reprogramming after the direct effect of HDACi has diminished. Additionally, when we characterized HDACi sensitive genes, we noted that 17% of DEGs were downregulated by HDACi. This result suggests that direct effects of HDACi activating repressive regulatory complexes, which then secondarily target downstream genes for silencing.

Supporting this hypothesis, we detected consistent upregulation of the repressive CoREST epigenetic complex after HDACi, as well as of its DNA binding cofactor tramtrack and repressive histone modifying cofactor RPD3/HDAC1. Together, these complex members plausibly assemble into a 'mature' CoREST repressive complex before silencing downstream targets. Interestingly, the most intense downregulation of DEGs is detected when animals are harvested 3h after HDACi treatment, which is the same timepoint exhibiting upregulation of the DNA-binding factor (ttk) for CoREST. Thus, one model for reprogramming is direct, immediate (e.g. 1 hour) stimulation of RPD3, CoREST, and other HDACi induced genes cause indirect (e.g. 3 hour) activation of tramtrack through an unknown downstream regulatory mechanism. DNA

binding of ttk to its DNA response elements then recruits the CoREST complex to silence target genes. Juvenile hormone esterase (JHe) and Juvenile hormone epoxide hydrolase (JHeh) are two important regulators of juvenile hormone (JH) levels. Increased JH is associated with behavioral transitions from nursing to foraging. Importantly for this model, we detect downregulation of JHe and JHeh 3h, but not 1h, after HDACi treatment. Downregulation of JH antagonists is expected to elevate JH levels. Thus, we hypothesize that the mature CoREST complex or another HDACi induced silencing complex assembles upstream of JHe and JHeh and causes stable repression of these genes.

To address this hypothesis, we compared changes in H3K27ac and H3K27me3 enrichment in individual brains after HDACi by ChIP-seq. We detected the strongest enrichment of H3K27ac peaks 1h after injection, and found H3K27me3 peaks are not consistently altered by HDACi treatment, supporting acetylation-specific effects of HDACi. Comparing to H3K27ac-gained peaks 1h after HDACi, we detect modest enrichment after 3h, and lower enrichment in control samples. These results mirror our transcriptional findings, in that 1h appears to be the most dramatic timepoint for transcriptional and hPTM differences caused by HDACi. We compared K27ac and K27me3 peaks over 1h upregulated HDACi DEGs, and detected a similar pattern, in which K27ac peaks are enriched in 1h and 3h HDACi treatments compared with controls. Finally, we averaged hPTM enrichment over TSS's for the list of 20 DEGs that overlap 1h and 3h comparisons between HDACi and control. Similarly, we detect the greatest enrichment at 1h, modest enrichment at 3h, and lower enrichment in controls. As before, we do not detect consistent patterns of H3K27me3 response to HDACi in any of these comparisons. We then examined individual genes, and found that whereas RPD3 and CoREST gain H3K27ac peaks upstream of their TSS, JHe and JHeh exhibit an upstream loss of H3K27ac after HDACi. Taken together, these results indicate H3K27ac is a key target of HDACi treatments, and argue that direct activation of RPD3/CoREST/ttk by increased H3K27ac enrichment may serve to activate the CoREST repressive complex, which in turn deacetylates histones upstream of key regulators of foraging behavior, JHe and JHeh, serving to repress them.

## Future directions

We present evidence supporting a role for histone acetylation, and specifically H3K27ac, in programming differences in caste-specific behaviors, arguing for a role of epigenetic mechanisms in division of labor strategies. Our results indicate that interplay between JH and Ec naturally impose caste-specific behaviors during early adulthood. To address this hypothesis, it will be important to experimentally manipulate components of JH and Ec biosynthesis pathways. Future endeavors to understand the importance of JH and Ec in regulating *Cflo* worker behaviors will include injection of RNAi and small molecule drugs targeting both the biosynthesis and metabolism of these key steroid hormone factors.

We find significant differences in the neurologic makeup between Major and Minor castes, and specifically detect increased GABA signaling and GABA receptor subunits expressed in Minor brains. Important follow up work will be to address the importance of the dual Grd paralogs found in *Cflo* in foraging behavior, perhaps via RNAi treatments targeting Grd vs Grd2. Further, computational analyses of the evolution of Grd2 and its related genes in eusocial vs. solitary insects may reveal a case of novel gene function, in which Grd and Grd2 function to control caste-specific differences in foraging.

We detect significantly enriched heat shock proteins in the longer-lived Major caste. One hypothesis for the underpinnings of disparate lifespans among *Cflo* castes is that each caste harbors innate differences in aging-related pathways. This hypothesis is supported by our data, which suggest that even in the earliest stages of adult life, Major tissues may be more protected against stressors. Thus, experimental manipulation of Hsps, as well as detection of these genes in the long-lived Queen caste, will contribute broadly to our understanding of how aging may be differentially regulated between castes at a transcriptional level.

We observed paradoxical upregulation of the HDAC RPD3 after HDACi treatment. Indeed, RPD3 was consistently among the top 2 activated DEGs after HDACi. This suggests that RPD3 or other HDACs regulate their own transcriptional loci. One plausible model for this is that RPD3 expression is naturally balanced by its own HDAC activity, wherein elevated expression

acts as a negative feedback loop when RPD3 deacetylates its own promoter/TSS sequence. In this model, under HDACi, RPD3 expression enters an 'always on' state when unable to deacetylate these regions. An important extension of this work will be to study a longer time-course of transcriptional changes after HDACi, to determine whether falling RPD3 expression overlaps with reactivation of HDAC activity.

Finally, our observations suggest that the CoREST regulatory complex is activated by HDACi, and is specifically responsible for secondary downregulation of HDACi-repressed genes, including JHe and JHeh. The following are two direct tests of this key hypothesis. Firstly, *ttk*/CoREST are predicted to directly activate JHe and JHeh. ChIP-seq of CoREST after HDACi-treatment should reveal its association at repressed genes. Preliminary results suggest that a mammalian RCOR1/CoREST antibody recognizes *Cflo* CoREST, and we are piloting RCOR1 ChIP-seq in HDACi treated tissues. Based on our current model, we predict RCOR1 enrichment will increase upstream of HDACi repressed genes 3h after HDACi, notably JH and JHeh. A second key prediction of the model is that RPD3, CoREST, and *ttk* are crucial to behavioral reprogramming. We have acquired RNAi constructs targeting these genes, and have begun piloting RNAi injections after HDACi, to determine whether we can block behavioral reprogramming after HDACi by inhibiting the CoREST complex.

## Chapter 4 Bibliography

1. Simola, Daniel F., et al. "A chromatin link to caste identity in the carpenter ant *Camponotus floridanus*." *Genome Research* (2012): gr-148361.
2. Simola, Daniel F., et al. "Epigenetic (re) programming of caste-specific behavior in the ant *Camponotus floridanus*." *Science* 351.6268 (2016): aac6633.
3. Wheeler, Diana E., and H. Frederik Nijhout. "Soldier determination in ants: new role for juvenile hormone." *Science* 213.4505 (1981): 361-363.
4. Jindra, Marek, Subba R. Palli, and Lynn M. Riddiford. "The juvenile hormone signaling pathway in insect development." *Annual review of entomology* 58 (2013): 181-204.
5. Sauman, Ivo, and Steven M. Reppert. "Molecular characterization of prothoracicotropic hormone (PTTH) from the giant silkworm *Antheraea pernyi*: developmental appearance of PTTH-expressing cells and relationship to circadian clock cells in central brain." *Developmental biology* 178.2 (1996): 418-429.
6. Liu, Nan, et al. "The microRNA miR-34 modulates ageing and neurodegeneration in *Drosophila*." *Nature* 482.7386 (2012): 519.
7. Liu, Suning, et al. "Antagonistic actions of juvenile hormone and 20-hydroxyecdysone within the ring gland determine developmental transitions in *Drosophila*." *Proceedings of the National Academy of Sciences* 115.1 (2018): 139-144.
8. Rewitz, Kim F., et al. "The insect neuropeptide PTTH activates receptor tyrosine kinase torso to initiate metamorphosis." *Science* 326.5958 (2009): 1403-1405.
9. Mizoguchi, Akira, et al. "Immunohistochemical localization of prothoracicotropic hormone-producing neurosecretory cells in the brain of *Bombyx mori*." *Development, growth & differentiation* 32.6 (1990): 591-598.
10. Li, Kang, Qiang-Qiang Jia, and Sheng Li. "Juvenile hormone signaling—a mini review." *Insect science* (2018).
11. Yamanaka, Naoki, et al. "Neuroendocrine control of *Drosophila* larval light preference." *Science* 341.6150 (2013): 1113-1116.
12. Yan, Hua, et al. "Eusocial insects as emerging models for behavioural epigenetics." *Nature Reviews Genetics* 15.10 (2014): 677.
13. Cheung, Samantha K., and Kristin Scott. "GABAA receptor-expressing neurons promote consumption in *Drosophila melanogaster*." *PloS one* 12.3 (2017): e0175177.
14. Delgado, Teresa Cardoso. "Glutamate and GABA in appetite regulation." *Frontiers in endocrinology* 4 (2013): 103.
15. Kiya, Taketoshi, and Takeo Kubo. "Analysis of GABAergic and non-GABAergic neuron activity in the optic lobes of the forager and re-orienting worker honeybee (*Apis mellifera* L.)." *PloS one* 5.1 (2010): e8833.

16. Arshavsky, Yuri L., et al. "Gamma-aminobutyric acid induces feeding behaviour in the marine mollusc, *Clione limacina*.." *Neuroreport: An International Journal for the Rapid Communication of Research in Neuroscience* (1991).
17. Gisselmann, Günter, et al. "Drosophila melanogaster GRD and LCCH3 subunits form heteromultimeric GABA-gated cation channels." *British journal of pharmacology* 142.3 (2004): 409-413.
18. Selcho, Mareike, et al. "Central and peripheral clocks are coupled by a neuropeptide pathway in Drosophila." *Nature communications* 8 (2017): 15563.
19. Kay, Janina, et al. "The Circadian Clock of the Ant *Camponotus floridanus* Is Localized in Dorsal and Lateral Neurons of the Brain." *Journal of biological rhythms* 33.3 (2018): 255-271.
20. Gospcic, Janko, et al. "The neuropeptide corazonin controls social behavior and caste identity in ants." *Cell* 170.4 (2017): 748-759.
21. Yang, Shi Ping, et al. "Characterization of the shrimp neuroparsin (MeNPLP): RNAi silencing resulted in inhibition of vitellogenesis." *FEBS open bio* 4.1 (2014): 976-986.
22. Palm, Wilhelm, et al. "Lipoproteins in Drosophila melanogaster—assembly, function, and influence on tissue lipid composition." *PLoS genetics* 8.7 (2012): e1002828.
23. Yokoyama, Hiroshi, et al. "Lipid transfer particle from the silkworm, *Bombyx mori*, is a novel member of the apoB/large lipid transfer protein family." *Journal of lipid research* (2013): jlr-M037093.
24. Calderwood, Stuart K., Ayesha Murshid, and Thomas Prince. "The shock of aging: molecular chaperones and the heat shock response in longevity and aging—a mini-review." *Gerontology* 55.5 (2009): 550-558.
25. Warrick, John M., et al. "Suppression of polyglutamine-mediated neurodegeneration in Drosophila by the molecular chaperone HSP70." *Nature genetics* 23.4 (1999): 425.
26. Johnson, Brian R., and Neil D. Tsutsui. "Taxonomically restricted genes are associated with the evolution of sociality in the honey bee." *BMC genomics* 12.1 (2011): 164.
27. Feldmeyer, B., D. Elsner, and S. Foitzik. "Gene expression patterns associated with caste and reproductive status in ants: worker-specific genes are more derived than queen-specific ones." *Molecular Ecology* 23.1 (2014): 151-161.
28. Yang, Yi, et al. "Histone demethylase LSD2 acts as an E3 ubiquitin ligase and inhibits cancer cell growth through promoting proteasomal degradation of OGT." *Molecular cell* 58.1 (2015): 47-59.
29. Brown, Nicholas G., et al. "RING E3 mechanism for ubiquitin ligation to a disordered substrate visualized for human anaphase-promoting complex." *Proceedings of the National Academy of Sciences* (2015): 201504161.
30. Huang, Ju, and Azad Bonni. "A decade of the anaphase-promoting complex in the nervous system." *Genes & development* 30.6 (2016): 622-638.

31. Mao, Diane D., et al. "A CDC20-APC/SOX2 signaling axis regulates human glioblastoma stem-like cells." *Cell reports* 11.11 (2015): 1809-1821.
32. van Roessel, Peter, et al. "Independent regulation of synaptic size and activity by the anaphase-promoting complex." *Cell* 119.5 (2004): 707-718.
33. Zheng, Ning, et al. "Structure of the Cul1–Rbx1–Skp1–F box Skp2 SCF ubiquitin ligase complex." *Nature* 416.6882 (2002): 703.
34. Carrano, Andrea C., et al. "SKP2 is required for ubiquitin-mediated degradation of the CDK inhibitor p27." *Nature cell biology* 1.4 (1999): 193.
35. Delgado-Esteban, Maria, et al. "APC/C-Cdh1 coordinates neurogenesis and cortical size during development." *Nature communications* 4 (2013): 2879.
36. Dui, Wen, et al. "The Drosophila F-box protein dSkp2 regulates cell proliferation by targeting Dacapo for degradation." *Molecular biology of the cell* 24.11 (2013): 1676-1687.
37. Boix-Perales, Hector, et al. "The E3 ubiquitin ligase skp2 regulates neural differentiation independent from the cell cycle." *Neural development* 2.1 (2007): 27.
38. Bostick, Magnolia, et al. "UHRF1 plays a role in maintaining DNA methylation in mammalian cells." *Science* 317.5845 (2007): 1760-1764.
39. Cheng, Jingdong, et al. "Structural insight into coordinated recognition of trimethylated histone H3 lysine 9 (H3K9me3) by the plant homeodomain (PHD) and tandem tudor domain (TTD) of UHRF1 (ubiquitin-like, containing PHD and RING finger domains, 1) protein." *Journal of Biological Chemistry* 288.2 (2013): 1329-1339.